

In presenting the dissertation as a partial fulfillment of the requirements for an advanced degree from the Georgia Institute of Technology, I agree that the Library of the Institute shall make it available for inspection and circulation in accordance with its regulations governing materials of this type. I agree that permission to copy from, or to publish from, this dissertation may be granted by the professor under whose direction it was written, or, in his absence, by the Dean of the Graduate Division when such copying or publication is solely for scholarly purposes and does not involve potential financial gain. It is understood that any copying from, or publication of, this dissertation which involves potential financial gain will not be allowed without written permission.

J

3/17/65
b

MASS SPECTROMETRIC STUDIES OF THE
SYNTHESIS, ENERGETICS, AND CRYOGENIC STABILITY
OF THE LOWER BORON HYDRIDES

A THESIS

Presented to
The Faculty of the Graduate Division

by
James Howard Wilson

In Partial Fulfillment
of the Requirements for the Degree
Doctor of Philosophy in the School of Chemical Engineering

Georgia Institute of Technology

May, 1966

MASS SPECTROMETRIC STUDIES OF THE
SYNTHESIS, ENERGETICS, AND CRYOGENIC STABILITY
OF THE LOWER BORON HYDRIDES

Approved: _____

Date approved by Chairman: May 15, 1966

ACKNOWLEDGMENTS

I am grateful to Dr. H. A. McGee, Jr., for the suggestion of this research problem and for his advice, interest, and encouragement during the progress of the research work. The suggestions and assistance given by my fellow graduate students, D. B. Bivens and T. J. Malone, are greatly appreciated as are the interest and suggestions of Dr. W. H. Eberhardt and Dr. W. T. Ziegler while serving on the reading committee. I am also thankful to Dr. E. C. Ashby for information concerning the details of a synthesis procedure.

The National Science Foundation, the Humble Oil and Refining Company, and the Standard Oil Company of California furnished me fellowships during my graduate study and my deepest appreciation is due for this assistance. I also wish to thank the National Aeronautics and Space Administration for its support through grant NSG-337 administered by the Engineering Experiment Station of the Georgia Institute of Technology.

The encouragement, assistance, and patience of my wife, Julia, as well as the motivation inspired by her and my daughter and son, Kristie and Mike, are gratefully acknowledged. The help and encouragement of my mother, Mrs. Pauline Hamrick, my stepfather, Mr. Ross T. Hamrick, and other relatives are also deeply appreciated.

TABLE OF CONTENTS

ACKNOWLEDGMENTS	Page ii
LIST OF TABLES	vi
LIST OF FIGURES	vii
SUMMARY	viii
NOMENCLATURE	xv
Chapter	
I. INTRODUCTION	1
Definition and Brief History of the Problem	1
Purpose of the Research	3
Review of Literature	4
II. APPARATUS AND EXPERIMENTAL TECHNIQUES	11
Introduction	11
Furnace Beam Inlet System	12
General Design Considerations	12
Mechanical Description	13
Experimental Procedure	18
Coaxial Furnace Inlet System	19
Hot Filament Inlet System	23
Radio Frequency Discharge Tube Inlet System	24
Cryogenic Inlet System	26
Pyrolysis Experiments	27
Radio Frequency Discharge Experiments	29
Energy Measurements	32
Dimethylanilineborane Synthesis Procedure	33
Purity of Gases Used in Synthesis Experiments	34
III. RESULTS AND DISCUSSION	35
Review of Preliminary Experiments	35
Furnace Beam Inlet System	35

TABLE OF CONTENTS (Continued)

Chapter	Page
III. (Continued)	
Hot Filament Pyrolysis	36
Coaxial Furnace Inlet System	37
rf Discharge Experiments	38
Pyrolysis Studies of BH_3 and BH_2	39
Energetics of the BH_3 - $^3\text{B}_2\text{H}_6$ System	42
Appearance Potential Data	42
Derived Ionization Potentials, Bond Energies, and Thermodynamic Values	47
Discussion of Experimental Measurements and Derived Data	47
Kinetic Considerations	58
Summary of BH_2 Results	62
Synthesis and Cryogenic Quenching of BH_3	65
Synthesis and Cryogenic Quenching of HBF_2 and H_2BF	66
IV. CONCLUSIONS AND RECOMMENDATIONS	69
APPENDICES	
A. BLANKING CIRCUIT	74
B. MODIFICATION OF THE RETARDING POTENTIAL DIFFERENCE CIRCUITRY	77
C. CALCULATION AND ESTIMATION PROCEDURES FOR BOND ENERGIES AND IONIZATION POTENTIALS FROM APPEARANCE POTENTIAL DATA	81
D. THERMODYNAMIC DATA DERIVED FROM BOND ENERGIES	89
E. RATE EQUATION DESCRIBING THE PYROLYSIS OF B_2H_6 IN THE INITIAL STAGE OF REACTION	94
F. CALCULATIONS OF KINETIC RATE CONSTANTS	100
G. RAW DATA FROM H_2BF QUENCHING EXPERIMENTS	105
H. CALCULATION OF PRESSURE IN THE PYROLYSIS REGION OF THE COAXIAL FURNACE INLET SYSTEM	109

TABLE OF CONTENTS (Continued)

APPENDICES (Continued)	Page
I. IONIZATION EFFICIENCY CURVES FOR EXPERIMENTAL APPEARANCE POTENTIALS	113
BIBLIOGRAPHY	120
VITA	125

LIST OF TABLES

Table	Page
1. Appearance Potentials of Fragment Ions From BH_3 and B_2H_6	43
2. Bond Energies and Ionization Potentials Calculated or Estimated from Appearance Potential Measurements	48
3. Thermodynamic Data Derived from Experimental Bond Energies	49
4. Kinetic Rate Constants for Several Reactions Involved in the Pyrolysis of B_2H_6	60
5. Raw Data for a Typical H_2BF Synthesis Experiment	106

LIST OF FIGURES

Figure	Page
1. Schematic Diagram of Furnace Beam Inlet System	14
2. Flow Arrangement for the Furnace Beam Inlet System	17
3. Coaxial Furnace Inlet System	20
4. Radio Frequency Discharge Tube Inlet System	25
5. Schematic Diagram for Pyrolysis and Quench of B_2H_6	28
6. Schematic Diagram for rf Discharge and Cryogenic Quenching Experiments	31
7. Ionization Efficiency Data for $I(BH_3)$ and $A(BH_3^+)$ from B_2H_6 Using the Semi-Log Matching Method	44
8. Ionization Efficiency Data for $I(BH_3)$ Using the Retarding Potential Difference Method	45
9. Schematic Diagram of Blanking Circuit	75
10. Electron Gun for RPD Studies in Normal Arrangement	78
11. Modification of Electron Gun for RPD Studies	78
12. Ionization Efficiency Data for $I(N_2)$ Using the Semi-Log Matching Method	114
13. Ionization Efficiency Data for $A(BH_3^+)$ from BH_3 Using the Semi-Log Matching Method	115
14. Ionization Efficiency Data for $A(BH_2^+)$ from BH_3 Using the Semi-Log Matching Method	116
15. Ionization Efficiency Data for $A(B^+)$ from B_2H_6 Using the Semi-Log Matching Method	117
16. Ionization Efficiency Data for $A(BH_2^+)$ from B_2H_6 Using the Semi-Log Matching Method	118
17. Ionization Efficiency Data for $A(B_2H_5^+)$ from B_2H_6 Using the Semi-Log Matching Method	119

SUMMARY

The work reported in this thesis involved the synthesis of BH_3 by pyrolysis or electrical discharge of suitable parent compounds, the identification and determination of the energetics of this molecule by mass spectrometric techniques, and an attempt to prepare the species as a stable liquid or solid phase by utilization of a unique cryogenic reactor inlet system which has been designed, constructed, and used successfully in related studies in this laboratory. A secondary effort was made to produce H_2BF in order to obtain more information concerning unstable trivalent compounds of boron.

The boron hydrides, particularly B_2H_6 , and also the higher alkylated boranes have received considerable attention over the past fifteen years or so because of their practical usefulness, especially as rocket and jet aircraft fuels. In addition, much interest and controversy has been focused upon the unusual bonding present in these compounds due to the so-called "electron deficient" nature of the boron atom. In contrast, BH_3 and also the free radical BH_2 have been the subject of comparatively few studies, evidence for their existence at the onset of this thesis work being only of a hypothetical nature. For example, kinetic studies, such as those on the pyrolysis of B_2H_6 ¹⁵⁻¹⁸, gave results explicable in terms of the intermediate BH_3 . The possibility that BH_3 might exist as a cryogenic material arose when a liquid helium quench of the products of a B_2H_6 microwave discharge produced an unidentified phase with a triple point of approximately 60°K ³⁶. In addition to the experimental evidence

for the existence of the reactive BH_3 molecule, estimated free energy values⁵⁵ indicated that the equilibrium between B_2H_6 and BH_3 should highly favor BH_3 at temperatures of about 1000°C .

During the preliminary experiments of this thesis research, two reports were published concerning the mass spectrometric detection of reactive intermediates in the pyrolysis of B_2H_6 . Although both BH_3 and BH_2 were included in the results of one group³⁹, the other research team identified only BH_3 ³⁸. Besides this discrepancy about the particular species observed in the pyrolysis, one study determined the dissociation energy of B_2H_6 into BH_3 fragments as ≥ 55 kcal/mole³⁸ while a value of 39 kcal/mole was obtained in the work that supposedly observed both BH_3 and BH_2 ³⁹. Consequently, the resolution of the differences between these two independent sources became one of the objectives of this thesis.

Initial attempts to detect BH_3 in the pyrolysis of B_2H_6 and dimethylanilineborane involved the introduction of the pyrolysis products into the ionization region of the mass spectrometer by effusion through small diameter orifices. This approach had been used successfully in this laboratory in the study of CF_2 ⁵² as well as in other investigations of unstable molecules and free radicals⁵⁹. However, BH_3 could not be detected in a lengthy series of hot filament and tubular furnace pyrolysis experiments. When BH_3 was finally observed by introducing the pyrolysis products directly into the electron beam without the presence of a beam collimating orifice, it became clear that future investigations of unstable species should be conducted, if possible, in this manner. Whereas CF_2 was not lost upon effusion through a 0.032 inch diameter orifice⁵², BH_3 suffered decomposition or reaction under similar experimental conditions.

A radio frequency discharge of B_2H_6 failed to produce evidence of BH_3 . If BH_3 were actually formed in the discharge, it would have been depleted by the time the discharge products reached the ionization region of the mass spectrometer approximately one foot away. This became apparent during the cryogenic quenching experiments when BH_3 could not be transferred through a 1-1/2 foot long by 3/8 inch diameter tube which had been cooled to a temperature approximately that of the melting point of oxygen ($54.8^\circ K$).

BH_3 was detected by pyrolysis of B_2H_6 in tubular furnaces of quartz, aluminum, and stainless steel at pressures of 10^{-4} to 10^{-2} mm Hg and temperatures of 250° to $400^\circ C$. BH_3 was also synthesized by pyrolysis of B_2H_6 on incandescent filaments of platinum, tungsten, nichrome, zirconium, molybdenum, niobium, titanium, and tantalum. The ionization potential of BH_3 was determined by the semi-log matching method and the Fox retarding potential difference method to be 12.32 ± 0.1 ev. By combining this with a value of 14.88 ± 0.05 ev for $A(BH_3^+)$ from B_2H_6 , $D(BH_3 - BH_3^+)$ may be calculated as 2.56 ev or 59 kcal/mole.

The appearance potentials of B^+ , BH^+ , BH_2^+ , BH_3^+ , and $B_2H_5^+$ from B_2H_6 , as well as from BH_3 wherever applicable, were determined. Although several of these values are in major disagreement with other studies, the numbers presented are considered to be accurate. This follows from the agreement between the semi-log matching method and the retarding potential difference method on the values of several of the appearance potentials and also from the self-consistency of the experimental numbers. The latter is demonstrated by three determinations of $D(BH_3 - BH_3^+)$ as approximately 2.6 ev from the appearance potentials of three separate

fragment ions.

The experimental appearance potentials permitted the direct determination of either the values of or the lower and/or upper bounds for $D(B^+ - H)$, $D(BH^+ - H)$, $D(BH_2^+ - H)$, $D(BH_3 - BH_3)$, $D(BH_3^+ - BH_3)$, $I(B_2H_6)$, and $I(B_2H_5)$. The calculation of $D(B - H)$, $D(BH - H)$, $D(BH_2 - H)$, and $I(BH_2)$ was made possible by introducing the spectroscopic value of $I(BH) = 9.77$ ev⁶⁷. The values are consistent with some of the data from spectroscopic, kinetic, and mass spectrometric studies and also are upheld by theoretical arguments in several cases.

The utilization of the derived bond energies to calculate the heat of formation of B_2H_6 as -40.9 kcal/mole at $298^\circ K$ allowed an analysis of the errors in the experimental bond energies from this research. This was accomplished by comparing the calculated heat of formation with an experimental value of 7.53 kcal/mole^{69,70}. This calculation involved $D(BH_3 - BH_3)$, the heat of sublimation of boron, the dissociation energy of hydrogen, and two times the value of the heat of atomization of BH_3 . If all values except the latter are assumed to be accurate, it may be seen that an error of 24.2 kcal/mole in the heat of atomization of BH_3 , i.e., $D(BH_2 - H) + D(BH - H) + D(B - H)$, would produce the rather large disagreement between the two heats of formation. That is, an average error of approximately 8 kcal/mole or 0.35 ev exists in the derived bond energies of BH , BH_2 , and BH_3 . This is believed to be the case as opposed to assigning what would be a considerable error to $D(BH_3 - BH_3)$. The errors are not believed to be due to the experimental appearance potential values, but to be inherent in the electron impact method of energy determinations.

Attempts to detect free BH_2 in the pyrolysis of B_2H_6 failed even though the experimental conditions under which BH_2 was reportedly synthesized were essentially reproduced. Other than the possibility that the reported observation of BH_2 was due to another species, the only explanation for this discrepancy that can be given by this author is that the presence of a 0.0001 inch diameter platinum:platinum-rhodium (90-10) thermocouple centered in the furnace and the gas stream, as described by Fehlner and Koski^{39,41}, catalyzed the formation of BH_2 (such an arrangement was not used in this work). However, this seems unlikely because of the small heating surface area of the wire as compared to the furnace walls (Fehlner and Koski report two to three times more BH_2 than BH_3).

Equilibrium partial pressures calculated from free energies of reaction based on the bond energies from this thesis research and entropy values from estimated thermodynamic tables showed that the pyrolysis of B_2H_6 should produce approximately equal amounts of BH_2 and BH_3 . In addition, the partial pressures were calculated by applying the previously mentioned correction to the BH_3 bond energy and also by assigning an unlikely error to $D(\text{BH}_3 - \text{BH}_3)$ of 24 kcal/mole. These results led to the same conclusion of approximately equal amounts of BH_2 and BH_3 . However, by again employing the experimental bond energies, the magnitudes of the activation energies for the dissociation of B_2H_6 into BH_2 and into BH_3 were estimated and a comparison of the resultant kinetic rate constants indicated that BH_2 should not play a significant role in the kinetics of the pyrolysis of B_2H_6 . This appeared more acceptable when a mechanism for the pyrolysis of B_2H_6 involving BH_3 and not BH_2 was proposed and then used to show agreement of the value of $D(\text{BH}_3 - \text{BH}_3)$ deduced from several

kinetic studies¹⁵⁻¹⁸ and the value determined from this work. Also, by relating the kinetic rate equation describing the pyrolysis mechanism to experimental results, pre-exponential factors were calculated for several steps in the pyrolysis mechanism that were entirely reasonable for the order of reaction in question as seen by comparison with experimental pre-exponential factors^{79,80}. This gave further support to the correctness of the proposed mechanism.

The quench of the products of the pyrolysis of B_2H_6 in the cryogenic reactor inlet system at temperatures as low as approximately the melting point of oxygen ($54.8^\circ K$) failed to produce evidence of stabilized BH_3 . That is, BH_3 was not observed either by monitoring the pyrolysis and quenching operation or by monitoring the gas evolved from the deposit upon warm-up. However, the observation of an increase in the H_2^+ ion peak at approximately $60^\circ K$ followed by a decrease in intensity at higher temperatures led to the initial conclusion that BH_3 had been stabilized at the quenching temperature, but was reacting or decomposing to liberate H_2 as the temperature of the system was increased. This concurred with an earlier x-ray detection of an unidentified phase with a triple point of $60^\circ K$ in the quenched products of a microwave discharge of B_2H_6 ³⁶. A subsequent experiment in which unpyrolyzed B_2H_6 and H_2 were subjected to the cryogenic quench produced the same variation of the H_2^+ ion peak upon warm-up. The final conclusion was that H_2 was trapped in the B_2H_6 matrix and liberated at approximately $60^\circ K$.

H_2BF was not detected in similar cryogenic quenching experiments on the products of an rf discharge of BF_3 and B_2H_6 . However, HBH_2 was observed upon warm-up of the quenched discharge products to about $90^\circ K$.

The lowering of $A(\text{BF}_2^+)$ to approximately 13 ev was evidence that HBF_2 and not BF_3 was the parent compound. Also, the appearance of HBF^+ and BF_2^+ peaks at a temperature slightly lower than that at which peaks from BF_3 begin to appear agreed with the reported similarity of the vapor pressures of HBF_2 and BF_3 ⁴⁶. Finally, the approximate 1:1 ratio of m/e ion peaks 31 and 49 concurred with a mass spectrometric study of HBF_2 ⁴⁶.

A modification of the standard arrangement of the electron gun grids of the Bendix mass spectrometer in the retarding potential difference mode of operation enabled an increase in sensitivity by a factor of approximately 5. This was advantageous in the determination of ionization and appearance potentials of species that were present in small concentrations in the gas samples introduced into the mass spectrometer. The modification was found to have no adverse effects upon the reliability of the energy measurements.

NOMENCLATURE

The following symbols are so defined unless otherwise specified in the text.

a	= inside radius.
A	= pre-exponential or frequency factor of reaction rate constant.
$A_{\text{expt.}}$	= experimentally determined pre-exponential factor.
$A(X)$	= appearance potential of X, ev.
$D(X-Y)$	= dissociation or bond energy of X-Y, ev or kcal/mole.
E	= activation energy, ev or kcal/mole.
$E_{\text{expt.}}$	= experimentally determined activation energy.
F	= conductance of a tube, liters/sec.
g	= gaseous state of X when used as X(g).
G	= Gibb's free energy, $H - TS$, ev or kcal/mole.
ΔG_f°	= free energy of formation, reactants and products in the ideal state.
ΔG_T°	= free energy of reaction at temperature T ($^\circ\text{K}$), reactants and products in the ideal state.
H	= enthalpy, ev or kcal/mole.
ΔH_f°	= heat of formation, reactants and products in the ideal state.
ΔH_r°	= heat of reaction, reactants and products in the ideal state.
ΔH_s°	= heat of sublimation, ideal state.
ΔH_T°	= heat of reaction at temperature T ($^\circ\text{K}$), reactants and products in the ideal state.
$I(X)$	= ionization potential of X, ev.

k	= reaction rate constant.
$k_{\text{expt.}}$	= experimentally determined reaction rate constant.
K_{eq}	= equilibrium constant.
K_p	= equilibrium constant in terms of partial pressures.
l	= length of tube, inches.
L	= mean free path of gas, cm.
m/e	= mass to charge ratio.
M	= molecular weight.
MFD	= capacitance, microfarads.
n	= number of moles.
P	= pressure.
P_{mm}	= pressure in millimeters of mercury.
P_X	= partial pressure of X.
R	= gas constant.
s	= solid state of X when used as X(s).
ΔS_T^0	= entropy of reaction at temperature T ($^{\circ}\text{K}$), cal/mole/ $^{\circ}\text{K}$ or kcal/mole/ $^{\circ}\text{K}$, reactants and products in the ideal state.
T	= temperature, $^{\circ}\text{K}$ or $^{\circ}\text{C}$.
VAC	= volts alternating current.
VDC	= volts direct current.
W	= watts.
η	= viscosity of gas, poise.
Ω	= resistance, ohms.

CHAPTER I

INTRODUCTION

Definition and Brief History of the Problem

This thesis problem is concerned with the preparation of highly reactive and unstable compounds which could ultimately be of practical use rather than existing only as laboratory curiosities. Included in such a study is the development of synthesis techniques for these new compounds, the determination of the energetics of the system involved (which allows one to positively identify the new species as well as to calculate bond energies, heats of formation, etc.) and the utilization of equipment designed to operate at cryogenic temperatures for the stabilization of the reactive substance in relatively pure form by effectively "freezing out" the activation energy of reaction. It should be pointed out that the synthesis process may actually take place at cryogenic temperatures as well as at room temperatures and above.

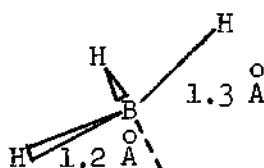
Since the pioneering work of Stock¹ and later Schlesinger and Burg², the boron hydrides had received relatively little attention prior to the last decade or so. The renewed interest in these compounds resulted from their potential usefulness as high energy fuels for rockets and jet aircraft. Compared to conventional solid and liquid fuels such as kerosene or saturated hydrocarbons, combustion of the boron hydrides produces up to 50 percent more heat per unit mass. The heat of combustion is lower than that of hydrogen, but the boron hydrides are much denser and,

in general, they do not require the additional weight of thermal insulation such as is necessary for hydrogen.

Besides their use as rocket fuels, as catalysts, as reducing agents, as semi-conductor doping agents, etc., the boron hydrides have received considerable interest and have been the subject of much controversy concerning their electronic structure. The fact that boron is "electron deficient," in the sense that there are more orbitals available for bonding than can be filled by the number of valence electrons present, results in the interesting structural and bonding properties of the boron hydrides. Diborane, B_2H_6 , the lowest boron hydride that is reasonably stable, is a good example. This molecule has, in addition to four ordinary covalent bonds between boron and hydrogen atoms, two "banana" bonds each involving two boron atoms and one hydrogen atom. These are three-centered, two-electron bonds formed from the hydrogen orbital and one hybridized $2sp^3$ orbital from each of the two boron atoms^{3,4}.

In comparison with the available knowledge of and with the amount of work done on diborane and the higher boron hydrides such as B_4H_{10} , B_5H_9 , B_5H_{11} , and $B_{10}H_{14}$, little has been accomplished in regard to the lower boron hydrides, BH , BH_2 , and BH_3 . BH has been studied experimentally by spectroscopic methods and its ionization potential and dissociation energy determined. However, at the beginning of this thesis research no direct experimental evidence of either BH_2 or BH_3 had been offered. The formation of BH_2 and stabilization by cryogenic quenching as a relatively pure phase appears to be highly unlikely as the species is a free radical and the quenching of low molecular weight free radicals is usually accomplished only in a frozen matrix in concentrations of at most a few tenths

of a percent. In contrast, BH_3 would seem to be a likely candidate for synthesis and subsequent quenching experiments. It would be expected to exist in a singlet electronic ground state with a planar structure formed by the bonding of three 2sp^2 orbitals of boron with the hydrogen orbitals⁵. In a theoretical treatment of the BH_3 molecule⁶, the first excited state was considered. This state was calculated to have an excitation energy of 5.06 eV, possibly an important point when one considers the existence of free BH_3 in a condensed phase. It is described as being a pyramidal biradical having one elongated B-H bond as shown below.



The dotted line shows the approximate direction of the non-bonding orbital. This description makes the B_2H_6 bridge structure rather more understandable. From a practical point of view, the development of a synthesis technique that may lead to economic production of BH_3 would be of considerable interest in that the heat of combustion of B_2H_6 , which has already been used as a propulsion fuel, would be increased by the amount of its dissociation energy into two BH_3 molecules.

Purpose of the Research

The main purpose of this thesis research has been to synthesize the BH_3 molecule by pyrolysis or electrical discharge of suitable parent compounds, to determine the energetics of the molecule by electron impact measurements, and to prepare the species as a stable phase at cryogenic

temperatures. This species was chosen because of its potentially practical usefulness, as previously mentioned, and because of its plausible existence based upon theoretical and experimental grounds, the former having been briefly discussed and the latter to be described shortly.

Although BH_2 and BH_3 had not been directly observed at the onset of this study, experimental results concerning these two species were published soon afterwards. The data presented showed considerable disagreement between the separate sources and questions arose as to what species were actually present in the synthesis steps. Consequently, much emphasis was placed upon attempting to resolve the existing differences between the published data and upon ascertaining the actual existence of certain reported species.

In order to obtain more information concerning unstable trivalent compounds of boron and hydrogen, a secondary effort was made to produce H_2BF . This molecule along with BH_3 would complete the series of compounds from BH_3 to the well-known substance BF_3 , that is, BF_3 , HBF_2 , H_2BF , and BH_3 .

Review of Literature

Although BH_3 and BH_2 had not been directly observed at the beginning of this research, a considerable amount of work had been published concerning indirect evidence primarily for BH_3 . These reports have appeared only recently. Prior to the first part of 1950, work on the thermal decomposition of boron hydrides had been published^{1,2,7-14} and in several cases the existence of BH_3 as an unstable intermediate had been postulated. However, the only evidence of the intermediate BH_3 was of a

chemical nature². That is, chemical reactions of various compounds with boron hydrides resulted in the addition of BH_3 to the starting material, e.g., the reaction of B_2H_6 and CO under suitable conditions produced BH_3CO .

In approximately a fifteen year period beginning in 1951, numerous reports appeared which were concerned with investigations of systems that produced experimental results explicable in terms of the BH_3 molecule. These investigations, which contained no direct observations of BH_3 or BH_2 , included studies such as the following:

- a) the pyrolysis of compounds such as B_2H_6 ¹⁵⁻¹⁹ and BH_3CO ^{20,21};
- b) the reactions of B_2H_6 with H_2O ²², C_2H_4 ²³, and PH_3 ²⁴;
- c) the exchange reactions between deuterium and B_2H_6 ^{25,26} and between isotopically normal B_2H_6 and enriched $\text{B}_2^{10}\text{H}_6$ ²⁷;
- d) the photolysis of B_2H_6 ²⁸ and B_5H_9 ²⁹;
- e) the photosensitized reaction of B_2H_6 by excited Hg atoms³⁰;
- f) the shock tube pyrolysis of B_2H_6 ^{31,32}.

Examples of methods used for following these reactions were chromatography, pressure rise, hydrogen production, and mass spectrometry. The main results of these experiments were kinetic analyses to determine the order of the reaction and the experimental activation energy and to suggest a mechanism, which invariably included BH_3 as an intermediate, consistent with the rate equation fitting the experimental data. In some instances, the dissociation energy of B_2H_6 into two BH_3 molecules was deduced. This value was also determined by a thermochemical procedure involving the reaction of B_2H_6 with gaseous methylamines³³.

In 1956, Bauer³⁴ presented an analysis of the data from the kinetic

studies available at that time to deduce upper and lower bounds for the heat of dissociation of diborane. He stated that the published mechanism for the decomposition of BH_3CO by Burg²⁰ was wrong and proposed an alternate mechanism supposedly giving the correct form for the observed pressure-time dependence. From his consideration of eight independent kinetic studies^{14,15,16,20,22-25}, Bauer was led to upper bounds for the dissociation energy of diborane which ranged from 27 to 38.4 kcal/mole. He also calculated rough lower bounds of 25 and 30.5 kcal/mole. These results are comparable with the thermochemical value of 28.4 kcal/mole³³.

Later, Garabedian and Benson³⁵ refuted Bauer in stating that Burg's kinetic data were in excellent agreement with his original mechanism. Their reanalysis of the data fixed the bond dissociation energy of B_2H_6 between 32 and 38.3 kcal/mole. From the remaining seven kinetic studies considered by Bauer, Garabedian and Benson were led to the conclusion that in six systems no calculation of the value of the heat of dissociation of B_2H_6 was warranted. The remaining one, they felt, fixed a lower bound at 33 kcal/mole. Examples of a few of the considerations upon which they based their conclusions were the questionable homogeneity and the lack of establishment of stoichiometry of some of the reactions and the "impossible" Arrhenius pre-exponential factors calculated in some cases.

At this point, it is quite obvious that such indirect means as those just discussed leave much to be desired for the absolute determination of the existence of reactive intermediates and for the accurate calculation of the energetics of the reactions involved. Experimental results obtained by spectroscopic and mass spectrometric methods, which permit the determination of bond energies, ionization potentials, appearance potentials,

etc., would appear to be subject to much less doubt and controversy.

It appeared possible that the first direct experimental observation of BH_3 was made by Bolz, Mauer, and Peiser³⁶. In an attempt to stabilize hydrogen atoms by frozen matrix trapping, diborane was subjected to a microwave discharge and the products quenched at the temperature of liquid helium. Hydrogen atoms were not stabilized since warm-up occurred suddenly from 4.2° to 33°K as a result of the recombination of the hydrogen atoms. However, by means of x-ray diffraction, a new phase was observed which exhibited a triple point of approximately 60°K . It was postulated that this unidentified phase could be BH_3 , although the possibility that it was only a previously unreported metastable phase of B_2H_6 could not be ruled out.

Morrey, Johnson, Fu, and Hill³⁷ studied the pyrolysis of B_2H_6 and followed the reaction with an infrared spectrometer. Infrared peaks were observed that did not correspond to any known boron hydrides. On the assumption that the observed frequencies at 3.9, 6.4, and 8.4 microns were the normal fundamental frequencies of BH_3 , force constants were calculated for the molecule. Assuming the same force constants for BD_3 , the authors stated that it was possible to predict the frequencies that would appear if deuterated B_2H_6 were pyrolyzed. This reaction was studied and although the results were thought encouraging, more refined measurements were believed necessary before the assignment to BH_3 could be proven.

In 1964, the first direct experimental observations of the BH_3 molecule and the BH_2 radical were reported. Sinke, Pressley, Baylis, and Stafford³⁸, utilizing a Knudsen-type cell in conjunction with a mass spectrometer, deduced a value of the dissociation energy of $\text{B}_2\text{H}_6 \geq 55$

kcal/mole from the observed equilibrium between BH_3 and B_2H_6 . Fehlner and Koski³⁹, who also employed mass spectrometric detection and used a fast flow pyrolysis technique, determined, by controlled energy electron impact methods, the ionization potential of BH_3 , $I(\text{BH}_3)$, and the appearance potential of BH_3 , $A(\text{BH}_3^+)$, from B_2H_6 to be 11.4 ± 0.2 ev and 13.1 ± 0.2 ev respectively. These results gave a value of 1.7 ev or 39 kcal/mole for the energy of dissociation of B_2H_6 . Diesen⁴⁰ reported a mass spectrometric identification of BH_3 from a shock tube study. Again, we find a discrepancy in the results of independent studies even though the measurements must be considered to be extremely reliable in comparison to the indirect methods which were discussed previously. One interesting point of which to take note is that Fehlner and Koski state that their data imply the BH_2 concentration to be about two to three times as large as the BH_3 concentration, while Sinke, *et al.*, assume the BH_2 peak resulted from the fragmentation of BH_3 .

Fehlner and Koski⁴¹ studied the pyrolysis of BH_3CO in a low pressure flow system using a mass spectrometer. The bond dissociation energy of BH_3CO was estimated from the data which, when combined with Burg's²⁰ equilibrium data, gave the energy of dissociation of diborane as 37.1 ± 4 kcal/mole. BH_3 was also observed in this study as confirmed by rough appearance potential measurements. In this paper, Fehlner and Koski noted that the coating of the reactor with Al_2O_3 did not affect the production of BH_3 from BH_3CO or B_2H_6 , but did greatly inhibit the formation of BH_2 from B_2H_6 . Based on the work with the pyrolysis of B_2H_6 and BH_3CO , Fehlner⁴² described a mechanism for the pyrolysis of B_2H_6 that included BH_2 and BH_3 as intermediates. He noted that this mechanism was very

similar to the Rice-Herzfeld mechanism for the pyrolysis of hydrocarbons.

Again utilizing a Knudsen-type cell and mass spectrometric detection, Baylis⁴⁰, et al., investigated the pyrolysis of B_2H_6 in order to observe any mono-, tri-, or tetraborane species that had been heretofore unobserved but postulated in reaction mechanisms. Their attempt resulted in data which indicated the presence of a B_3H_x molecule and a tetraborane that could possibly be B_4H_8 . In addition, BH_3 was again observed. Thus, the experimental observations of Baylis, et al., appeared to be in accord with the arguments of Schaeffer¹⁹, Clarke and Pease¹⁶, Lipscomb⁴³, and others^{18,31} concerning the existence of BH_3 , B_3H_7 , and B_3H_9 as intermediates in the pyrolysis of B_2H_6 and concerning the formation of a tetraborane prior to pentaborane. However, these results did not agree with the mechanism proposed by Fehlner⁴². The intermediate species of his mechanism did not include the triborane intermediates, but were concerned mainly with H , BH_2 , BH_3 , BH_4 , and B_2H_5 . H , BH_4 , and B_2H_5 have not been reported in the pyrolysis of B_2H_6 , although B_2H_5 has been postulated in the photolysis of B_2H_6 ²⁸.

This review of the literature points out the controversy that existed concerning the reaction mechanisms, the energetics, and the possible existence of certain unstable intermediates involved in the pyrolysis of B_2H_6 and other boron hydride compounds. Both indirect and direct experimental measurements had failed to fix the dissociation energy of B_2H_6 with any certainty, the values obtained thus far ranging from approximately 27 to 55 kcal/mole. And even though the existence of BH_3 had been fairly well established due to three independent observations, BH_2 had not been included in the published work of one group which observed BH_3 under

conditions similar to those reportedly producing both BH_2 and BH_3 . These were the existing differences which, among other problems, were to be examined and for which solutions were hopefully to be found.

The secondary effort made to synthesize H_2BF was not supported by quite the experimental evidence that has been presented for the existence of BH_3 . In fact, the only mention of a reactive monohaloborane (H_2BX , $\text{X} = \text{F}, \text{Cl}, \text{Br}, \text{or I}$) found in the literature was the suggestion of H_2BCl as an intermediate in the reaction of BCl_3 and B_2H_6 ⁴⁴. HBF_2 had been prepared in large yields and found to be quite stable at approximately -169°C ⁴⁵⁻⁵⁰. Of course, the very stable compound BF_3 is well known. The existence of H_2BF with properties intermediate to the very reactive BH_3 molecule and to the considerably more stable HBF_2 molecule appeared plausible if from nothing more than the idea of continuity in the series of compounds from BH_3 to BF_3 .

CHAPTER II

APPARATUS AND EXPERIMENTAL TECHNIQUES

Introduction

The major piece of equipment used in this work was a Bendix Time-of-Flight Mass Spectrometer, Model 12-107. A detailed description of the mass spectrometer, its auxiliary equipment, and circuitry for the retarding potential difference (RPD) method of ionization potential measurements by Fox, *et al.*⁵¹, is given in a thesis from this laboratory by Martin⁵². However, two modifications have since been made for application in this work. A blanking circuit for the elimination of large interfering ion signals is described in Appendix A. The other modification, concerned with the increase of trap current (intensity of the ionizing electron beam) for greater sensitivity in the RPD mode, is dealt with in Appendix B.

The cryogenic inlet system used for the quenching experiments is described in part by Martin⁵². A more complete discussion of the design considerations, mechanical description, and operation of a combination reactor and inlet system that has been developed in this laboratory is presented by Malone^{53,54}. The auxiliary equipment and experimental procedure for quenching experiments with BH_3 and H_2BF , as well as for the pyrolysis and rf discharge experiments involving the synthesis and the appearance potential studies of BH_3 , are described here. Of the equipment involved in the latter experiments, only the coaxial furnace inlet system

and one of the hot filament inlet systems actually produced evidence of BH_3 . Although the use of the furnace beam inlet system and the rf discharge tube inlet system did not result in the synthesis of BH_3 , future studies of other unstable species may well employ these inlet systems quite successfully.

The details for the synthesis of dimethylanilineborane that was also used in pyrolysis experiments for the production of BH_3 are presented in this chapter.

Furnace Beam Inlet System

General Design Considerations

As mentioned in Chapter I, although BH_3 had not been directly observed by experimental means when this thesis work was initiated, indirect evidence had been presented for its existence in many pyrolysis experiments, particularly in the pyrolysis of B_2H_6 . Therefore, a rather obvious first step in this series of experiments was the construction of a suitable furnace for the production of BH_3 from B_2H_6 . Rather than the usual static system employed by previous experimentalists who were mainly concerned with kinetic studies, a steady-state flow system was desirable from the standpoint of the stability required for energy measurements and of the need to readily investigate various pyrolysis conditions for the optimum production of BH_3 . The latter followed primarily from the anticipated quenching experiments. Relatively high temperatures appeared desirable since ΔG of the reaction



is approximately 0 at 800°K, as calculated from estimated thermodynamic data⁵⁵, becoming increasingly negative at higher temperatures. This indicates, of course, a very favorable equilibrium constant for the formation of BH_3 . The high temperatures pose the disadvantage, however, of the possibility of decomposition of BH_3 and B_2H_6 into boron and hydrogen. Therefore, another purpose of the fast-flow system was to overcome the rates of decomposition of the reactant and product. Low pressures were also deemed necessary. First of all, this would mean a shift to the right in Equation (1) according to LeChatelier's principle. Secondly, lower pressures would result in fewer intermolecular collisions and hinder the reactions of the BH_3 molecule in forming higher boron hydrides.

From the preceding considerations, the furnace beam inlet system was constructed. The arrangement is similar in some ways to inlet systems first used by Eltenton⁵⁶ and subsequently highly developed by Lossing⁵⁷, Dibeler⁵⁸, and others⁵⁹.

Mechanical Description

The furnace beam inlet system is shown schematically in Figure 1. The main parts are a 3/8 inch OD stainless steel furnace tube (1) through which the gas sample is admitted, a 1-1/2 inch OD stainless steel exhaust tube (2) which contains the furnace tube and acts as an exhaust tube and cooling tube for the gas from the furnace, and a 4-1/2 inch OD stainless steel piston (3) which moves in a double O-ring gland into a vacuum lock and which is connected to a 3 inch OD extension can (4) that moves to within 3/16 inch of the ion grids of the mass spectrometer. The physical arrangement of the inlet system in place is essentially identical to that of the cryogenic inlet system as illustrated by Malone^{53,54}. In operation,

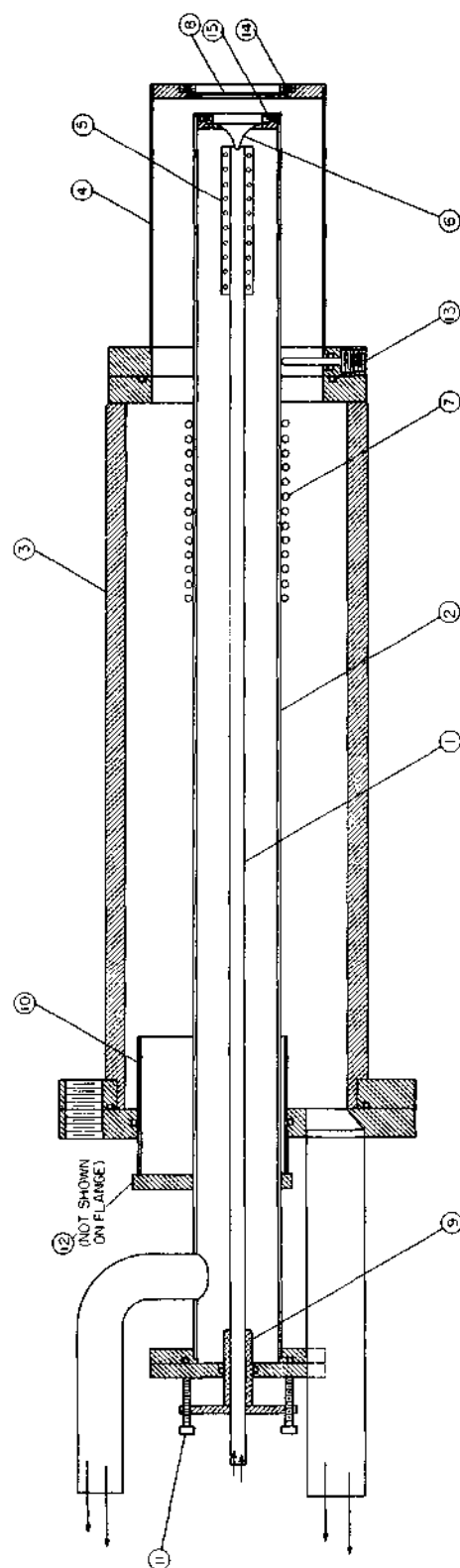


Figure 1. Schematic Diagram of Furnace Beam Inlet System.

the gas sample travels down the furnace tube, is heated by a length of nichrome wire wound furnace (5) (whose upper temperature limit is approximately 1000°C), and impinges upon a thin metal foil (6) which is mechanically sealed into the end of the exhaust tube. A cooling coil (7) is provided should it be necessitated by the furnace temperature and gas flow rate. The thin metal foil (about 0.010 inch thick) allows a jet of the gas to be admitted into the intermediate pumping space. The foil may be nipple shaped as shown to allow the orifice, in the deepest part of the nipple, to extend into the furnace region and consequently to be at approximately the same temperature as the gas from the furnace. The intermediate pumping space, which is that volume lying within the piston and extension can and outside of the exhaust tube, is evacuated by a diffusion pump system. The jet of gas then strikes another thin metal foil (8) which is located within 1-1/8 inches of the electron beam and which serves to collimate the stream of gas. Under the conditions of pressure in the intermediate space and assuming the gas leaving the first foil is at approximately the same temperature as the furnace, it would be expected that molecular flow is experienced through the final foil and therefore the mass spectrometer would essentially be recording the composition of the reactant gas as it exists in the furnace.

Several features were incorporated in the design of the apparatus to provide for flexibility and convenience in operation and maintenance of the system. For instance, the furnace tube and exhaust tube are mounted through flanges by sleeves (9) and (10) which are free to slide in O-ring seals. By means of adjusting screws (11) and (12) on the tubes, the distance between the end of the furnace tube and the first foil may be varied

as may the distance between both foils. Adjustment of these two parameters would presumably produce an optimum sample beam for analysis by the mass spectrometer. Also, for alignment of the holes in the foils, three positioning screws (13) are provided which enter through O-ring seals in the flange on the extension can at right angles to and bear upon the exhaust tube.

Concerning the maintenance of the system, it was believed that plugging of the orifices by deposited boron might prove to be a problem. Therefore, the design is such that for removal and replacement or cleaning of the foils the apparatus may be withdrawn from the mass spectrometer, the compression nut (14) and the foil(8) removed from the outside, and then through the resulting opening the remaining compression nut (15) and foil (6) may be removed.

The headers on the exhaust tube and the piston were provided with terminals for power and thermocouple connections. The temperature of the furnace was measured by a chromel-alumel thermocouple imbedded in the furnace insulation. Thermocouples were also placed at several points, such as near the O-ring seals and wherever else it was felt that overheating might occur.

Figure 2 shows a simplified flow diagram of the experimental setup. The flow rate from the diborane cylinder (1) was measured by a Fischer and Porter flow meter (2). The leak valve (3) and the throttle valve (4), Veeco Model FR-100-S, were manipulated to control the flow rate and the furnace pressure, which may be varied from a few microns to several millimeters of mercury. For pressures greater than approximately one millimeter of mercury, an Edwards High Vacuum Model LB2A leak valve was

PI - PRESSURE INDICATING GAUGE

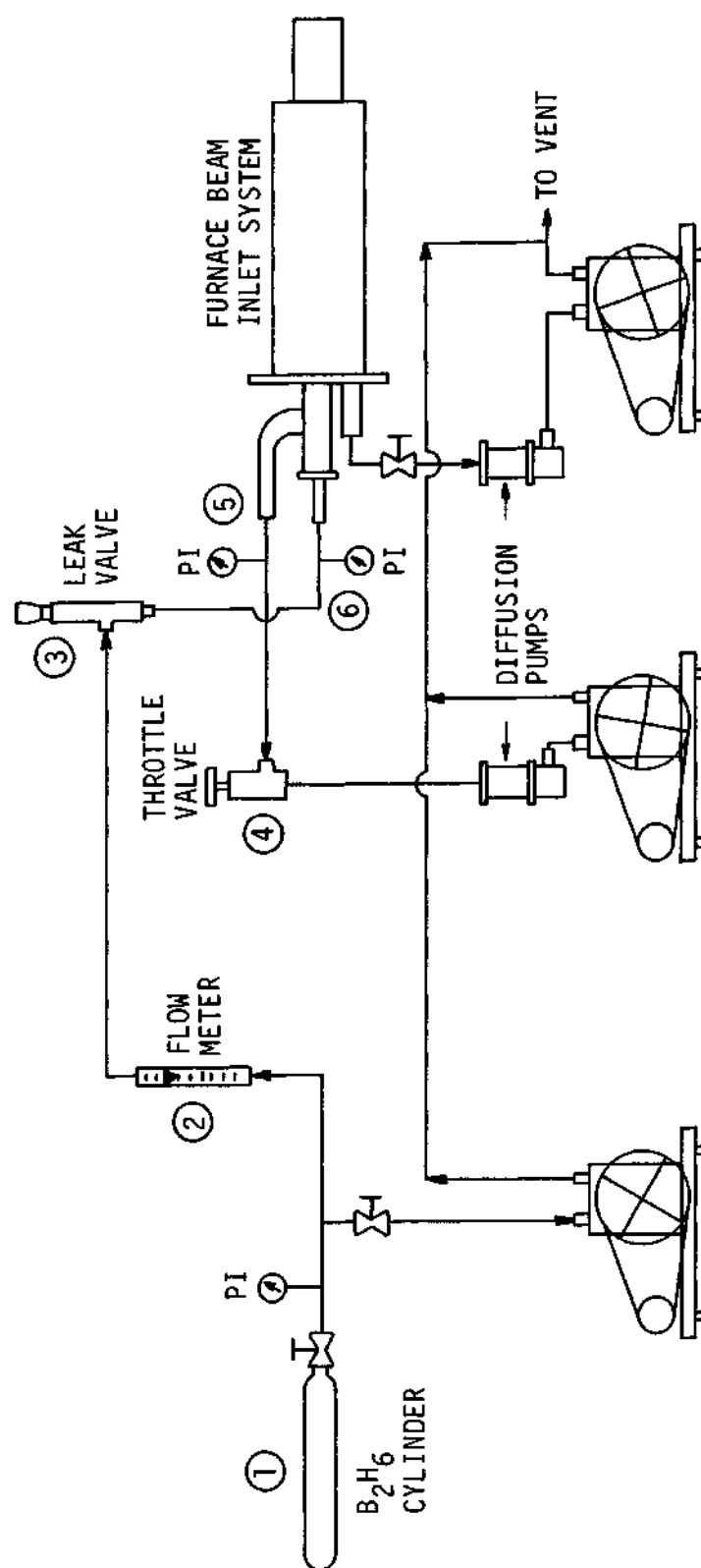


Figure 2. Flow Arrangement for the Furnace Beam Inlet System.

used, whereas a Vactronic Model VV-50 leak valve was employed for lower pressures. Vacuum gauges (5) and (6) indicated the pressure drop through the system and also the approximate furnace pressure. Again depending upon the range of pressures involved, a Dubrovin vacuum gauge, a McLeod vacuum gauge, or a Veeco cold cathode discharge gauge was utilized. Both the intermediate pumping space and the furnace exhaust tube were evacuated by diffusion pump systems, though for pressures above one millimeter of mercury only a mechanical pump was used to exhaust the furnace.

Experimental Procedure

The pyrolysis of B_2H_6 was investigated by means of the furnace beam inlet system over a wide range of operating conditions. Flow rates up to a maximum of 150 std cm^3/min were studied at pressures of 20 to approximately 10^{-4} mm Hg. The flow rates at the lower pressures were too low to permit determination, though the Vactronic leak valve will supposedly allow control down to 0.01 std cm^3/sec . Temperatures as high as $900^\circ C$ were involved. The pyrolysis furnace was packed with stainless steel turnings in several experiments.

Although rough calculations were made to determine the amount of gas that would be admitted through the two orifices and into the ionization region of the mass spectrometer, a trial-and-error method was used to determine a satisfactory orifice size for different operating conditions. In all cases, the orifice must allow a quantity of gas to enter the ionization region which is sufficient for appearance potential measurements, yet must not permit a quantity so large to enter that either the multiplier plates become saturated (the blanking circuit had not been installed at this time) or the pressure in the mass spectrometer rises above 2×10^{-5}

mm Hg, a maximum pressure as recommended by Bendix if ion-molecule reactions are to be of no significance. The orifice sizes varied from 0.010 to 0.063 inches in diameter. Additional experiments were conducted in which only one foil was present and in which both foils were removed and the furnace tube exit advanced as close to the electron beam as possible, a distance of 1-1/2 inches. The pyrolysis reaction was monitored by recording the mass spectrum on a Honeywell 906 Visicorder and determining whether or not the $m/e = 14$ peak, corresponding to $B^{11}H_3$, or the ratio of $m/e = 14$ to $m/e = 27$, the latter corresponding to $B_2^{11}H_5$, experienced any significant increase that would indicate the presence of BH_3 as a free species. In addition, by noting the value of electron energy at which the $m/e = 14$ peak vanished, the presence of free BH_3 would be signified by a lowering of the vanishing point by an amount approximately equal to the dissociation energy of B_2H_6 .

Coaxial Furnace Inlet System

The tubular furnace shown in Figure 3 was constructed for pyrolysis studies at inlet pressures up to 0.5 mm Hg and temperatures as high as 500°C. The furnace was mounted coaxially with the drift tube of the mass spectrometer inside the fast reaction chamber (1) of the ion source header. The most desirable feature of this system was that it allowed the furnace exit to be positioned anywhere from being completely immersed in the electron beam to about one inch away. In comparison, the furnace exit of the furnace beam inlet system could be advanced no closer to the electron beam than 1-1/2 inches.

The furnace tube (2) was a 1/8 inch OD stainless steel tube which

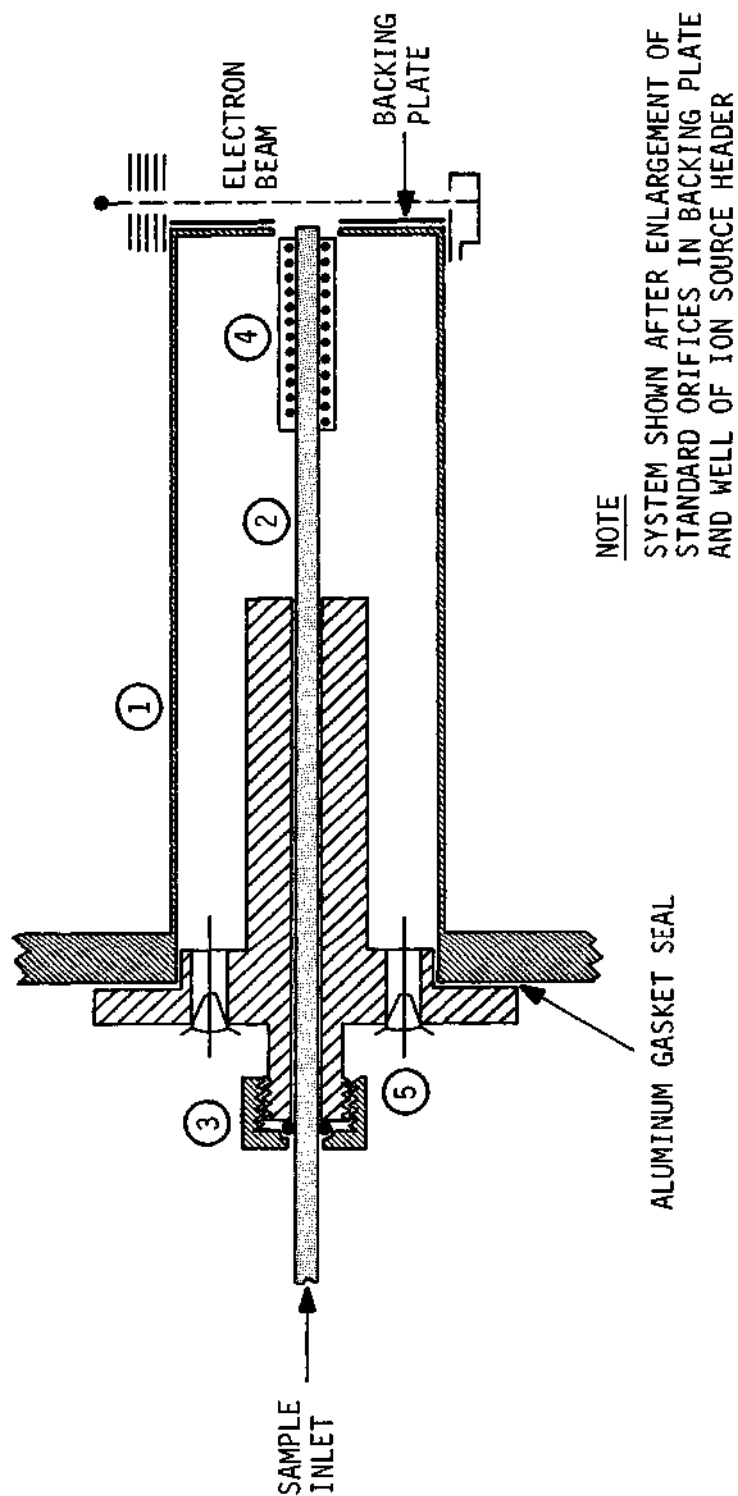


Figure 3. Coaxial Furnace Inlet System.

could be positioned by sliding through an O-ring sealed quick-disconnect joint (3). The heated region (4), usually one inch in length, was wound with nichrome wire coated with Sauereisen Insa-Lute Adhesive Cement for uniform heating as well as for insulation between the wire and the furnace tube itself. The temperature of the furnace was measured by a chromel-alumel thermocouple imbedded in the Sauereisen. Power and thermocouple leads were introduced through high vacuum electrical feed throughs (5). Furnaces of alumina and quartz (one inch in length and one millimeter ID) were also employed by simply sealing them into the end of the 1/8 inch tube with Sauereisen. In some instances, the stainless steel furnace was packed with five or six one inch lengths of monel capillary tubing.

In operation the sample gas was introduced by means of a Vactronic Model VV-50 leak valve connected to a suitable delivery system (usually a lecture bottle filled with B_2H_6). The inlet pressure was determined by either a thermocouple gauge, a Veeco cold cathode discharge gauge, or a Consolidated Type 41550 micromanometer. The production of the species of interest was maximized by varying pressure and temperature. It was found that in most cases a temperature greater than approximately $400^{\circ}C$ would result in a decrease in BH_3 production, probably due to its decomposition into boron and hydrogen. This upper temperature depended, of course, upon the dimensions of the particular furnace.

In initial experiments with this system, the sample gas from the furnace traveled into the ionization region of the mass spectrometer through the standard 0.032 inch orifice in the fast reaction chamber of the ion source header and then through a similar orifice in the backing plate located slightly less than 0.5 millimeters away. It was later found

necessary to enlarge both orifices to 1/4 inch and to cover the opening in the backing plate with the fine mesh that is used on the ion grids. With the backing plate removed, the furnace exit could be positioned directly in the electron beam. However, this caused a lowering of the appearance potentials of all species present, including the inert calibrating gas, argon. When the exit was positioned at the bottom of the fast reaction chamber, this effect was not noticeable. At first it was believed that the potential existing on the furnace windings was accelerating the ionizing electrons to an energy a few volts higher than that indicated by the electron energy potentiometer. These observations were made with furnaces having a single winding of heating wire. Later, when using a furnace with a double winding of wire, the appearance potential lowering was again noted even though the furnace exit was not advanced into the ionizing region and the grounded end of the windings was located at the furnace exit. Now, the most reasonable explanation of this phenomenon appeared to be that the alternating magnetic field created by the furnace was causing acceleration of the electron beam, the effect being more noticeable for a furnace with a double winding of heating wire than with a single winding. The use of a noninductively wound furnace would have clarified this situation, but was not done in these experiments.

A few pyrolysis experiments were conducted using the furnace attachment for the cryogenic inlet system as described by Malone⁵³. This consisted of a 1-1/2 inch long alumina tube (one millimeter ID), heated over a one inch length by a coil of tungsten wire, which replaced the extension piece of the inlet system. The exit of the furnace tube could be positioned in the edge of the electron beam of the mass spectrometer.

Temperature was measured by a copper-constantan thermocouple imbedded in the Sauereisen Insa-Lute Cement which coated the heater wire and furnace tube.

Hot Filament Inlet System

Pyrolysis of B_2H_6 was carried out by means of the hot filament inlet system described by Martin⁵² which was positioned in the fast reaction chamber of the ion source header. Filaments of platinum, tungsten, and nichrome were studied. The maximum temperature examined in each case was that at which the metallic filament collapsed. This temperature was about $1700^\circ C$ for platinum, $1100^\circ C$ for nichrome, and $3000^\circ C$ for tungsten. Temperatures were determined by sighting through an observation port with a Leeds and Northrup Model 8622-C optical pyrometer. Pressures ranged from approximately 10^{-4} to greater than 10^{-2} mm Hg as indicated by a Veeco cold cathode discharge gauge. This series of experiments was conducted before the orifices in the fast reaction chamber of the ion source and in the backing plate were enlarged.

The hot filament system described by Malone⁵³ was also used for a few pyrolysis studies. In this arrangement, a coiled wire filament was installed directly across the exit port in the extension piece of the cryogenic reactor inlet system. With the inlet system positioned so that the wire filament was tangent to the electron beam, a species could be pyrolyzed by a single collision with the filament and analyzed immediately. Temperatures were again determined by optical pyrometry. Filaments of zirconium, molybdenum, niobium, titanium, and tantalum, in addition to those just mentioned, were utilized.

Radio Frequency Discharge Tube Inlet System

Prompted by the observations of Bolz, Mauer, and Peiser³⁶ on the microwave discharge of B_2H_6 , a radio frequency discharge of B_2H_6 was attempted to produce BH_3 . The experimental arrangement is shown in Figure 4. The 3/8 inch OD pyrex or quartz discharge tube (1) was sealed into the fast reaction chamber (2) of the ion source by an O-ring sealed quick-disconnect joint (3). The orifices in the fast reaction chamber and the backing plate were enlarged at this time. A carrier gas and diborane were admitted through Vactronic Model VV-50 leak valves (4) and (5). The discharge was generated by means of a 50 turn, one inch diameter coil (6) powered by a Hallicrafter's BC-610 radio transmitter.

The discharge circuitry is described in detail in a thesis by Bivens⁶⁰ from this laboratory. A 650 volt potential supplied by several batteries in series (7) was applied between two parallel metal strips (8) placed on either side of the discharge tube. This was necessary to prevent ions produced by the discharge from entering the ionization region of the mass spectrometer and creating noise. Several turns of aluminum foil (9) situated on either side of the discharge coil confined the visible glow of the discharge within the region between the aluminum foil. Otherwise, the discharge glow would extend over the entire length of tube, heating up the tygon connections to the valves, thereby introducing impurities, and causing noise in the spectrometer. An attempt was made to conduct an in-line discharge, i.e., with the discharge tube coaxial with the drift tube. However, all efforts to prevent ions from entering the ionization region failed. It was decided that the 3000 volt drop across the discharge coil was creating highly energetic ions which could not be deflected into

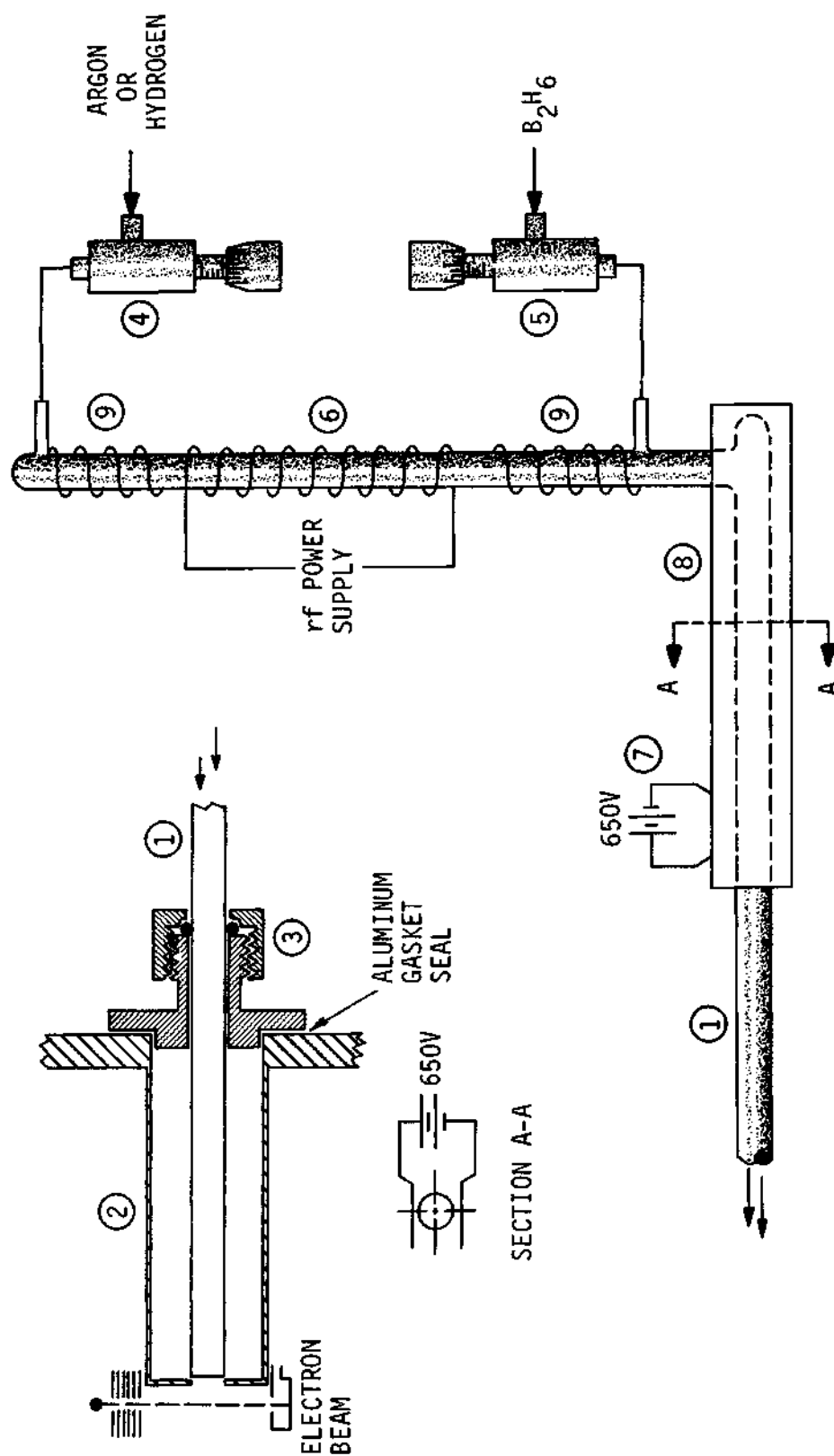


Figure 4. Radio Frequency Discharge Tube Inlet System.

the walls, in order to allow neutralization, by the methods used. The 90 degree bend in the discharge tube of Figure 4 was successful in eliminating the majority of the ions, but the parallel metal strips were necessary for their complete elimination.

In operation, argon or hydrogen was introduced upstream of the discharge coil and the pressure adjusted until a fairly intense discharge was obtained (about 0.05 mm Hg for argon and considerably higher for hydrogen). Diborane was injected downstream of the discharge coil in order to prevent deposition of boron in the region of the coil, which would result in a decrease in the efficiency of the discharge. The flow rates of diborane were varied from so low a rate that the B_2H_6 peaks were barely detectable to so large a rate as to cause saturation of the multiplier plates (approximately 0.1 mm Hg), the blanking circuit having yet to be installed. The intensity of the carrier gas discharge was also varied. Argon was found to be the better carrier gas for the discharge in that lower pressures could be utilized and a greater fraction of the diborane could be dissociated. Evidently, for the dissociation of B_2H_6 argon is a better energy transfer agent than is hydrogen. Although the visible glow of the discharge did not extend to the B_2H_6 inlet, metallic boron was coated on the tube walls over a length of several inches where the glow was present. Evidently, the diborane was diffusing upstream and discharging in the glow region.

Cryogenic Inlet System

As previously mentioned, the mechanical description and operation of the cryogenic inlet system proper is presented in detail by Malone^{53,54}.

Only the adaptations for pyrolysis and discharge experiments are given here.

Pyrolysis Experiments

Figure 5 shows the experimental arrangement for the production of BH_3 and its subsequent cryogenic quench. The 1/8 inch OD stainless steel furnace (1), which was used for pyrolysis studies in the coaxial arrangement, was silver soldered into the end of a 5/16 inch OD monel tube (2) and the assembly mounted in a brass header (3) provided with power and thermocouple lead throughs. The assembly was connected to the reactor header (4) of the cryogenic inlet system so that the furnace exit was positioned within 1/2 inch of the tapered region (5) within the outer refrigerant chamber. The monel tube was wrapped with insulating tape to prevent freezing of B_2H_6 on the walls, though the possibility appeared remote. B_2H_6 was introduced through a Vactronic Model VV-50 leak valve (6) and the pressure measured by a thermocouple gauge (7).

The optimum conditions for producing BH_3 with this particular furnace had already been determined as a pyrolysis temperature of 380°C and an inlet pressure of 0.1 mm Hg. The pyrolysis of B_2H_6 was conducted at these conditions and the furnace effluent was quenched to about 55°K during an approximately one hour run. The products were analyzed mass spectrometrically during gentle warm-up of the system. The analysis was accomplished by the usual technique of approximate appearance potential measurements and by the recording of mass spectra at different temperatures. The pressures involved were low enough to permit the pyrolysis to take place with the cryogenic inlet system extension piece advanced into place tangential to the electron beam. Hence, the volatile species at the quenching temperature of about 55°K could be monitored during the pro-

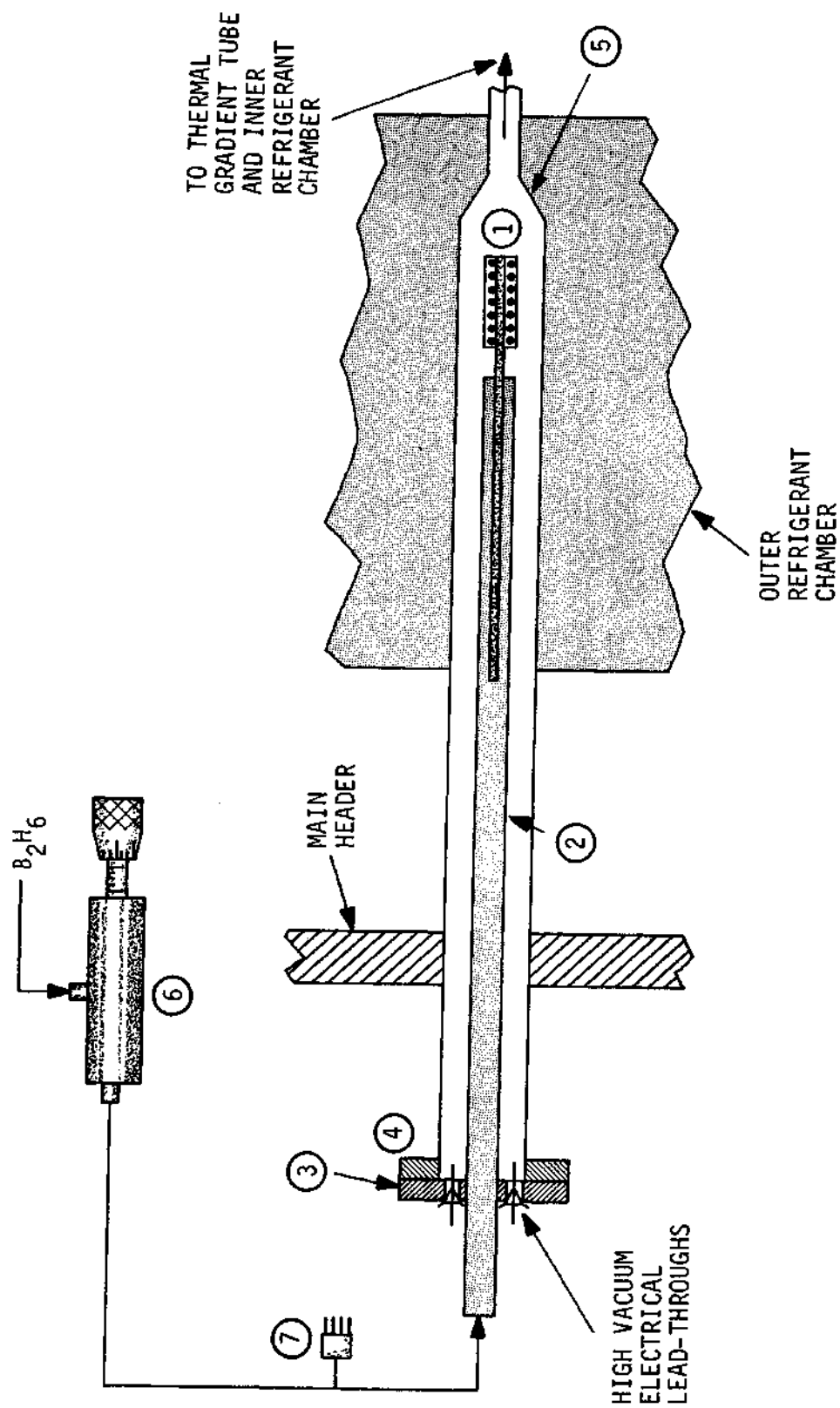


Figure 5. Schematic Diagram for Pyrolysis and Quench of B_2H_6 .

duct quench itself. The reactor space was continuously evacuated by a diffusion pump system.

The quenching temperature was attained by flooding the two refrigerant chambers with liquid O_2 and then pumping on each chamber with a mechanical pump. The inaccuracy of the thermocouples prevented the determination of the actual temperatures involved. However, the temperature dropped approximately 30° to $35^\circ K$ in a fifteen minute period and leveled off for another fifteen minutes before decreasing at a very slow rate. Thus, it appeared that the O_2 had frozen and then the solid O_2 had further cooled to a few degrees below the melting point. Once the temperature had experienced its initial drop, the pyrolysis could be conducted at $380^\circ C$ for approximately one hour before the outer refrigerant chamber began to warm. The inner chamber would hold the quenching temperature nearly fifteen minutes longer. Of course, after both chambers had been emptied of O_2 , no control over warm-up of the cryogenic inlet system was possible. However, as long as the refrigerant chambers were evacuated, the warm-up rate to room temperature was slow enough to permit a reasonable analysis of evolved products.

Experiments were performed in which pyrolysis products were quenched on the metal reactor space walls and also in which the reactor space was glass lined. In addition, conditions corresponding to low deposition rates were investigated should a lack of sufficient rate of heat transfer allow heating of the deposited film of gases.

Radio Frequency Discharge Experiments

The experimental arrangement for the production of H_2BF involved the radio frequency discharge coupled to the cryogenic inlet system as

shown in Figure 6. The pyrex discharge tube (1) seated into a taper joint (2) which was attached by means of a glass-to-metal seal (3) to the reactor header (4). The end of the discharge tube extended to the center of the outer refrigerant chamber. The one millimeter ID glass capillary (5) extended to the end of the discharge tube for some experiments and to within one inch of the end for others. The discharge tube within the refrigerant chamber was wrapped with aluminum foil to prevent freezing of B_2H_6 in the capillary. The discharge coil (6) operated as mentioned previously and B_2H_6 , BF_3 , and argon were admitted through high vacuum leak valves. Pressure was indicated by a thermocouple gauge located upstream of the discharge coil. The experiments were performed with the reactor space glass lined. Again, operating conditions permitted the reaction to be performed with the cryogenic inlet system advanced into proper analytical position. Both liquid O_2 and liquid N_2 were used as coolants, the lowest temperature investigated being approximately $55^\circ K$ obtained by pumping on liquid O_2 .

The experimental procedure involved introducing argon to a pressure of about 0.06 mm Hg to obtain a fairly intense discharge and then admitting BF_3 until the total pressure was 0.5 to 1.0 mm Hg. The diborane flow was adjusted to produce an inlet pressure of about 0.1 mm Hg. Naturally, the desired quenching temperature of about $55^\circ K$ or $77^\circ K$ had already been attained and the discharge was carried out for approximately 1 to 1-1/2 hours. Product analysis was conducted upon warm-up as previously described. Analysis of the unreacted feed gases in both the pyrolysis and the discharge experiments was also performed.

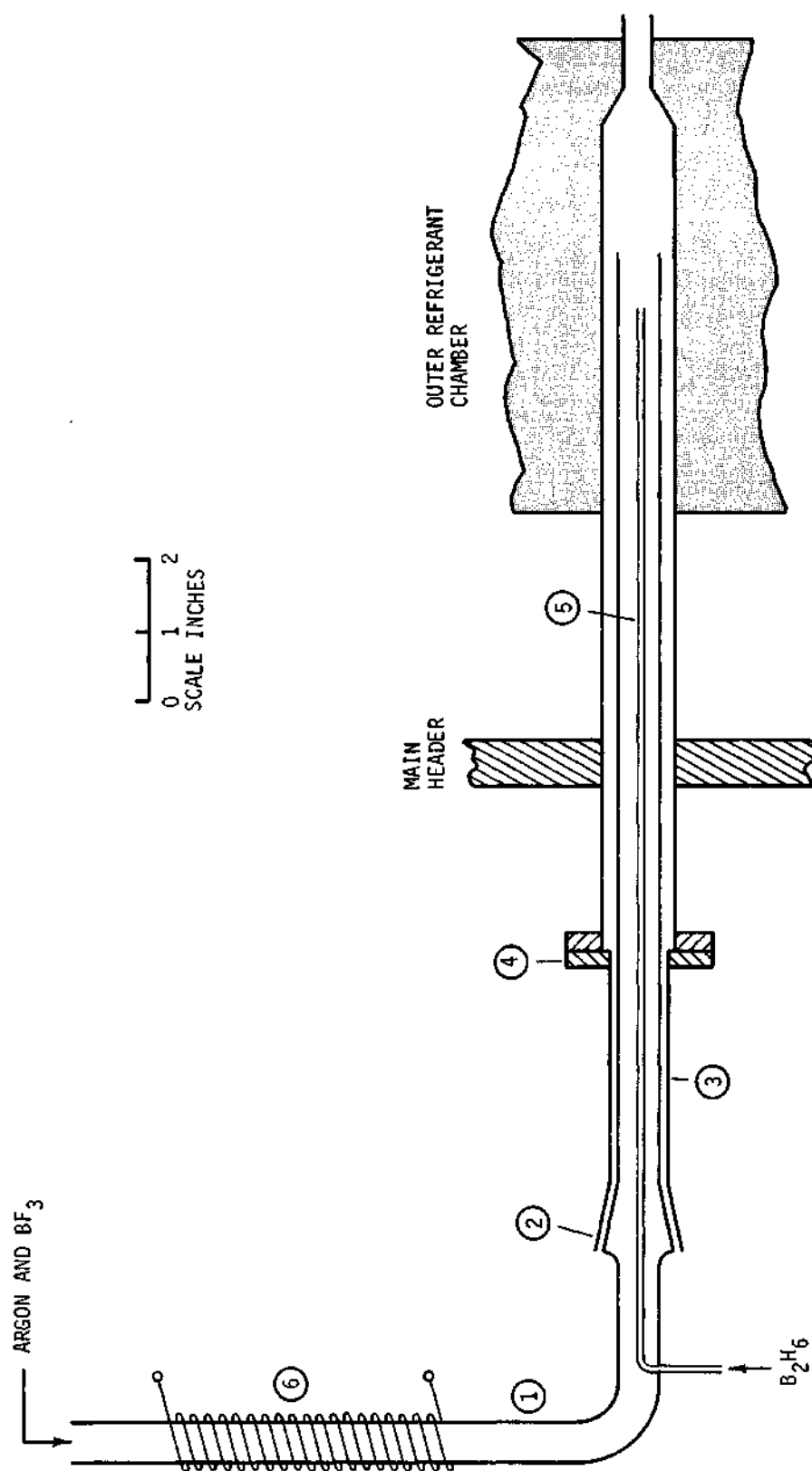


Figure 6. Schematic Diagram for RF Discharge and Cryogenic Quenching Experiments.

Energy Measurements

Martin⁵² gives a fairly complete discussion of the theory and experimental methods for determining the energetics of molecules and free radicals by mass spectrometric techniques utilizing the Bendix time-of-flight spectrometer. However, the semi-log matching method of Foner and Hudson⁶¹, which was not discussed by Martin⁵², was the primary technique employed in this work.

The energy scale was usually calibrated with argon each time the appearance potential of a particular ion was determined. Since the species of interest was present in the majority of cases only as a small fraction of a considerable flow of sample, it was much simpler to adjust the peak height of the ion of interest to match that of argon rather than employing the reverse procedure, which is normally followed. In contrast to experiences with compounds such as the oxygen fluorides⁵³, the calibration of the energy scale essentially did not change even in day-to-day operation. In fact, the cleaning of the electron grids and replacement of the filament had practically no effect on calibration. On the basis of this, later appearance potential measurements were made by performing only one calibration even when the appearance potentials of up to four different ions were desired during a single experiment. In all pyrolysis experiments, the calibration was conducted with the furnace on in view of the appearance potential lowering effect that had been observed and which was discussed earlier.

*
Dimethylanilineborane Synthesis Procedure

Approximately 100 milliliters of dimethylaniline were dried with several grams of sodium aluminum hydride. The dry product was then distilled under vacuum in an atmosphere of nitrogen, the total pressure being about 10 mm Hg. The reaction between diborane and dimethylaniline was performed by bubbling diborane through a 1:1 mixture of the aniline compound and diethyl ether in a stirred reactor (the synthesis was carried out in a hood). The reactor was a three-necked flask provided with a magnetic stirrer, a diborane inlet line with a fritted end which extended below the liquid level in the flask, a thermometer, and a water-cooled outlet line. The entire system was flushed with nitrogen prior to reaction and the synthesis was conducted under a positive nitrogen pressure of a few millimeters of mercury. The outlet line was equipped with a check valve, simply a U-tube filled with several inches of mercury, to prevent air from being sucked back into the system in the event of a loss of positive pressure. Diborane was bubbled through the dimethylaniline for approximately two hours at such a rate that the temperature of the liquid did not rise above 30°C. The observation of a significant increase in the viscosity of the reaction mixture and of a greenish flame when the outlet gas was ignited indicated that the reaction was essentially complete. The conversion was almost 100 percent as demonstrated by a titration of the reaction product.

Dimethylanilineborane was found to be very stable at room temperature when a system containing the compound was evacuated for several days

*Dr. Eugene C. Ashby of the Georgia Institute of Technology School of Chemistry is acknowledged for providing the synthesis procedure for dimethylanilineborane.

by a mechanical pump without any noticeable loss of sample. In contrast, an equal amount of dimethylaniline could be pumped away within a few hours.

Purity of Gases Used in Synthesis Experiments

Diborane was obtained from the Callery Chemical Company, Callery, Pennsylvania, as a compressed gas in 100 gram lots. The diborane was stored at dry ice temperature to prevent decomposition and reaction. For the experimental work, a lecture bottle was filled with the diborane to a total pressure of about 30 psig. An analysis by means of the mass spectrometer revealed no detectable impurities. However, after the diborane lecture bottle had been used for several days while at room temperature, hydrogen and higher boranes such as B_4H_{10} could be detected. At this time the lecture bottle was refilled from the main cylinder.

Boron trifluoride of a 99.5 percent minimum purity was obtained from the Matheson Company. The reported impurities were air, SO_2 , SiF_4 , and sulfates.

CHAPTER III

RESULTS AND DISCUSSION

Review of Preliminary ExperimentsFurnace Beam Inlet System

The pyrolysis of B_2H_6 in the furnace beam inlet system shown in Figure 1 failed to produce evidence of free BH_3 either by appearance potential lowering or by a significant change in the $BH_3^+/B_2H_5^+$ ratio. The reasons for this failure became clear after later pyrolysis experiments in the fast reaction chamber of the ion source header were performed using the apparatus shown in Figure 3 and after a study of the variation of sensitivity as a function of distance from the electron beam was conducted by Malone⁵³. First of all, it became apparent that any BH_3 that may have been produced was being lost by decomposition or recombination during passage through the beam collimating metal foils. In addition, a decrease in sensitivity by a factor of 200 for an unstable species with the furnace exit positioned 3 centimeters from the edge of the electron beam was indicated by Malone's calculations. These calculations were, incidentally, verified experimentally. Considering the fact that the eventual maximum output of the mass spectrometer electrometer due to BH_3 was 5 millimicroamp (at an electron energy low enough to prevent interference of BH_3 from B_2H_6 by fragmentation), such a decrease in sensitivity would fall in the region of minimum detectable output of the electron multiplier and electrometer system. Had the mole fraction of

BH_3 in the effluent gas been on the order of 0.1 or greater, as indicated by free energy considerations at temperatures of approximately 1000°C , the observation of BH_3 by means of the furnace beam inlet system may well have been successful. However, as discussed later, the decomposition of both the B_2H_6 and the pyrolysis products at approximately 350° to 400°C limited the maximum BH_3 production.

Hot Filament Pyrolysis

The failure of the furnace beam inlet system to produce BH_3 led to pyrolysis experiments in the fast reaction chamber of the ion source header in order to decrease the distance between the electron beam and the region of pyrolysis. In this series of experiments and later preliminary experiments with the tubular coaxial furnaces, the orifices in the fast reaction chamber and the backing plate had not been enlarged and were the standard 0.032 inch as supplied by Bendix. This was not thought to be of any concern because molecular flow would be expected at the temperatures and pressures involved and, most convincingly, previous work by Martin⁵² had resulted in the production and observation of CF_2 after the pyrolysis products had effused through the 0.032 inch hole in the fast reaction chamber.

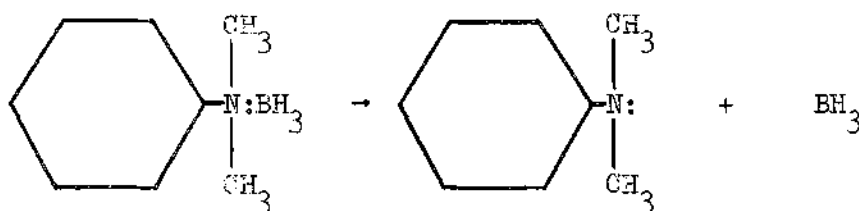
The pyrolysis of B_2H_6 on filaments of platinum, nichrome, and tungsten failed to indicate the presence of BH_3 by appearance potential lowering. However, a change in the $\text{BH}_3^+/\text{B}_2\text{H}_5^+$ ratio was noted in these experiments. For example, the pyrolysis of B_2H_6 on a nichrome filament at temperatures of 900° to 1000°C and pressures of 10^{-4} to 10^{-3} mm Hg in the fast reaction chamber produced a $\text{BH}_3^+/\text{B}_2\text{H}_5^+$ ratio of 1.5×10^{-3} . This ratio at room temperature was half as great. This was not a signifi-

cant change and could be attributed to the variation in the mass spectrum of parent compounds with temperature⁵². If the increase was actually due to BH_3 , it was too small to be detected by the appearance potential lowering method.

Coaxial Furnace Inlet System

The results of the pyrolysis of B_2H_6 before enlargement of the orifices between the furnace exit and the electron beam in the ion source header were essentially identical to those just described. That is, there was no evidence of BH_3 from appearance potential lowering even though the $\text{BH}_3^+/\text{B}_2\text{H}_5^+$ ratio was seen to increase with temperature. In view of the fact that BH_3 was observed with the furnace exit in essentially the same position, approximately 1/4 inch from the electron beam, after the orifices were enlarged, it became clear that the relatively few wall collisions suffered by the BH_3 molecules in passing through the 0.032 inch holes were sufficient to cause decomposition or recombination, probably the former.

The pyrolysis of dimethylanilineborane, again before enlargement of the orifices in the fast reaction chamber and the backing plate, produced no BH_3 as would be expected from the previous discussions. The pyrolysis was expected to occur according to



When an increase in the $m/e = 14$ peak was observed at a pyrolysis temperature of approximately 400°C , it was at first believed to be resulting from BH_3 . However, during a subsequent pyrolysis of dimethylaniline, the identical effect was observed. The conclusion was that CH_2^+ was causing the increase in the $m/e = 14$ peak.

The pyrolysis of dimethylanilineborane was not carried out after the orifice modifications. However, its instability with temperature increase should prove dimethylanilineborane to be a suitable compound for the production and study of the BH_3 molecule. This became apparent when B_2H_6 was observed as a result of heating the dimethylanilineborane sample to 35°C in order to increase its vapor pressure for greater flow rates into the pyrolysis furnace.

rf Discharge Experiments

The rf discharge of B_2H_6 with and without a carrier of argon or hydrogen did not result in the observation of BH_3 . The discharge experiments were performed both before and after the orifice enlargements. The reasons for the failure to observe BH_3 in the former case have been made obvious. The inability of the BH_3 molecule to survive a travel of 12 inches in the quartz discharge tube from the discharge region to the electron beam was made clear in the cryogenic quenching experiments. This, of course, presupposes that BH_3 was actually produced in the discharge. It is very likely that the rf discharge is so energetic as to cause decomposition into boron and hydrogen rather than forming BH_3 .

A discharge of air and argon generated NO and N_2O along with N and O atoms which could be observed by the mass spectrometer. However, even the stable products NO and N_2O were produced in such relatively small

quantities that the possibility of observation of BH_3 by rf discharge appeared even less likely.

An obvious improvement on this experiment would be to position the discharge tube so that the products would be exhausted immediately into the electron beam. However, the problem of noise with the discharge tube in the coaxial position has been mentioned. A perpendicular arrangement, similar to that of the cryogenic inlet system, might lessen this problem since externally produced ions would enter perpendicularly to the mass spectrometer drift tube. This would mean less coaxial drift between the occurrence of ion pulses, which is the source of the noise. Another difficulty is introduced, though, in that the very strong magnetic field of the rf discharge coil would have a very pronounced effect on the electron beam. Whether or not this could be compensated for by means of a calibrating gas, as was done with the coaxial pyrolysis furnace, is a matter of conjecture.

Pyrolysis Studies of BH_3 and BH_2

BH_3 was first observed in pyrolysis experiments with the hot filament arrangement on the extension piece of the cryogenic inlet system described by Malone⁵³. BH_3 was synthesized upon pyrolysis of B_2H_6 by every filament listed in Chapter II. No quantitative analysis was made of the relative amounts of BH_3 produced due to the high noise levels created by the filaments in the temperature range of the pyrolysis, i.e., 700°-900°C. Also, the amount of BH_3 was relatively small compared to the tubular furnace pyrolysis experiments because of smaller heating surface area and also due to the lack of orientation of flow into the electron beam after

contact with the hot metal filament. However, by studying the mass spectra of the pyrolysis products displayed on the oscilloscope, it appeared that the quantity of BH_3 produced did not depend on the type of filament used, thus indicating no catalytic effect in the dissociation of B_2H_6 into BH_3 fragments.

The pyrolysis of B_2H_6 for the synthesis of BH_3 was also conducted by means of the tubular alumina furnace attachment to the cryogenic inlet system again described by Malone⁵³. A few preliminary appearance potential measurements were made. However, due to the difficulty in removing and reinstalling the cryogenic inlet system when furnaces of different materials and dimensions were desired, future pyrolysis experiments were carried out in the coaxial furnace arrangement shown in Figure 3. It was at this time that the 0.032 inch orifices in the fast reaction chamber and the backing plate were enlarged to 1/4 inch. The difference in sensitivity between the coaxial and the perpendicular arrangement was of some concern, but little change was subsequently found. This was also later indicated by Malone's^{53,54} calculations.

The quantity of BH_3 produced under particular conditions of temperature and pressure was found to be independent of the furnace material. The BH_3 signal rose in intensity with temperature, beginning at approximately 200°C, leveled out at about 400°C, and decreased at higher temperatures, the rate of decomposition into the elements becoming predominate. This temperature of maximum concentration at a particular pressure naturally varied with the furnace dimensions. For example, a 1.9 millimeter ID furnace required a temperature of approximately 390°C for maximum BH_3 production, whereas a temperature of 320°C for a 1.0 millimeter ID furnace re-

sulted in the maximum concentration.

No attempt was made to measure the relative peak heights of the BH_x and the B_2H_x species in order to estimate the concentration of BH_3 at the conditions of maximum BH_3 signal output. This was because the intensities of the B_2H_x peaks were so large that the blanking circuit was required for their elimination. If the blanking circuit were not in operation, the multiplier was essentially at its saturation level, at which stage the output readings became erroneous.

Essentially no higher boron hydrides were formed in these experiments even at furnace pressures as high as 10^{-2} mm Hg (the calculation of the pressure in the pyrolysis region is given in Appendix H). An exception was the 1/8 inch stainless steel furnace packed with four monel tubes with a total heated length of 1 inch. The deposition of boron eventually caused this furnace to plug. Shortly before this occurred, the formation of B_4H_{10} , B_5H_{11} , and possibly higher boron hydrides was observed. The gradual build-up of boron necessitated a higher and higher upstream pressure in order to maintain a constant flow through the furnace. Naturally, this resulted in higher pressures in the pyrolysis region and therefore sufficient numbers of intermolecular collisions for formation of higher boranes. Baylis⁴⁰, et al., in their study of triborane and tetraborane intermediates in the pyrolysis of diborane, began to detect higher boron hydrides at 250°C and 4×10^{-3} mm Hg in a baffled furnace. The use of a baffled furnace would explain product formation at the slightly lower pressure because of increased contact time. The importance of these observations is seen later in discussions of the BH_2 molecule.

The reported detection of the BH_2 molecule in the pyrolysis of

B_2H_6 by Fehlner and Koski^{39,41}, prompted a search for its presence, along with BH_3 , in these experiments. In an attempt to reproduce Fehlner and Koski's experimental conditions as closely as possible, B_2H_6 was pyrolyzed in a coaxial, 1 millimeter ID quartz furnace with a heated length of 1 inch. A 0.0001 inch diameter platinum: platinum-rhodium (90-10) thermocouple was not positioned in the gas stream in the pyrolysis region although such an arrangement was used by Fehlner and Koski⁴¹. The pressure was varied from at least 10^{-4} to 10^{-2} mmHg and the temperature range was 250° to $430^\circ C$. Since BH_2 was supposedly observed at a pressure of 5×10^{-4} mm Hg and $270^\circ C$ in a quartz furnace of similar dimensions, these conditions were certainly covered. However, at no time did there appear to be evidence for the existence of this free radical. During these experiments, the ratio of m/e ion peaks 13 and 14 underwent no change that could not be attributed to temperature effects. Crude appearance potential measurements showed only the presence of free $B^{10}H_3$ and $B^{11}H_3$. The backing plate, the 1/4 inch opening in which had been covered with metal gauze, was removed for these experiments because of the reported loss of BH_2 due to the presence of materials other than quartz⁴¹.

Energetics of the $BH_3 - B_2H_6$ System

Appearance Potential Data

The appearance potential data for the $BH_3 - B_2H_6$ system are presented in Table 1. All values were determined by means of the semi-log matching method⁶¹ with exception of the ionization potential of BH_3 which was also determined by the RPD method^{51,52,64}. Representative ionization efficiency curves shown in Figures 7 and 8 demonstrate the semi-log matching

Table 1. Appearance Potentials of Fragment Ions from BH_3 and B_2H_6

Fragment Ion	Appearance Potential from Parent in ev (This Work) ^c		Appearance Potential from Parent in ev (Literature)		
	BH_3	B_2H_6	BH_3	B_2H_6	
B^{10+}	15.83 ^a	18.39 ± 0.02		18.7 ± 0.1^d	19.5 ± 0.2^e
B^{10}H^+	13.66 ± 0.02^b	16.39 ± 0.3		14.9 ± 0.1	16.6 ± 0.2
$\text{B}^{10}\text{H}_2^+$	12.95 ± 0.05	15.5 ± 0.05		13.4 ± 0.1	13.5 ± 0.5
$\text{B}^{11}\text{H}_3^+$	12.32 ± 0.1	14.88 ± 0.05	11.4 ± 0.2^f	13.1 ± 0.2^g	12.1 ± 0.2^g
$\text{B}^{11}\text{H}_2^+$		11.84 ± 0.1		11.9 ± 0.2	11.3 ± 0.5
$\text{B}^{10}\text{H}_6^+$				11.9 ± 0.1	12.1 ± 0.2
$\text{B}^{10}\text{H}_5^+$				11.9 ± 0.1	12.0 ± 0.3

a. Calculated as $(18.39 - 2.56)\text{ev}$. See Appendix C.

b. Error represents maximum deviation from average of experimental values.

c. Average of experimental values.

d. Values in column from Reference 62.

e. Values in column from Reference 63.

f. Values in column from Reference 39.

g. Fragment ion is $\text{B}^{10}\text{H}_3^+$.

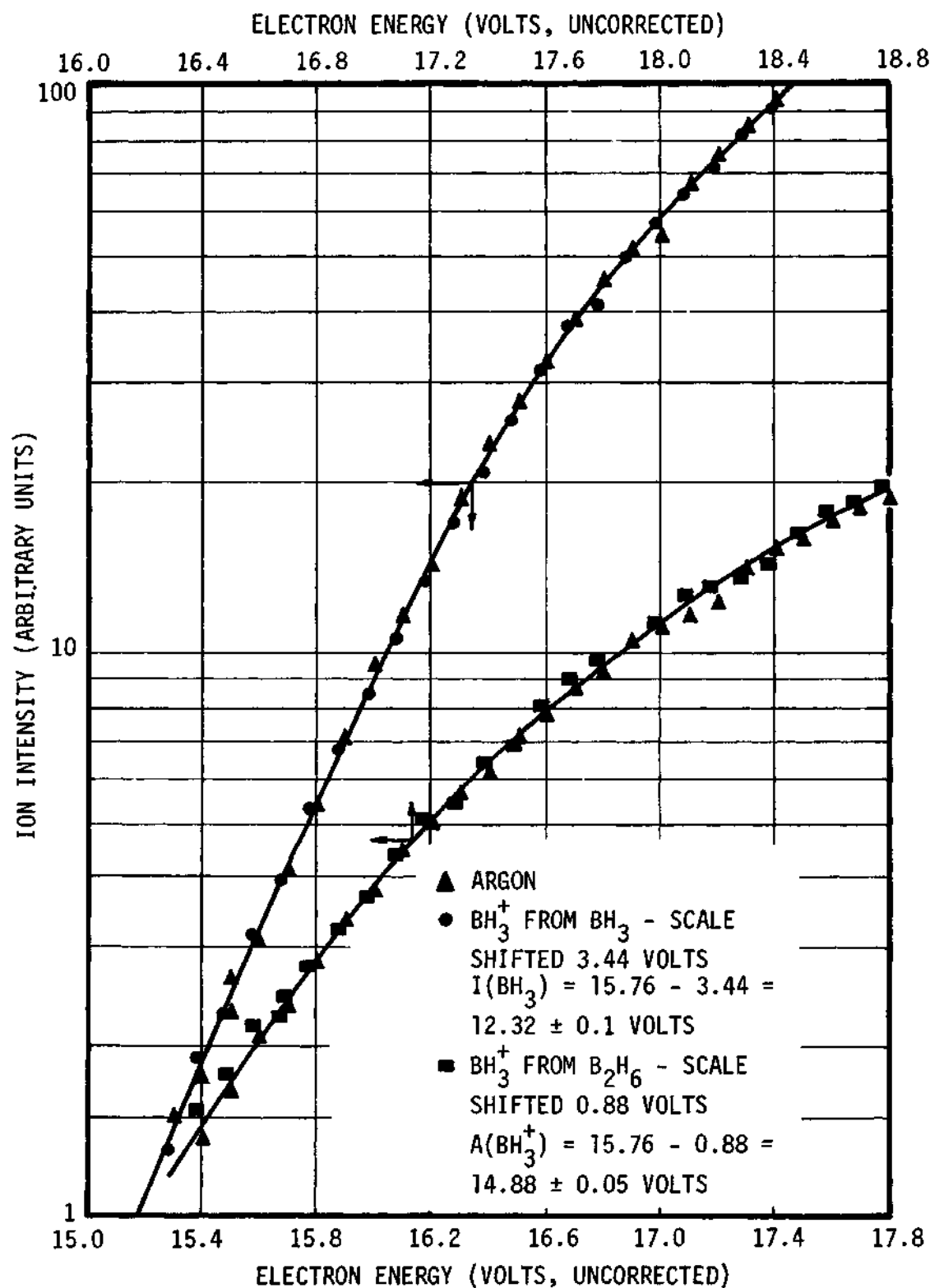


Figure 7. Ionization Efficiency Data for $I(\text{BH}_3)$ and $A(\text{BH}_3^+)$ from B_2H_6 Using the Semi-Log Matoning Method.

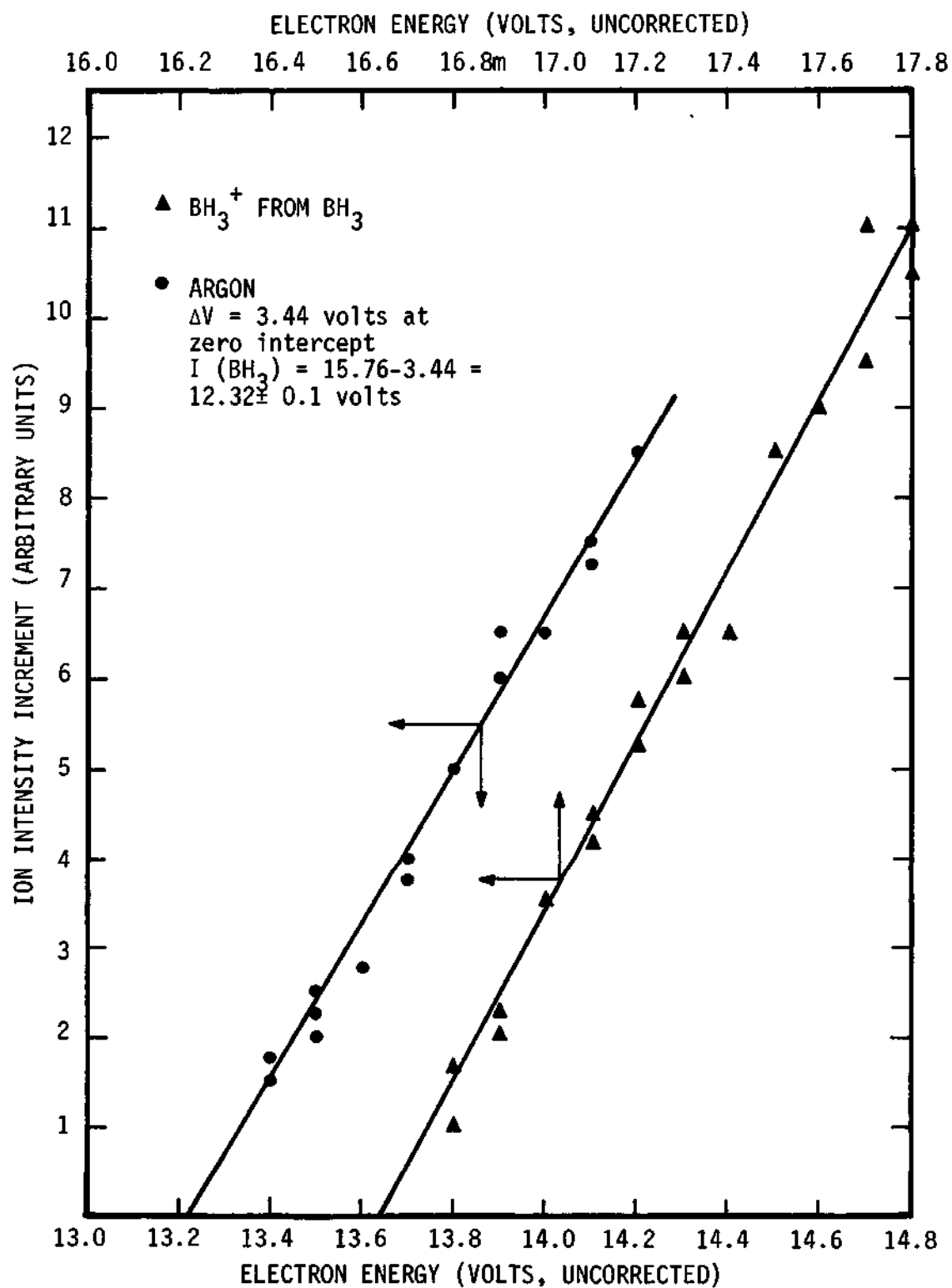


Figure 8. Ionization Efficiency Data for $\text{I}(\text{BH}_3)$ Using the Retarding Potential Difference Method.

method for $I(\text{BH}_3)$ and $A(\text{BH}_3^+)$ from B_2H_6 and the RPD method for $I(\text{BH}_3)$ respectively. Appendix I presents the ionization efficiency curves for the remaining experimental appearance potentials and also for $I(\text{N}_2)$, used to verify the semi-log matching method.

Appearance potentials of the indicated fragments were determined to avoid interference from other species. For example, if the appearance potential of B^{11}H^+ were determined, interference from $\text{B}^{10}\text{H}_2^+$ would be expected since it appears at a lower value than B^{11}H^+ . However, by performing the measurement on B^{10}H^+ , interference is avoided since $A(\text{B}^{11}\text{H}^+)$ is considerably higher than $A(\text{B}^{10}\text{H}^+)$. On the other hand, even though $A(\text{B}^{11}\text{H}^+)$ is only slightly greater than $A(\text{B}^{10}\text{H}_2^+)$, the cracking pattern of both B_2H_6 and BH_3 is such that the ratio $\text{B}^{11}\text{H}/\text{B}^{10}\text{H}_2$ is approximately 1/20 at low electron energies, thereby eliminating interference of B^{11}H^+ with $\text{B}^{10}\text{H}_2^+$. The value of $A(\text{B}^{10}\text{H}^+)$ from BH_3 could not be determined because of the lack of sufficient ion intensity. In attempts to measure this quantity, it was found that $A(\text{B}^{10}\text{H}^+)$ from B_2H_6 was lowered upon pyrolysis, indicating the presence of B^+ from BH_3 . However, the value obtained was much higher than was to be expected for $A(\text{B}^{10}\text{H}^+)$ from BH_3 and it was subsequently found that B^+ from B_2H_6 was the major contributor to the observed signal. The value of $A(\text{B}^{10}\text{H}^+)$ from B_2H_6 is thought to be accurate to within only ± 0.3 ev. This is due to the interference of noise that permitted only the top third or less of the ionization efficiency curve to be utilized for matching with argon. The nature of the interference was such that at the lower electron energies the noise became more and more the major contributor to the ion signal.

Derived Ionization Potentials, Bond Energies, and Thermodynamic Values

The bond energies and ionization potentials derived from the preceding experimental appearance potentials, in addition to available literature values, are given in Table 2. Table 3 presents the thermodynamic values that have been calculated by utilizing the derived bond energies. Several of these values are important in arguments to be presented later. All calculation procedures, including any assumptions and additional data that may have been necessary, are described in detail in Appendices C and D.

Discussion of Experimental Measurements and Derived Data

Much confidence is placed in the experimentally determined appearance potentials even though considerable disagreement exists between these values and the values from the literature. First of all, the experimental values appear to be self-consistent in that for all fragment ions considered (with the exception of B^{10+} which has been previously discussed), the difference in the appearance potentials of a certain fragment from BH_3 and from B_2H_6 is essentially equal to 2.56 ev (to see that this condition should hold, refer to Appendix C). The slight deviation due to $B^{10+}H$ has already been explained. Also very significant, indeed, is the extremely good agreement of $D(B^+ - H)$, as calculated directly from the experimental appearance potentials, with the spectroscopic results of Bauer, Herzberg, and Johns⁶⁷. $D(BH^+ - H)$ and $D(BH_2^+ - H)$ agree quite well with values obtained from isoelectronic curves prepared by Price, Passmore, and Roessler⁶⁸. In contrast, the values for the three ion dissociation energies as calculated from other appearance potential studies^{62,63} not only disagree with the just mentioned sources but with one another. Several of these values appear to be quite unreasonable. For example, a

Table 2. Bond Energies and Ionization Potentials
Calculated or Estimated from Appearance
Potential Measurements

Bond Energy or Ionization Potential	Energy, ev		
	This Research	Literature	
		Experimental	Calculated or Estimated
D(B - H)	3.64	$< 3.51^{67}$	$3.39^{65}, 3.40^{66}$
D(BH - H)	4.83		4.7^{68}
D(BH ₂ - H)	3.58	3.2^{39}	3.2^{68}
D(B ⁺ - H)	2.17	$< 2.04^{67}$	3.0^{68}
D(EH ⁺ - H)	5.23		5.2^{68}
D(BH ₂ ⁺ + H)	0.63		0.9^{68}
D(BH ₃ - BH ₃)	2.56	$1.7^{39}, > 2.39^{38}$	$1.23^{33}, 1.61^{41}$ $2.25^{16}, < 1.66^{35}$
D(BH ₃ ⁺ - BH ₃)	$< 3.67; > 3.04$		
I(B ₂ H ₆)	$< 11.84; > 11.21$	$11.9^{62}, 12.1^{63}$	
I(BH ₂)	9.37	9.8^{39}	8.2^{68}
I(B ₂ H ₅)	> 8.26		7.86^{62}

Table 3. Thermodynamic Data Derived from Experimental Bond Energies

Thermodynamic Quantity of Interest	Calculated Value (kcal/mole or mm Hg)	Literature Value (kcal/mole or mm Hg)
ΔH_f° of B_2H_6 at 298°K	- 40.9	7.53 ^{69,70} , 6.73 ⁷¹ 5.8 ⁷²
ΔG_f° of B_2H_6 at 298°K	- 28.7	19.78 ⁵⁵
partial pressure of $BH_3^{a,b}$	1.4×10^{-7}	
partial pressure of BH_3^c	3.1×10^{-3}	5.5×10^{-4} ⁷³ (473°K)
partial pressure of $BH_2^{b,d}$	3.6×10^{-9}	
partial pressure of $BH_2^{b,e}$	4.9×10^{-7}	
partial pressure of $BH_2^{c,e}$	4.2×10^{-4}	

^a All equilibrium values correspond to a total B_2H_6 pressure of 10^{-2} mm Hg and a temperature of 600°K.

^b Calculated using $D(BH_3 - BH_3) = 59$ kcal/mole from this work.

^c Calculated using $D(BH_3 - BH_3) = 35$ kcal/mole from the literature^{35,41}.

^d Calculated using $D(BH_2 - H) = 3.58$ ev from this work.

^e Calculated using $D(BH_2 - H) = 3.2$ ev which represents a correction to the value from this work as seen from the comparison made in the text of the heats of formation of B_2H_6 .

value of 7.62 ev for $D(BH^+ - H)$ is calculated from the data of one report⁶³. This is well over 2 ev greater than any other estimate or measurement of $D(BH^+ - H)$. Finally, the reproducibility of the measurements, the verification of the semi-log matching method by measurements of known ionization potentials ($I(N_2)$ is shown in Appendix I), and the agreement of $I(BH_3)$ as determined by both the semi-log matching method and the RPD method lend strong support to the accuracy of the experimental numbers.

Of the derived bond energies and ionization potentials in Table 2, only the values of $D(B - H)$, $D(BH - H)$, $D(BH_2 - H)$, and $I(BH_2)$ required introduction of an experimentally determined quantity from other sources, excluding of course the well known values of $I(B)$ and $D(H - H)$. The introduction of $I(BH) = 9.77$ ev, as given by Bauer, et al.,⁶⁷ permits these calculations but automatically fixes $D(B - H) - D(B^+ - H) = 1.47$ ev and vice versa, as shown in Appendix C. Obviously, as a result of this assumption $D(B - H)$ and $D(B^+ - H)$ exhibit the same apparent agreement with Bauer, et al.⁶⁷.

The value of $D(BH - H)$, and consequently $D(BH_2 - H)$, depended upon the estimation of the polarization stability acquired by $BH^+ - H$ relative to the neutral BH_2 ⁶⁸. A similar effect is observed in the case of B_2H_6 which is discussed below. $I(BH_2)$ then is automatically fixed since, as shown in Appendix C, $I(BH_2) = I(BH) - [D(BH^+ - H) - D(BH - H)]$. If we accept the estimate of 8.2 ev for $I(BH_2)$ ⁶⁸ from isoelectronic curves with the explanation that this is to be associated with the fact that a non-bonding π electron is removed (8.3 ev in $B, {}^2P_{1/2}$), this sets $D(BH^+ - H) - D(BH - H) = 1.57$ ev, assuming $I(BH) = 9.77$ ev⁶⁷. The resulting values of $D(BH - H) = 3.66$ ev and $D(BH_2 - H) = 4.75$ ev are accordingly inconsistent

with the general order of bond strengths of hybrid bonds as a result of the amount of overlapping, i.e., $sp^3 < sp^2 < sp$.⁷⁴ In addition, an increase of 1.57 ev due to polarization stability appears rather excessive. The estimated value of $I(BH_2) = 9.4$ ev in Table 2 seems more reasonable if we consider that the electron removed in ionization came from a lower lying orbital than the $p\pi$ orbital. This would correspond to BH in which the ionization may be described as that of the unbonded $sp\sigma$ electron produced in the promotion which results in two oppositely directed $sp\sigma$ orbitals⁶⁸. The difference in ionization potentials of BH and BH_2 would then be the result of several factors, the nature of which and the amount of whose influence would be difficult to evaluate. But one might guess, for example, that the electronic repulsion in the BH_2 molecule could be slightly greater than in BH, consequently leading to a lower ionization potential of BH_2 than BH.

In contrast to the polarization stability acquired by $BH^+ - H$, $D(B^+ - H)$ is less than $D(B - H)$ by 1.47 ev⁶⁷. This could possibly be explained by a considerable loss of electron shielding between the nuclei in the BH^+ ion, whose repulsion would then be a greater factor than the acquisition of polarization stability. In the case of BH_2 , the shielding would probably not be as important since the electron removed upon ionization would have been involved in shielding between two pair of nuclei instead of one.

The determination of the value of $D(BH_3^+ - BH_3)$ is ascribed to the following line of reasoning. $A(B_2H_5^+)$ from B_2H_6 can be written $A(B_2H_5^+) = I(B_2H_6) + D(B_2H_5^+ - H)$. Since $D(BH_2^+ - H) = 0.63$ ev and the bonding of the terminal hydrogens in B_2H_6 is sp^3 as compared with sp^2 in BH_3 , we would

expect $D(B_2H_5^+ - H) < 0.63$ ev and therefore 11.84 ev $> I(B_2H_6) > 11.21$ ev. Since $A(BH_3^+)$ from B_2H_6 may also be written as $A(BH_3^+) = I(B_2H_6) + D(BH_3^+ - BH_3) < 11.84$ ev $+ D(BH_3^+ - BH_3)$, it follows that $D(BH_3^+ - BH_3) > 14.88$ ev $- 11.84$ ev $= 3.04$ ev. By similar reasoning, $D(BH_3^+ - BH_3) < 3.67$ ev. The strength of the $BH_3^+ - BH_3$ bond is verified by the abundance of $B_2H_5^+$ in the mass spectrum of B_2H_6 , the lack of B_2H_6 being due to the weak $B_2H_5^+ - H$ bond. These results are evidence that ionization in B_2H_6 is occurring by removal of an electron involved in terminal B - H bonding. This is in agreement with a theoretical study of the B_2H_6 molecule by Burnelle and Kaufman⁷⁵. Here, it was found that ionization should occur from a B - B antibonding orbital which contributed strongly to the terminal B - H bond overlap population. If we now take the results of Fehlnner and Koski³⁹ and Koski, et al.,⁶² we find that $D(BH_3^+ - BH_3) = 13.1$ ev $- 11.9$ ev $= 1.2$ ev, as compared with their result of $D(BH_3 - BH_3) = 1.7$ ev. This would appear to indicate that ionization of B_2H_6 was occurring by removal of a bridge electron. This strength of the $BH_3^+ - BH_3$ bond, the terminal B - H bonds supposedly being relatively unaffected, would imply that a considerable $B_2H_6^+$ ion intensity should be observed in the mass spectrum of B_2H_6 , which is certainly not the case.

If we again assume that the general order of the strength of hybrid bonds is $sp^3 < sp^2 < sp$, then $D(B_2H_5 - H) < D(BH_2 - H) = 3.58$ ev. Therefore, $I(B_2H_5) > 11.84$ ev $- 3.58$ ev $= 8.26$ ev, as seen in Appendix C. This is to be expected if we consider ionization to be occurring from the lone non-bonding electron of B_2H_5 that would result from the removal of a neutral terminal hydrogen atom from B_2H_6 . This electron, in a sp^3 non-bonding orbital, would require approximately the same energy for removal

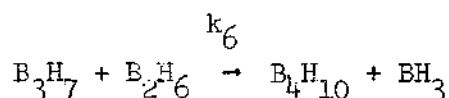
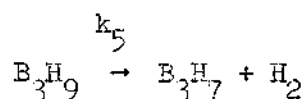
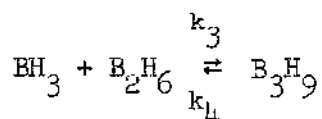
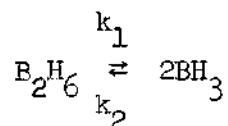
as does the electron in the 2p orbital of boron (8.3 ev).

$I(B_2H_6)$ was estimated to lie between 11.84 and 11.21 ev. The literature values in Table 2 are seen to be slightly higher. The presence of nitrogen prevented the direct measurement of $I(B_2H_6)$. An isotopically enriched $B_2^{10}H_6$ sample would obviously solve this problem.

The widely varying results of the measurement of $D(BH_3 - BH_3)$ have been mentioned in Chapter I, the range of values given in Table 2. This work agrees with only two of the reported values. Sinke, *et al.*,³⁸ reported $D(BH_3 - BH_3) \geq 55 \pm 8$ kcal/mole in a mass spectrometric study of the equilibrium between BH_3 and B_2H_6 . Maximum values for temperatures between 775° and 925°K increased systematically from 61.9 to 67.4 kcal/mole. If we assume that in all cases studied herein, the transitions occurring upon electron impact are between the ground vibrational, electronic, and rotational levels with all resulting fragments at zero kinetic energy (usually a good assumption for positive ions resulting from the rupture of single bonds⁷⁶), then all bond energies correspond to the standard change in enthalpy at 0°K. The assumption of no excess energy also implies no activation energy is required for the decomposition⁷⁶. Therefore, correcting $D(BH_3 - BH_3)$ as shown in Appendix D to 775° and 925°K, values of 60.6 and 60.2 kcal/mole are obtained.

This work also agrees with a value of 52 kcal/mole for $D(BH_3 - BH_3)$ determined by Clarke and Pease¹⁶ in a kinetic study of the pyrolysis of B_2H_6 . This value was obtained from the relation of the experimental activation energy to $1/2 \Delta H$ of the reaction $B_2H_6 \rightarrow 2BH_3$. This is seen from a comparison of the experimental rate equation to the rate equation fitting a postulated mechanism of the pyrolysis. Interestingly though,

three other kinetic studies^{15,17,18} of the pyrolysis of diborane revealed the same order of reaction and experimental activation energy, 25.5 to 29 kcal/mole, but produced essentially identical rate constants which disagreed with Clarke and Pease. Although Bauer³⁴ deduced $D(\text{BH}_3 - \text{BH}_3) < 38$ kcal/mole from these kinetic studies using a somewhat different method, no other attempt was made to relate the experimental activation energies to $D(\text{BH}_3 - \text{BH}_3)$. Consequently, based upon the available literature on the pyrolysis of B_2H_6 and to some extent upon the work of this thesis, this author has selected what appears to be the most reasonable mechanism for the initial steps in the pyrolysis of B_2H_6 , determined the rate equation, and related the experimentally determined activation energies to $D(\text{BH}_3 - \text{BH}_3)$. The mechanism is as follows:



The procedure is described in Appendix E and most of the results are presented later in this chapter. As before, $D(\text{BH}_3 - \text{BH}_3)$ was found to be

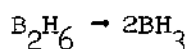
equal to twice the value of the experimental activation energy. Therefore, $D(\text{BH}_3 - \text{BH}_3) = 51$ to 58 kcal/mole from the concurring data of three independent kinetic studies as developed in this thesis work.

The standard heats and free energies of formation presented in Table 3 are seen to differ considerably from the reported literature values. Especially interesting is the agreement between two separate sources^{69,70} on ΔH_f° of B_2H_6 as 7.53 kcal/mole, since this would lead one to seriously question the values determined in this work. However, an investigation of the method of calculation of ΔH_f° of B_2H_6 as described in Appendix D clarifies this situation.

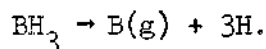
ΔH_f° of B_2H_6 is seen to be equal to

$$2\Delta H_s^\circ(\text{B}) + 6\Delta H_f^\circ(\text{H}) - \Delta H_r^\circ(1) - 2\Delta H_r^\circ(2)$$

where $\Delta H_r^\circ(1)$ and $\Delta H_r^\circ(2)$ are experimental values from this research and $\Delta H_r^\circ(1)$ refers to

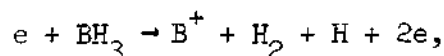


and $\Delta H_r^\circ(2)$ is the heat of atomization of BH_3 : i.e., the enthalpy change of the process

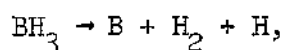


If we assume that 7.53 kcal/mole is correct for ΔH_f° of B_2H_6 , which is believed to be the case, and that $\Delta H_s^\circ(\text{B})$ and $\Delta H_f^\circ(\text{H})$ are accurately known quantities ($\Delta H_s^\circ(\text{B})$ is discussed in Appendix D), then the sum $\Delta H_r^\circ(1) + 2\Delta H_r^\circ(2)$ is too great by 48.4 kcal/mole. If the recombination of the very

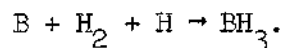
reactive BH_3 molecules is similar to the recombination of free radicals, in that these reactions have negligible activation energies^{77,78}, then $\Delta H_r^\circ(1)$ would be an accurate number, which again is thought to be so, and $\Delta H_r^\circ(2)$ is therefore in error by 24.2 kcal/mole. This implies an average error of approximately 8 kcal/mole or 0.35 ev in the derived bond energies of BH , BH_2 , and BH_3 . A minimum error of 0.13 ev or 3 kcal/mole in $D(\text{B} - \text{H})$ is immediately evident by comparing the experimental value of 3.64 ev to $D(\text{B} - \text{H}) < 3.51$ ev from the spectroscopic results of Bauer, *et al*⁶⁷. Recalling that any excess energy required for decomposition, such as an activation energy, must be imparted to the molecule-ion by the impacting electron⁷⁶, the error in the bond energies may be attributed to the experimental value of $A(\text{B}^+)$ from BH_3 (Appendix C demonstrates that the sum $D(\text{B} - \text{H}) + D(\text{BH} - \text{H}) + D(\text{BH}_2 - \text{H})$ may be calculated from this appearance potential). That is, since $A(\text{B}^+)$ from BH_3 is represented by the process



the experimental appearance potential must be equal to the activation energy of



because of the reasons just discussed, plus the ionization potential of boron. Now the activation energy of the above equation is essentially equal to $D(\text{B} - \text{H}) + D(\text{BH} - \text{H}) + D(\text{BH}_2 - \text{H}) - D(\text{H} - \text{H}) + E'$ where E' is the activation energy of the reverse process



A value of 24.2 kcal/mole for E' is quite reasonable and it is this activation energy that results in a value of $A(B^+)$ from BH_3 which subsequently leads to the calculation of erroneous bond energies from the appearance potential data.

It is interesting to note that applying these "corrections" to the experimental values, along with a lower estimate of the gain of polarization stability of $BH^+ - H$, would lead to bond energies of $B - H$, $BH - H$, and $BH_2 - H$ which almost coincide with the results of Price, et al⁶⁸. Thus, we have an example where what appear to be rather small errors arising from electron impact measurements result in significant disagreements when the experimental numbers are used in certain calculations.

The calculated equilibrium partial pressures of BH_2 and BH_3 that would be produced by the dissociation of B_2H_6 are also shown in Table 3. Since the value of $D(BH_3 - BH_3)$ is believed to be fairly accurate, the equilibrium constant for the formation of BH_3 , and consequently the value of its partial pressure, is considered more reliable than that for the formation of BH_2 . The uncertainty of the latter lies in the possible error of $D(BH_2 - H)$ which has been brought forth in the comparison of calculated and experimental heats of formation of B_2H_6 . Consequently, two calculations of the partial pressure of BH_2 were made involving the experimental value of $D(BH_2 - H)$ and also a corrected value of this bond energy. The partial pressures of BH_3 and BH_2 were again calculated, but with the assumption that $D(BH_3 - BH_3) = 35$ kcal/mole in agreement with earlier estimations of this bond energy as discussed in Chapter I. With the exception of the partial pressure calculated for $D(BH_2 - H) = 3.58$ ev,

all other values in Table 3 indicate that the dissociation of B_2H_6 should produce approximately equal amounts of BH_3 and BH_2 at equilibrium. Calculations were not made for the dissociation of B_2H_6 into BH_2 and BH_4 which has been assumed to be the first step in the formation of BH_2 ^{39,42}. If BH_4 is actually involved, it would dissociate immediately into BH_2 and H_2 because of its probable high degree of instability.

The preceding determination of equilibrium partial pressures and heats and free energies of formation required the introduction of calculated entropy and $(H^\circ - H_{298}^\circ)$ values as given in the JANAF thermodynamic tables⁵⁵. Since the $(H^\circ - H_{298}^\circ)$ values resulted in additions of only 2 or 3 kcal/mole to bond energies on the order of 60 kcal/mole, any errors present in these enthalpy functions would be of no concern. However, the TS term in the free energy is a significant quantity and therefore the accuracy of the calculated entropy values becomes of importance. Although the structural and spectroscopic parameters used in the calculation of the ideal gas entropy are only estimates, Shepp and Bauer⁸⁶, who calculated entropies for the $B_2H_6 - BH_3$ system, state that the values should be accurate to half an entropy unit or better because of the slight dependence of the entropy on the estimated frequencies and on the logarithm of the products of the estimated moments of inertia. The estimated parameters are those of BH_2 and BH_3 since the values for B_2H_6 have been experimentally determined.

Kinetic Considerations

The failure to observe BH_2 in this work as described previously, even though its observation had been reported under almost identical ex-

perimental conditions³⁹ and thermodynamic considerations, as discussed in the preceding section, indicated that the formation of BH_2 from B_2H_6 is as favorable as the formation of BH_3 , led this author to the following consideration of the kinetics of the system. The purpose was to determine whether or not the formation of BH_2 in the pyrolysis of B_2H_6 is as kinetically favorable as BH_3 and also to test further the proposed mechanism for the pyrolysis of diborane which was previously used to determine $D(\text{BH}_3 - \text{BH}_3)$ from reported kinetic studies. The results are presented in Table 4 and the method of calculation and assumptions involved are given in Appendix F.

The ratio of the rate constant for the formation of BH_3 to that of BH_2 ($\text{B}_2\text{H}_6 \rightarrow 2\text{BH}_2 + \text{H}_2$) is seen to be approximately 10^{23} at 600°K for $D(\text{BH}_2 - \text{H}) = 3.58 \text{ ev.}$ (the use of two different bond energies is discussed in Appendix F.) If the reaction $\text{B}_2\text{H}_6 \rightarrow \text{BH}_2 + \text{BH}_4$ had been considered as has been proposed^{39,42}, the ratio would have been even greater. This statement assumes that $D(\text{BH}_3 - \text{H})$ is no greater than 1.32 ev. However, it is to be expected that $D(\text{BH}_3 - \text{H})$ would be less than this value since this would involve a one electron bond between H and the vacant orbital of the BH_3 molecule. (BH_4 is isoelectronic with CH_4^+ for which $D(\text{CH}_3^+ - \text{H}) = 1.3 \text{ ev.}$ ^{68,76}). The frequency factors of the rate constants in the formation of both BH_3 and BH_2 were assumed to be approximately equal. This is of little consequence since it would be necessary for their ratio to be an extremely unlikely number to have a significant effect on the ratio of the rate constants.

Fehlner⁴² postulated a mechanism for the pyrolysis of B_2H_6 which involved both BH_2 and BH_3 as intermediates. By relating the experimental

Table 4. Kinetic Rate Constants for Several Reactions Involved in the Pyrolysis of B_2H_6

Reaction	A	E, kcal/mole
(1) $B_2H_6 \xrightarrow{k_1} 2BH_3$	$4.0 \times 10^{14} \text{ sec}^{-1}$	61
(2) $2BH_3 \xrightarrow{k_2} B_2H_6$	$3.6 \times 10^8 \frac{\text{liter}}{\text{mole sec}}$	≈ 0
(3) $BH_3 + B_2H_6 \xrightarrow{k_3} B_3H_9$	$3.6 \times 10^8 \frac{\text{liter}}{\text{mole sec}}$	≈ 0
(4) $B_2H_6 \xrightarrow{k_4} 2BH_2 + H_2$	assumed equal to A_1	125^a
(5) $B_2H_6 \xrightarrow{k'_4} 2BH_2 + H_2$	assumed equal to A_1	107^b

^a calculated using $D(BH_2 - H) = 3.58 \text{ ev}$ from this work.

^b calculated using $D(BH_2 - H) = 3.2 \text{ ev}$ which represents a reasonable correction to the value from this work as seen from the comparison made in the text of the heats of formation of B_2H_6 .

activation energy^{15,17} to that predicted by the rate equation of the postulated mechanism, Fehlner determined the activation energy, E_{BH_4} , of $\text{B}_2\text{H}_6 \rightarrow \text{BH}_2 + \text{BH}_4$ as 44 kcal/mole. This involved estimating all the individual activation energies in the rate equation, with the exception of E_{BH_4} , from the thermochemical bond energies and by the application of Semenov's rule⁷⁸ and then solving for E_{BH_4} . It is interesting to note that he could have calculated E_{BH_4} directly from the thermochemical data as 111 kcal/mole, assuming $D(\text{BH}_3 - \text{H}) = 0$. To arrive at the value of 44 kcal/mole, $D(\text{BH}_3 - \text{H})$ would have to be estimated as 67 kcal/mole or 2.9 ev, a seemingly impossible number. Fehlner also calculated the frequency factor of this reaction as 10^{18} sec^{-1} . He states that although this is a large value for a unimolecular decomposition, it is not uniquely so and is not an impossible value for this reaction. However, a brief search⁷⁸⁻⁸⁰ uncovered only one example of such a high frequency factor, that being an estimated value of $10^{17.3} \text{ sec}^{-1}$ for $\text{C}_2\text{H}_6 \rightarrow 2\text{CH}_3$.

Fehlner also states that his mechanism accounts for the change to first order of the pyrolysis of B_2H_6 with temperature rise. This was in reference to a shock tube study by Skinner and Snyder³² in the temperature range 600-700°K. The data from this study demonstrated a frequency factor of $10^{10.1} \text{ sec}^{-1}$. Assuming this value applies to the dissociation of B_2H_6 , it appears that this is a quite low value for this reaction. Skinner and Snyder also took the rate constants from work^{15,16,37} showing 3/2 order for the pyrolysis of B_2H_6 at lower temperatures and recalculated the constants as first order rate constants. By plotting the log of the recalculated rate constants against $1/T$ along with the constants from the shock tube study, a straight line was drawn which appeared to fit the points reasonably well. However, as noted previously, the rate constants of

Clark and Pease¹⁶ have been disputed by three other studies^{15,18,19}. If the constants of Clark and Pease are not taken into account, this author does not feel that the remaining points can reasonably be considered as fitting a straight line. It might also be mentioned that an earlier kinetic study¹⁵ indicated that the order of the pyrolysis tended toward second order as the temperature approached 400°K in contrast to the results of Skinner and Snyder.

The frequency factor for k_3 in Table 4 was calculated by relating the experimental frequency factor from the B_2H_6 pyrolysis¹⁵ to that of the rate equation developed in Appendix E. This involved the relationship $\ln A_1/A_2 = \Delta S/R$ ⁸⁰ for which ΔS was calculated from estimated thermodynamic tables⁵⁵. A_3 is seen to be consistent with the frequency factors for bimolecular reactions^{79,80}. A_1 and A_2 were then determined by assuming $A_2 = A_3$ and then solving for A_1 from the previous relationship. A_1 also appears to be a reasonable number as compared with unimolecular frequency factors^{79,80}. E_1 and E_4 followed directly from the experimental bond energies and E_2 and E_3 were assumed to be negligible. The assumption that E_2 is approximately zero has been discussed and it was necessary to set E_3 equal to zero to show agreement between kinetic studies and this thesis for $D(BH_3 - BH_3)$. The latter assumption may be subject to some criticism but it does not appear too unlikely in consideration of the reactivity of the BH_3 molecule and the probability that reaction 3 in Table 4 is exothermic since it occurs with the net formation of one bond.

Summary of BH_2 Results

Although free energy considerations demonstrated that the formation

of BH_2 from B_2H_6 is just as favorable as BH_3 , this experimental work taken by itself would lead one to the conclusion that BH_2 is not present in sufficient quantities under the experimental conditions described herein to permit its detection. Coupled with the kinetic rate constant study, it would also seem fairly obvious that the dissociation of B_2H_6 into BH_2 is not a factor in the pyrolysis of B_2H_6 .

The results of Fehlner and Koski^{39,41}, however, are in direct contradiction to this work. Since the results of this work include strong evidence of an error in Fehlner and Koski's ionization potential value of BH_3 , $I(\text{BH}_3) = 11.4$ ev, one might be tempted to attribute their measurement of the ionization potential of the $m/e = 13$ ion peak, $I(\text{BH}_2) = 9.8$ ev, as being due to B^{10}H_3 . This arises partly from the experimental observation that the vanishing point of a particular ion peak can vary as much as 2 to 3 volts depending upon its intensity, i.e., the higher the intensity the lower the vanishing point. Since the ratio of $m/e = 13$ to $m/e = 14$ is approximately 10 to 1 for both B_2H_6 and BH_3 , an error of 1.6 ev (11.4 ev - 9.8 ev from Fehlner and Koski) would seem entirely possible if the calibration were not correctly performed. It must be pointed out, though, that Fehlner and Koski's value for $I(\text{BH}_2) = 9.8$ ev is in close agreement with that predicted by this study. In fact, as seen previously, if $D(\text{BH}^+ - \text{H}) = D(\text{BH} - \text{H})$, then $I(\text{BH}) = I(\text{BH}_2) = 9.77$ ev.

The matter is further complicated by the reported difference in the recombination effects on BH_3 and BH_2 by argon³⁹, the inhibition of BH_2 formation by Al_2O_3 with no effect upon BH_3 formation⁴¹, and the detection of BH_3 but not BH_2 from BH_3CO pyrolysis⁴¹. This strongly indicates that a $m/e = 13$ ion peak not attributable to B^{10}H_3 was actually observed. How-

ever, considering that in this work and in that of Baylis⁴⁰, et al., higher boron hydrides could not be observed at pressures lower than 4×10^{-3} mm Hg, the detection of a lowering of recombination rate of BH_3 at the pressure of 5×10^{-4} mm Hg as used by Fehlner and Koski³⁹ would appear to be a bit unlikely due to the small number of intermolecular collisions that are seen to be present at this pressure.

This author has no reasonable explanation for the failure to observe BH_2 from the pyrolysis of B_2H_6 in this experimental work, assuming that Fehlner and Koski^{39,41} did in fact accomplish this feat, other than the possibility that the presence of the platinum: platinum-rhodium thermocouple previously mentioned could have catalyzed the formation of BH_2 . This was realized during the composition of this thesis and consequently the experimental setup did not include such a thermocouple in the pyrolysis region. The small heating surface area of the wire as compared to the furnace walls (Fehlner and Koski report two to three times more BH_2 than BH_3) makes such an effect appear unlikely. Their initial publication³⁹ promised a complete report to be forthcoming and further comments must be reserved until it is published or until more clarifying results are obtained in this laboratory.

There are several experiments which, if they had been included in Fehlner and Koski's report, would have further supported their detection of BH_2 or would have shown the $m/e = 13$ peak to arise from another species. For example, if appearance potential measurements on the $m/e = 12$ peak produced a value of 9.8 eV, this would be rather conclusive proof of the detection of free B^{10}H_2 as well as B^{11}H_2 . Also, if a successful attempt had been made to observe free B_2H_5 and B_2H_4 , the mechanism postulated by

Fehner⁴² for the pyrolysis of B_2H_6 , involving B_2H_5 and B_2H_4 due to the formation of BH_2 , would have been strongly supported.

Synthesis and Cryogenic Quenching of BH_3

The quenching experiments with the products of the B_2H_6 pyrolysis produced no evidence that BH_3 had been prepared as a liquid or solid phase at approximately 55°K. In addition to the failure to detect BH_3 upon warm-up of the cryogenic reactor, BH_3 could not be observed during the actual quenching of the pyrolysis products to temperatures of about 55° and 77°K. The apparent decomposition or reaction of the BH_3 molecule in traveling approximately 1-1/2 feet from the furnace exit to the electron beam even though the transfer tube was maintained at these low temperatures is not very encouraging for future quenching experiments with the reactor space maintained at even lower temperatures. No difference was found between the results of experiments conducted both with and without a glass lining in the cryogenic reactor.

Although BH_3 was not detected in these experiments, an increase in the H_2^+ ion peak was observed upon warm-up of the cryogenic reactor. The intensity of the peak reached a maximum at approximately 60°K and decreased at higher temperatures, rising again when the B_2H_6 vapor pressure became significant. This coincided with the results of Bolz, Mauer, and Peiser³⁶ who observed a slight increase in pressure at the time of disappearance of an unidentified phase at 60°K (refer to Chapter I). From all appearances, BH_3 had actually been quenched but had decomposed or reacted either in the condensed state or in the vapor phase upon warm-up with the production of H_2 . However, during a subsequent experiment in

which B_2H_6 and H_2 were quenched at about 55°K without pyrolysis, the same behavior of the H_2^+ ion peak was observed. The conclusion was that H_2 had been trapped in the frozen B_2H_6 matrix and liberated at 60°K.

Synthesis and Cryogenic Quenching of $HB\dot{F}_2$ and H_2BF

H_2BF was not detected in the products of the rf discharge of B_2H_6 and BF_3 . However, evidence was obtained which strongly indicated the presence of $HB\dot{F}_2$. First of all, the m/e ion peaks 31, 48, and 49 appeared slightly below the temperature at which BF_3 could be first detected in blank experiments, i.e., analyses of the undischarged feed gases by quenching them and monitoring the effluent gases upon warm-up. Ion peaks 48 and 49 would be due to both BF_3 and $HB\dot{F}_2$ (mostly $HB\dot{F}_2$ at this temperature) and the 31 peak was attributed to $HB\dot{F}_2^+$ from $HB\dot{F}_2$. This agrees with the reported proximity of the vapor pressures of BF_3 and $HB\dot{F}_2$ ⁴⁶. Secondly, the intensities of m/e ion peaks 31 and 49 were approximately equal, in agreement with a recent mass spectrometric observation of $HB\dot{F}_2$ ⁵⁰. Finally, rough appearance potential measurements gave $A(B^{11}F_2^+)$ as approximately 13 ev. This demonstrated that BF_2^+ was not due to fragmentation from BF_3 since $A(BF_2^+)$ from BF_3 is 16.2 ev⁸¹. It is interesting to note that $A(BF_2^+)$ from $HB\dot{F}_2$ is close to the value of $A(BH_2^+)$ from BH_3 as determined in this work. Also, the $BF_2^+ - H$ bond is extremely weak as evidenced by the undetectable BF_2H^+ ion intensity. This indicates that the values of $I(BH_3)$ and $I(HB\dot{F}_2)$ are similar with the electron being removed upon ionization from the B - H bond in both cases. As in the case of the BH_3 quenching experiments, no difference was noted between the experiments conducted with the cryogenic inlet system glass lined and those carried

out with no glass lining.

In comparison to the large amount of BF_3 evolved with increase in temperature of the cryogenic inlet system, the amount of HBF_2 produced was rather small. The low yield was expected when the discharge of BF_3 was found to be relatively inefficient. This followed from the observation of only a slight build-up of boron in the discharge tube and the detection of only a small decrease in BF_3 intensity when the discharge was ignited using the apparatus shown in Figure 6. Also, even though the B_2H_6 was introduced through a capillary downstream of the discharge, a heavy build-up of boron a few inches downstream of the B_2H_6 inlet indicated that much of the B_2H_6 was being decomposed by the discharge. In consideration of these statements and from comparison of the relative flow rates, the quantity of BH_3 produced in the pyrolysis experiments is believed to be as great, if not greater, than the amount of HBF_2 synthesized. Therefore, arguments to the effect that BH_3 was not detected in the quenching experiments because of a lack of product would appear to be unfounded since an apparently smaller amount of HBF_2 was detected.

Although the B_2H_6 inlet capillary extended essentially to the end of the surrounding tube carrying the BF_3 discharge products, deposits were present about two or three inches from the end of the capillary which was evidence that the B_2H_6 was diffusing upstream and then reacting. Therefore, any products that would not deposit on the discharge tube walls must diffuse back out of the tube before condensing on the walls of the cryogenic reaction chamber. If any H_2BF were formed, further reaction to HBF_2 would likely occur before the H_2BF could be quenched.

The rough data of this experiment with an identification of extraneous products is presented in Appendix G.

CHAPTER IV

CONCLUSIONS AND RECOMMENDATIONS

The work described in the preceding chapters has led to the following conclusions:

1) BH_3 was produced by the pyrolysis of B_2H_6 in tubular furnaces of alumina, quartz, and stainless steel. BH_3 was also synthesized by the pyrolysis of B_2H_6 on incandescent filaments of platinum, tungsten, nichrome, zirconium, molybdenum, niobium, titanium, and tantalum.

2) BH_3 could not be detected in the radio frequency discharge of B_2H_6 . If BH_3 had been formed in the discharge it would have been depleted before the discharge products reached the ionization region of the mass spectrometer, as was shown by subsequent cryogenic quenching experiments.

3) The appearance potentials of B^+ , BH^+ , BH_2^+ , BH_3^+ , and B_2H_5^+ from B_2H_6 , as well as from BH_3 wherever applicable, were determined and are presented in Table 1.

4) The values of or the upper and/or lower bounds for $D(\text{B}^+ - \text{H})$, $D(\text{BH}^+ - \text{H})$, $D(\text{BH}_2^+ - \text{H})$, $D(\text{BH}_3 - \text{BH}_3)$, $D(\text{BH}_3^+ - \text{BH}_3)$, $I(\text{B}_2\text{H}_6)$, and $I(\text{B}_2\text{H}_5)$ were calculated directly from the experimental appearance potentials. By introducing $I(\text{BH}) = 9.77 \text{ eV}^{67}$, $D(\text{B} - \text{H})$, $D(\text{BH} - \text{H})$, $D(\text{BH}_2 - \text{H})$, and $I(\text{BH}_2)$ were also calculated. The results are given in Table 2.

5) The heat of formation of B_2H_6 at 298°K was calculated as -40.9 kcal/mole by utilization of the derived bond energies. Comparison with

an experimental value of 7.53 kcal/mole^{69,70} gave an indication of the errors in the bond energies and consequently in the experimental appearance potentials. The errors are believed to be inherent in the electron impact method of energy determinations and not due to the experimental procedure.

6) Free BH_2 was not observed in this work even though the pyrolysis of B_2H_6 was investigated under conditions essentially identical to those that reportedly produced BH_2 ^{39,41}. The only discernible difference in the experimental setup was the absence of a 0.0001 inch diameter platinum-platinum-rhodium thermocouple in the furnace region which may possibly catalyze the formation of BH_2 .

7) Although equilibrium partial pressures calculated from free energies of reaction, which were determined from the bond energies in this thesis and entropy values from estimated thermodynamic data⁵⁵, showed that the pyrolysis of B_2H_6 should produce comparable amounts of BH_3 and BH_2 , BH_2 is kinetically unfavorable in comparison to BH_3 . This was concluded after a consideration of the activation energies, again determined from the experimental bond energies, for the dissociation of B_2H_6 into BH_2 and BH_3 .

8) A mechanism for the pyrolysis of B_2H_6 involving BH_3 but excluding BH_2 was proposed and utilized to show agreement between this work and several kinetic studies¹⁵⁻¹⁸ on the value of $D(\text{BH}_3 - \text{BH}_3)$. Also, by relating the kinetic rate equation describing the pyrolysis mechanism to experimental results, pre-exponential factors were calculated for several steps in the pyrolysis mechanism that were entirely reasonable for the order of reaction in question as seen by comparison with experimental pre-

exponential factors^{79,80}.

9) No evidence was obtained for the existence of BH_3 as a cryogenic material by monitoring the quenching operations at approximately 55°K and 77°K of the effluent gases from the pyrolysis of B_2H_6 in a tubular quartz furnace or by monitoring the gases evolved from the deposits during warm-up.

10) A similar procedure failed to produce evidence for H_2BF in the products from the rf discharge of BF_3 and B_2H_6 . However, the known compound HBF_2 was observed in the warm-up of the quenched products to approximately 90°K.

11) A modification of the standard RPD arrangement of the electron gun grids of the mass spectrometer allowed an increase in sensitivity of a factor of about 5. The modification was found to have no adverse effects upon the results of energy measurements.

Several extensions of the present work may be proposed.

Future studies of reactive and unstable molecules by techniques similar to those described in this thesis should be conducted so that the products of the synthesis operation, i.e., pyrolysis, rf discharge, etc., may be exhausted immediately into the ionization region of the mass spectrometer without passage through any beam collimating arrangement such as that described in Chapter II. Although other studies have made successful use of such arrangements, the initial frustrating attempts to detect BH_3 in reaction products effusing through small diameter orifices should certainly encourage adherence to this recommendation.

The pyrolysis of B_2H_6 in a tubular quartz furnace packed with platinum: platinum-rhodium (90-10) thermocouple wire should be investigated

to determine if BH_2 can be produced by a catalytic effect of the thermocouple wire. The pyrolysis of B_2H_6 on incandescent filaments of the thermocouple wire might also be studied. The synthesis of BH_2 and the subsequent determination of $\text{I}(\text{BH}_2)$ and $\text{A}(\text{BH}^+)$ and $\text{A}(\text{B}^+)$ from BH_2 would more completely determine the energetics of the BH_3 and B_2H_6 molecules, as well as the BH_2 free radical.

The attempts to prepare BH_3 as a solid or liquid phase should be performed at temperatures lower than 55°K and in equipment designed to allow synthesis, quench, and vaporization to occur in the immediate vicinity of the ionizing electron beam. The latter arises from the failure to transfer BH_3 through 1-1/2 feet of 3/8 inch diameter tube cooled to about 55°K .

An investigation of the variation of the BH_3^+ ion intensity with the distance of the furnace exit from the electron beam might give an indication of the lifetime of the BH_3 molecule. This could be done by a comparison with the variation of the argon ion intensity under similar conditions. The results of this experiment could possibly explain the failure to transfer BH_3 from the outer refrigerant chamber region of the cryogenic inlet system to the ionization region of the mass spectrometer. That is, if the investigation showed that BH_3 experienced a much greater decrease in intensity than argon as the distance between the furnace exit and the electron beam was increased, it could be postulated that the BH_3 was decomposing by an unimolecular process. Therefore, the possibility of transferring BH_3 for a distance of 1-1/2 feet in the cryogenic inlet system would appear to be remote.

The investigation of lower temperatures and operations in the

vicinity of the ionization region is also suggested for the synthesis of H_2BF . In addition, a system that would allow the products of the rf discharge to be subjected to immediate quench is highly desirable since it appeared that reaction was occurring a few inches upstream of the quenching region in these experiments. The use of a ceramic discharge tube rather than quartz is recommended because of SiF_4 and Si_2F_6 production from reaction of the discharge products with the tube walls.

Should BH_3 be stabilized at cryogenic temperatures, the study of the chemical reactivity of this compound with several species would prove of interest. Other than the products that would be expected from comparison with the known reactions of B_2H_6 , previously unobserved compounds might well be synthesized.

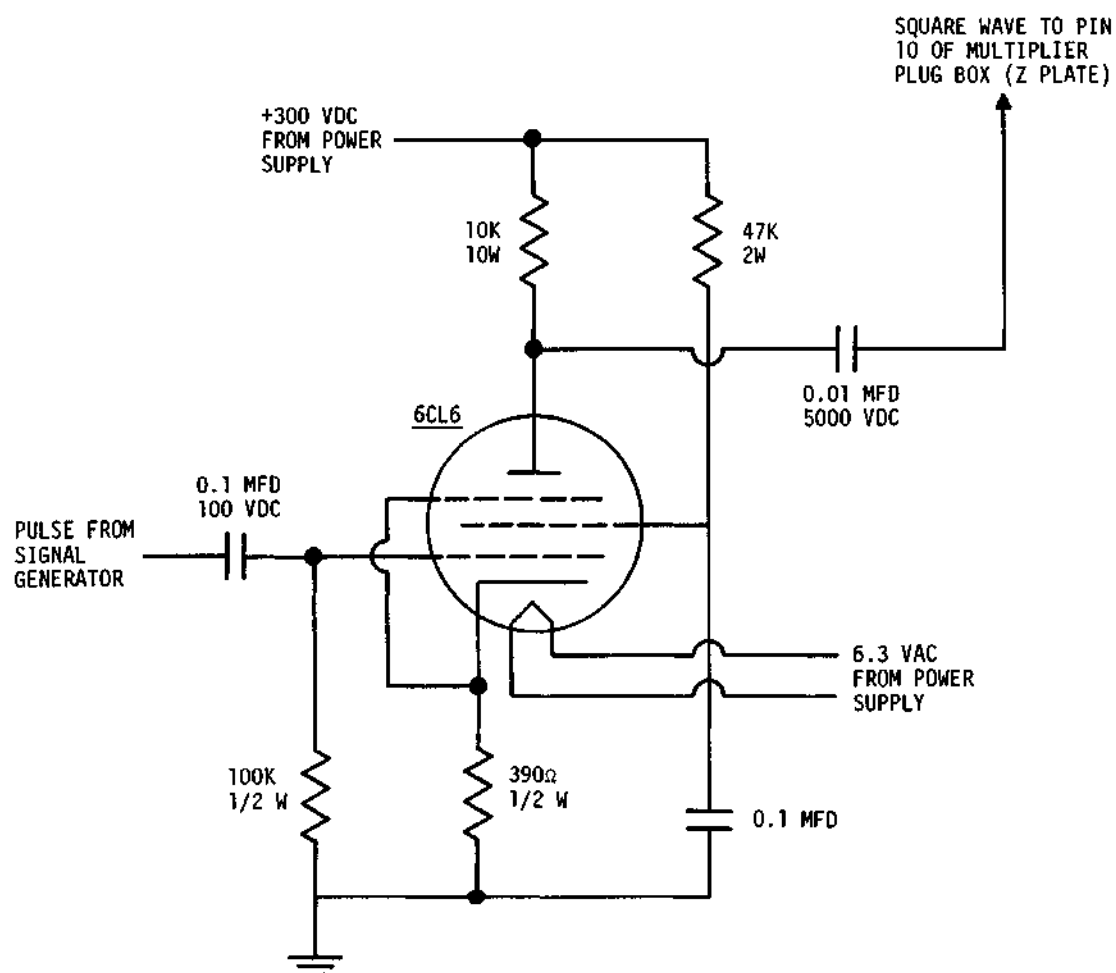
APPENDIX A

BLANKING CIRCUIT

The Bendix mass spectrometer has an undesirable feature in that the glass electron multiplier plates, which amplify the electron signal produced by the ions arriving into the collector, lose sensitivity quite rapidly and result in erroneous output readings when very large ion currents are present. Such was usually the case in the experiments herein since relatively large flows of B_2H_6 were necessary to produce sufficient BH_3 intensity for appearance potential measurements.

A blanking circuit, which removes the electron signal before it can reach the multiplier plates by applying a properly timed pulse to the "Z" plate, is available from Bendix and a similar circuit has been developed by Studier⁸². However, since the instrument available in this laboratory was not so equipped, it was necessary to assemble such a blanking circuit for use in appearance potential measurements on the $BH_3 - B_2H_6$ system.

The main pieces of equipment used for the blanking circuit were a General Radio Company Type 1205-B adjustable regulated power supply and a Rutherford Electronics Company Model B7B pulse generator. The circuit diagram is shown in Figure 9. Basically, the circuit provides a square wave, adjustable to a maximum of approximately 340 volts, to the "Z" plate of the multiplier. The duration of the pulse is adjustable from 0 to greater than 50 μ sec, which is the cycle time of the mass spectrometer.



NOTES

1. Signal Generator Triggered by Mass Spectrometer.
2. Standard Jumper Between Pin 10 (Z Plate) and Pin 11 (Grid) of Multiplier Plug Box Removed.
3. 100K, 1/2 W Resistor Installed Between Pin 10 and Pin 11.

Figure 9. Schematic Diagram of Blanking Circuit.

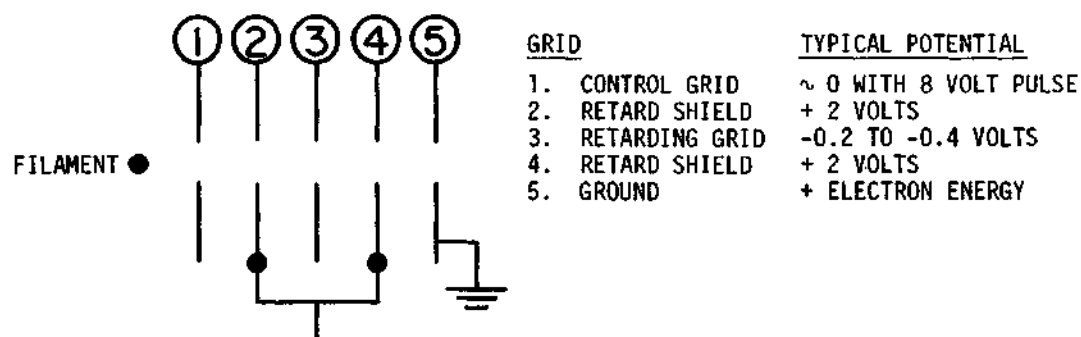
In addition, the pulse generator is equipped with a delay circuit so that the beginning of the square wave pulse may be varied from a value of m/e equal to zero to any value of m/e . In this way, if the mass peak of interest lies below the large mass peaks that are creating interference, by proper settings of the delay and pulse duration controls of the pulse generator, the interfering peaks may be blanked out. Such is also the case when the peak of interest lies above the interfering peaks. This circuit is to be compared to that of Bendix, which has no adjustable delay, and to that of Studier⁸², which is capable of blanking out interfering mass peaks on both sides of the peak of interest.

APPENDIX B

MODIFICATION OF THE RETARDING POTENTIAL DIFFERENCE CIRCUITRY

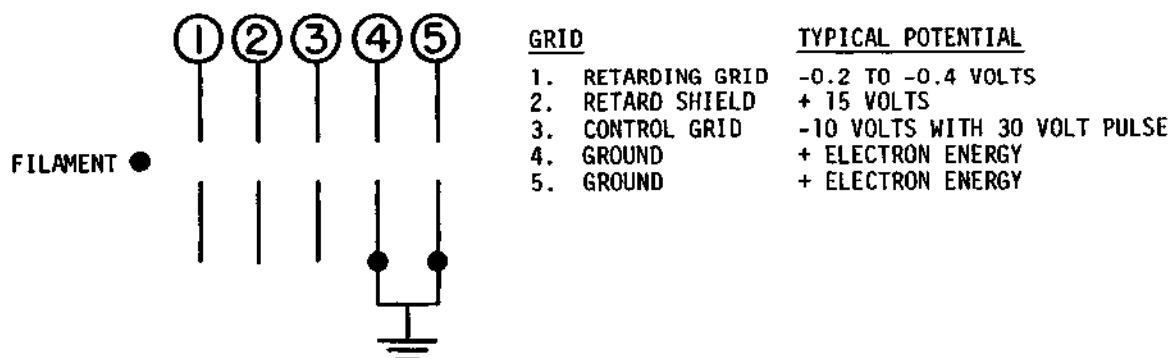
A disadvantage of the normal RPD arrangement of the grids of the electron gun, as described by Martin⁵² and shown in Figure 10, is that the maximum attainable trap current (ionizing electron beam) at electron energies normally used for ionization potential measurements (approximate 10-20 volts) had usually been no more than 0.03 microampere. In normal operation, the trap current can be increased to greater than 0.25 microampere, which is off scale. Melton and Hamill⁶⁴, who modified the Bendix mass spectrometer for the utilization of the RPD technique, attribute the loss of trap current to the defocussing action on the electron beam caused by the deceleration between the control grid (pulsed approximately + 8 volts relative to the filament) and the retarding grid (biased approximately - 0.2 to - 0.4 volts relative to the filament). This decrease in trap current and the resulting decrease in sensitivity of the mass spectrometer is then a considerable drawback for ionization potential measurements of species which are present only in very small concentrations.

An interesting observation was made on one occasion after the electron gun grids had been extremely well cleaned, the filament aligned very carefully, and the source magnets positioned for maximum trap current. The maximum trap current reading in the RPD mode of operation was found to be as great as in normal operation. However, the sensitivity of

NOTE

Potentials are with respect to Filament.

Figure 10. Electron Gun for RPD Studies in Normal Arrangement.

NOTE

Potentials are with respect to Filament.

Figure 11. Modification of Electron Gun for RPD Studies.

the machine appeared to be less, as was usual, and, in addition, a considerable amount of noise, i.e., diffuse mass peaks appearing at non-integral numbers, was present over the entire output range of the mass spectrometer.

During attempts to determine the origin of the noise, the mass spectrometer was switched into the normal pulsed mode of operation, all grids being at ground potential except the control grid which was as shown in Figure 10. Upon lowering the control grid bias to - 10 volts relative to the filament while increasing the pulse height, the noise was eliminated. Also, with the mass spectrometer in the pulsed Studier mode of operation, in which ions that are being continuously formed are held in the region of the electron beam by appropriate biases before pulsing, the noise was reduced considerably. These observations led to the conclusion that the noise was being caused by a continuous leakage of the electron beam due to the extremely low bias on the control grid. This would account for the same apparent low sensitivity of the machine even though the trap current had been increased by careful cleaning and alignment of the electron gun. It was further noted that after a period of operation during which the control grid had become dirty, the trap current had dropped to its usual low level in the RPD mode and the noise had simultaneously disappeared.

In order to increase the trap current (without introducing noise) and consequently the sensitivity of the machine in the RPD mode, several different arrangements of the electron gun grids along with changes in the biases and pulse heights were investigated. The arrangement shown in Figure 11 was found to be satisfactory. With a + 15 volt bias on the

retard shield, a trap current of approximately 0.1 microampere could be obtained, the operating level in normal pulsed operation being 0.125 microampere. However, increasing the bias resulted in the onset of noise. Evidently, the additional energy given to the electrons allowed them to overcome the - 10 volt bias on the control grid. Of course, the electrons do not possess the 25 ev necessary to overcome this 25 volt barrier, but do so as a result of "peak through" from the grids immediately behind the control grid. Such a phenomenon was responsible for the continuous electron leakage described previously when the grid bias was at a very low value.

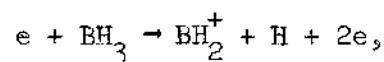
It has been suggested that for ionization and appearance potential measurements the control grid pulse height should be kept at a low value, preferably less than 10 volts. This was certainly not the case here, but no difficulty was experienced in performing energy measurements. This became obvious when a value determined by the RPD method was reproduced by the independent semilog matching method. It would appear that any effect that may be introduced by the higher pulse height is compensated for when measurements are performed on the calibrating gas under the identical operating conditions. A similar situation existed when in a pyrolysis experiment it was necessary to calibrate with the furnace on due to the effect of the magnetic field of the furnace windings. This effect was a lowering of the appearance potentials as a result of an added acceleration of the electron beam.

APPENDIX C

CALCULATION AND ESTIMATION PROCEDURES
FOR BOND ENERGIES AND IONIZATION POTENTIALS
FROM APPEARANCE POTENTIAL DATA

1. $D(\text{BH}_2^+ - \text{H})$

For the process



we can write

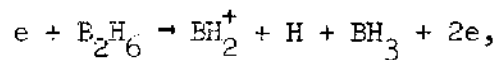
$$A(\text{BH}_2^+) = I(\text{BH}_3) + D(\text{BH}_2^+ - \text{H}),$$

or

$$D(\text{BH}_2^+ - \text{H}) = 12.95 \text{ ev} - 12.32 \text{ ev} = 0.63 \text{ ev},$$

where both $A(\text{BH}_2^+)$ and $I(\text{BH}_3)$ were experimentally determined in this thesis research.

Alternatively, from the process



$$A(\text{BH}_2^+) = A(\text{BH}_3) + D(\text{BH}_2^+ - \text{H}),$$

or

$$D(\text{BH}_2^+ - \text{H}) = 15.5 \text{ ev} - 14.88 \text{ ev} = 0.62 \text{ ev},$$

where both $A(\text{BH}_2^+)$ and $A(\text{BH}_3^+)$ are experimental values not dependent upon the above data. The agreement on $D(\text{BH}_2^+ - \text{H})$ is excellent.

2. $D(\text{BH}^+ - \text{H})$

For the process



$$A(\text{BH}^+) = A(\text{BH}_2^+) + D(\text{BH}^+ - \text{H}) - D(\text{H} - \text{H}),$$

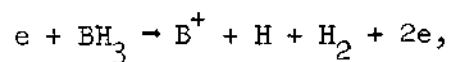
or

$$D(\text{BH}^+ - \text{H}) = 13.66 \text{ ev} - 12.95 \text{ ev} + 4.52 \text{ ev} = 5.23 \text{ ev},$$

where only the well known $D(\text{H} - \text{H})$ is not an experimental number from this thesis research.

3. $D(\text{B}^+ - \text{H})$

For the process



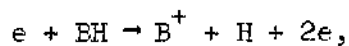
$$A(\text{B}^+) = A(\text{BH}^+) + D(\text{B}^+ - \text{H}),$$

where $A(\text{BH}^+)$ represents the process in 2. Hence

$$D(\text{B}^+ - \text{H}) = 15.83 \text{ ev} - 13.66 \text{ ev} = 2.17 \text{ ev}.$$

4. $D(\text{B} - \text{H})$ and Relationship Between $[D(\text{B} - \text{H}) - D(\text{B}^+ - \text{H})]$ and $I(\text{BH})$

If we consider the process



we can write

$$A(B^+) = I(BH) + D(B^+ - H)$$

and also

$$A(B^+) = D(B - H) + I(B).$$

Clearly,

$$I(BH) + D(B^+ - H) = D(B - H) + I(B),$$

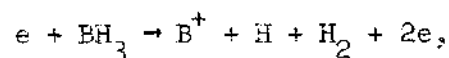
and therefore

$$I(BH) = I(B) + [D(B - H) - D(B^+ - H)].$$

The recent spectroscopic study by Bauer, Herzberg, and Johns⁶⁷ gives $I(BH) = 9.77$ ev. This value, combined with $I(B) = 8.3$ ev and $D(B^+ - H) = 2.17$ ev from 3, determines $D(B - H)$ as 3.64 ev.

5. $D(BH - H)$ and $D(BH_2 - H)$

From the process



it follows that

$$A(B^+) = D(BH_2 - H) + D(BH - H) + D(B - H) + I(B) - D(H - H),$$

or

$$D(BH_2 - H) + I(BH - H) = 15.83 \text{ ev} + 4.52 \text{ ev} - 8.3 \text{ ev} - 3.64 \text{ ev} =$$

$$8.41 \text{ ev},$$

where $A(B^+)$ is an experimental number from this thesis and $D(B - H)$ was calculated in 4. If we now assume that $D(BH^+ - H)$ is 0.4 ev greater than $D(BH - H)$ because of a gain of polarization stability, as indicated by isoelectronic curves⁶⁸, then

$$D(BH - H) = 5.23 \text{ ev} - 0.4 \text{ ev} = 4.83 \text{ ev},$$

where $D(BH^+ - H)$ was calculated in 2. Thus

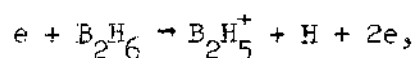
$$D(BH_2 - H) = 8.41 \text{ ev} - 4.83 \text{ ev} = 3.58 \text{ ev}.$$

6. $I(B_2H_6)$

Assuming that the sp^3 bonding in B_2H_6 is not as strong as the sp^2 bonding in BH_3 ,

$$0 < D(B_2H_5^+ - H) < D(BH_2^+ - H) = 0.63 \text{ ev}.$$

From the process of ionization of B_2H_6 and dissociation to $B_2H_5^+$,



it follows that

$$A(B_2H_5^+) = I(B_2H_6) + D(B_2H_5^+ - H),$$

or

$$I(B_2H_6) = 11.84 \text{ ev} - D(B_2H_5^+ - H).$$

$I(B_2H_6)$ is then bracketed as

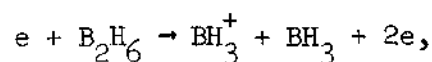
$$I(B_2H_6) < 11.84 \text{ ev for } D(B_2H_5^+ - H) > 0$$

and

$$I(B_2H_6) > 11.21 \text{ ev for } D(B_2H_5^+ - H) < 0.63 \text{ ev.}$$

$$7. \quad \underline{D(BH_3^+ - BH_3)}$$

The energy of symmetrical dissociation of $B_2H_6^+$ can also be bracketed by considering



from which it follows that

$$A(BH_3^+) = I(B_2H_6) + D(BH_3^+ - BH_3).$$

Thus

$$D(BH_3^+ - BH_3) > 3.04 \text{ ev for } I(B_2H_6) < 11.84 \text{ ev}$$

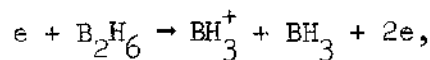
and

$$D(BH_3^+ - BH_3) < 3.67 \text{ ev for } I(B_2H_6) > 11.21 \text{ ev,}$$

where $A(BH_3^+)$ is an experimental number from this thesis.

$$8. \quad \underline{D(BH_3 - BH_3)}$$

For the process



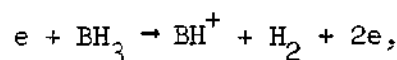
$$A(BH_3^+) = D(BH_3 - BH_3) + I(BH_3),$$

or

$$D(\text{BH}_3 - \text{BH}_3) = 14.88 \text{ ev} - 12.32 \text{ ev} = 2.56 \text{ ev},$$

where the numbers involved are experimental values from this thesis.

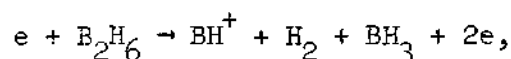
To demonstrate that the difference in appearance potentials of a particular fragment from B_2H_6 and from BH_3 should be equal to $D(\text{BH}_3 - \text{BH}_3)$, consider the fragment BH^+ as produced first from BH_3 by the process



for which

$$A(\text{BH}^+) = D(\text{BH}_2 - \text{H}) + D(\text{BH} - \text{H}) + I(\text{BH}) - D(\text{H} - \text{H}),$$

and then from B_2H_6 by



for which

$$A(\text{BH}^+) = D(\text{BH}_3 - \text{BH}_3) + D(\text{BH}_2 - \text{H}) + D(\text{BH} - \text{H}) + I(\text{BH}) - D(\text{H} - \text{H}).$$

It is obvious that the difference in the two appearance potentials is

$$D(\text{BH}_3 - \text{BH}_3).$$

9. $I(\text{BH}_2)$

For the process



$$A(\text{BH}^+) = D(\text{BH}_2 - \text{H}) + I(\text{BH}_2) + D(\text{BH}^+ - \text{H}) - D(\text{H} - \text{H}).$$

But, from 5,

$$D(\text{BH}_2 - \text{H}) = A(\text{B}^+) - D(\text{BH} - \text{H}) - D(\text{B} - \text{H}) - I(\text{B}) + D(\text{H} - \text{H}).$$

Therefore,

$$\begin{aligned} A(\text{BH}^+) &= A(\text{B}^+) - D(\text{BH} - \text{H}) - D(\text{B} - \text{H}) - I(\text{B}) + D(\text{H} - \text{H}) \\ &\quad + I(\text{BH}_2) + D(\text{BH}^+ - \text{H}) - D(\text{H} - \text{H}). \end{aligned}$$

Recalling from 3 that for a fixed process $A(\text{B}^+) - A(\text{BH}^+) = D(\text{B}^+ - \text{H})$ and from 4 that $D(\text{B} - \text{H}) - D(\text{B}^+ - \text{H}) = 1.47 \text{ ev}$,

$$I(\text{BH}_2) = I(\text{B}) + 1.47 \text{ ev} + D(\text{BH} - \text{H}) - D(\text{BH}^+ - \text{H}).$$

From 5,

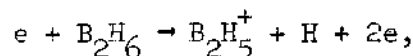
$$D(\text{BH} - \text{H}) - D(\text{BH}^+ - \text{H}) = 0.4 \text{ ev}.$$

Thus

$$I(\text{BH}_2) = 8.3 \text{ ev} + 1.47 \text{ ev} - 0.4 \text{ ev} = 9.37 \text{ ev}.$$

10. $I(\text{B}_2\text{H}_5)$

For the process



$$A(\text{B}_2\text{H}_5^+) = D(\text{B}_2\text{H}_5 - \text{H}) + I(\text{B}_2\text{H}_5).$$

Assuming that the sp^3 bonding in B_2H_6 is not as strong as the sp^2 bonding in BH_3 ,

$$I(\text{B}_2\text{H}_5 - \text{H}) < D(\text{BH}_2 - \text{H}) = 3.58 \text{ ev}$$

and

$$I(\text{B}_2\text{H}_5) > 11.84 \text{ ev} - 3.58 \text{ ev} = 8.26 \text{ ev}.$$

If $D(\text{BH}_2 - \text{H}) = 3.2 \text{ ev}$ as obtained from isoelectronic curves⁶⁸,

then

$$I(\text{B}_2\text{H}_5) > 8.64 \text{ ev}.$$

APPENDIX D

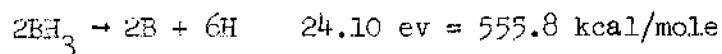
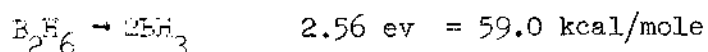
THERMODYNAMIC DATA DERIVED FROM BOND ENERGIES

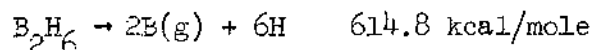
In this appendix, the heat of formation and free energy of formation of B_2H_6 are calculated by utilizing the bond energies determined in this research work. These calculated values are used to obtain an estimate of the magnitude of the errors in the bond energies by comparison with experimental values of ΔH_f° and ΔG_f° of B_2H_6 , as shown in Chapter III. In addition, equilibrium partial pressures of BH_3 and BH_2 are calculated in order to ascertain whether or not the reported observation³⁹ of two to three times more BH_2 than BH_3 in the pyrolysis of B_2H_6 is reasonable from a thermodynamic point of view, the kinetic considerations to be discussed later.

The temperature and total pressure for which the equilibrium constants are calculated were typical experimental conditions for the pyrolysis of B_2H_6 in this research work. The resultant negligible amounts of BH_3 and BH_2 at equilibrium justify the separate calculations of the equilibrium values.

Heat of Formation of B_2H_6

Consider the equations,





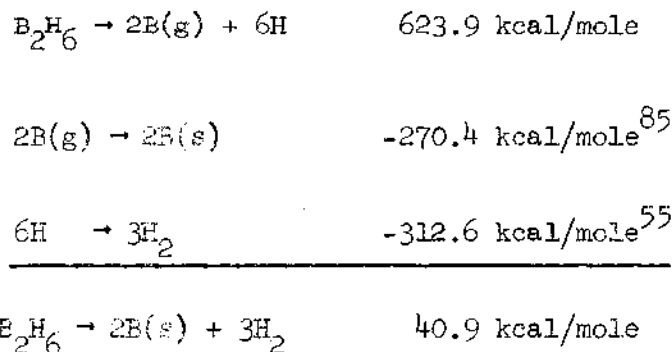
where the energetic quantities are from the electron impact studies of this thesis research. If the electron impact appearance potentials are assumed to include no electronic, vibrational, or rotational excitations and no excess kinetic energy, as discussed in Chapter III, then $614.8 \text{ kcal/mole} = \Delta H^\circ_{\text{O}}$, the heat of atomization of B_2H_6 at 0°K . Applying $(H^\circ - H^\circ_{298})$ values from JANAF DATA⁵⁵ to the last equation,

$$\Delta(H^\circ_{\text{O}} - H^\circ_{298}) = 3.0 - 8.9 + 2.8 = 9.1 \text{ kcal/mole}$$

and therefore

$$\Delta H^\circ_{298} = 614.8 + 9.1 = 623.9 \text{ kcal/mole.}$$

The heat of formation of B_2H_6 at 298°K may now be determined in the following manner.



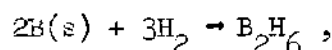
Thus, $\Delta H^\circ_{\text{f}}$ of B_2H_6 at $298^\circ\text{K} = -40.9 \text{ kcal/mole}$.

It must be noted that the value used for the heat of sublimation of boron differs from another literature value⁵⁵ by approximately 2.5 kcal/mole. This would mean a difference in the calculated heat of formation

of 5 kcal/mole. However, since the calculated ΔH_f° disagrees with experimental results by approximately 49 kcal/mole, the uncertainty of 5 kcal/mole is of little or no consequence. This follows from the semi-quantitative nature of the comparison made in Chapter III between the calculated and experimental values of ΔH_f° .

Free Energy of Formation of B_2H_6

For the reaction



$$\Delta S_{298}^\circ = 55.3 - 2.8 - 93.6 = -41.1 \text{ cal/mole/}^\circ K$$

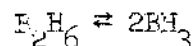
where the entropy values are taken from estimated thermodynamic tables⁵⁵.

Therefore,

$$\begin{aligned} \Delta G_f^\circ \text{ at } 298^\circ K &= \Delta H_f^\circ - T\Delta S_f^\circ \\ &= -40.9 + 12.2 = -28.7 \text{ kcal/mole.} \end{aligned}$$

Equilibrium Partial Pressures of BH_2 and BH_3 at $600^\circ K$

Consider the equilibrium



and again assume that the experimental bond energies correspond to heats of reaction at $0^\circ K$. By employing estimated thermodynamic tables⁵⁵, as before, along with $I(BH_3 - BH_3) = 2.56 \text{ ev}$ or 59.0 kcal/mole from this research, the following may then be written:

$$\Delta(H_{600}^{\circ} - H_0^{\circ}) = 2.2 \text{ kcal/mole}$$

$$\Delta H_{600}^{\circ} = 59.0 + 2.2 = 61.2 \text{ kcal/mole}$$

$$\Delta S_{600}^{\circ} = 103.1 - 68.1 = 35.0 \text{ cal/mole/}^{\circ}\text{K}$$

$$\Delta G_{600}^{\circ} = \Delta H_{600}^{\circ} - T\Delta S_{600}^{\circ}$$

$$= 61.2 - 600 \times 0.035 = 40.2 \text{ kcal/mole}$$

$$\ln K_p = \frac{-\Delta G}{RT} = -33.69$$

$$K_p = 2.4 \times 10^{-15} \text{ atm.}$$

If one sets the moles of B_2H_6 initially equal to 1 and the moles of B_2H_6 reacted equal to $x/2$, then the moles of BH_3 formed equal x . Since x will obviously be very small compared to 1, 1 and x will essentially be equal to the mole fractions of B_2H_6 and BH_3 , respectively. It then follows that

$$K_p = \frac{p_{BH_3}^2}{p_{B_2H_6}} = \frac{x^2 P^2}{1P} = x^2 P,$$

and thus

$$x = \sqrt{\frac{K_p}{P}} = 4.9 \times 10^{-8} P^{-1/2}$$

where P is the total reaction pressure in terms of atmospheres. Therefore,

$$p_{BH_3} = xP = 4.9 \times 10^{-8} P^{1/2}.$$

If $P = 10^{-2}$ mm Hg $= 1.3 \times 10^{-5}$ atm, then

$$p_{\text{BH}_3} = 4.9 \times 10^{-8} \times 3.6 \times 10^{-3} \text{ atm} \times \frac{760 \text{ mm Hg}}{\text{atm}} = 1.4 \times 10^{-7} \text{ mm Hg}.$$

The calculation of p_{BH_2} for the equilibrium $\text{B}_2\text{H}_6 \rightleftharpoons 2\text{BH}_2 + \text{H}_2$ is similar to that of p_{BH_3} ($\Delta H^\circ = D(\text{BH}_3 - \text{BH}_3) + 2D(\text{BH}_2 - \text{H}) - D(\text{H} - \text{H})$). The resultant expression for p_{BH_2} is

$$\begin{aligned} p_{\text{BH}_2} &= (2K_p P)^{1/3} \text{ atm} \\ &= 2 \times 10^{-10} P^{1/3} \text{ atm} \end{aligned}$$

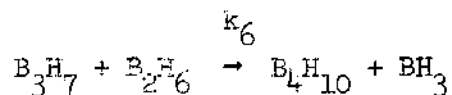
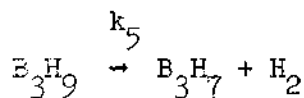
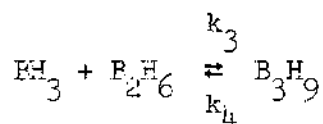
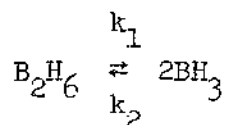
where the experimental value of $D(\text{BH}_2 - \text{H}) = 3.58$ ev was used in the calculation of the heat of reaction. However, since this value is possibly in error, as discussed in Chapter III, p_{BH_3} was also calculated utilizing $D(\text{BH}_2 - \text{H}) = 3.2$ ev which is in agreement with values determined from isoelectronic curves⁶⁸ and which also represents a reasonable correction to $D(\text{BH}_2 - \text{H})$ from this work. The expression for p_{BH_2} now becomes

$$p_{\text{BH}_2} = 2.7 \times 10^{-8} P^{1/3} \text{ atm}.$$

APPENDIX E

RATE EQUATION DESCRIBING THE PYROLYSIS
OF B_2H_6 IN THE INITIAL STAGE OF REACTION

The mechanism postulated from the present work for the initial stages of the pyrolysis of B_2H_6 is



This mechanism is essentially that as suggested by Enrione and Schaeffer¹⁸. The arguments supporting this mechanism are contained in Enrione and Schaeffer's article as well as in an earlier publication by Schaeffer¹⁹.

Although BH_2 has been suggested as an intermediate in the pyrolysis of B_2H_6 ^{39,42}, it was not included in this mechanism because of the failure to observe BH_2 in this work and of the comparison of rate constants of the dissociation of B_2H_6 to BH_3 and to BH_2 in Appendix F. Further support for

the above mechanism is found in the work on the pyrolysis of B_2H_6 by Baylis, et al.⁴⁰, who observed monoborane, triborane, tetraborane, and pentaborane species which appeared in the given order as pressure and temperature were increased.

To determine the rate equation for the above mechanism, let

$$[B_2H_6] = a$$

$$[BH_3] = b$$

$$[B_3H_9] = c$$

$$[B_3H_7] = e$$

where $[x]$ designates the molal concentration of x or the partial pressure of x . The following equations may then be written:

$$\frac{da}{dt} = -k_1a + k_2b^2 - k_3ab + k_4c - k_6ae \quad (1)$$

$$\frac{db}{dt} = 2k_1a - 2k_2b^2 - k_3ab + k_4c + k_6ae \quad (2)$$

$$\frac{dc}{dt} = k_3ab - k_4c - k_5c \quad (3)$$

$$\frac{de}{dt} = k_5c - k_6ae \quad (4)$$

Using a conventional stationary-state treatment for the intermediate species BH_3 , B_3H_9 , and B_3H_7 , the rate equation may be determined in the following manner:

From Equations (3) and (4),

$$\frac{dc}{dt} = 0 = k_3 ab - k_4 c - k_5 c,$$

or

$$c = \frac{k_3 ab}{k_4 + k_5},$$

and

$$\frac{de}{dt} = 0 = k_5 c - k_6 ae,$$

or

$$e = \frac{k_5 c}{k_6 a} = \frac{k_5 k_3 ab}{k_6 a (k_4 + k_5)} = \frac{k_3 k_5 b}{k_6 (k_4 + k_5)}.$$

Substitution into Equation (2) yields

$$\begin{aligned} \frac{db}{dt} = 0 &= 2k_1 a - 2k_2 b^2 - k_3 ab + \frac{k_4 k_3 ab}{(k_4 + k_5)} + \frac{k_6 a k_3 k_5 b}{k_6 (k_4 + k_5)} \\ &= 2k_1 a - 2k_2 b^2 + ab \left[\frac{-k_3 k_4 - k_3 k_5 + k_3 k_4 + k_3 k_5}{k_4 + k_5} \right] \\ &= 2k_1 a - 2k_2 b^2, \end{aligned}$$

or

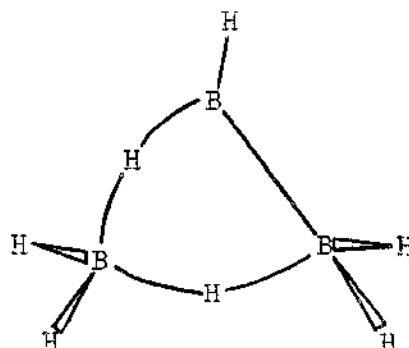
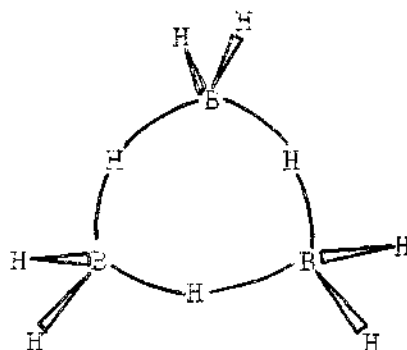
$$b = \sqrt{k_1 a / k_2} = \sqrt{K a}$$

where $K = k_1 / k_2$.

Finally, substitution into Equation (1) gives

$$\begin{aligned} \frac{da}{dt} &= -k_1 a + k_2 Ka - k_3 \sqrt{K} a^{3/2} + \frac{k_4 k_3 \sqrt{K} a^{3/2}}{k_4 + k_5} \\ &\quad - \frac{k_6 k_3 k_5 \sqrt{K} a^{3/2}}{k_6 (k_4 + k_5)} \\ &= -k_1 a + \frac{k_2 k_1 a}{k_2} + k_3 \sqrt{K} a^{3/2} \left[\frac{-k_4 - k_5 + k_4 - k_5}{k_4 + k_5} \right] \\ &= -\frac{2k_5 k_3 \sqrt{K} a^{3/2}}{k_4 + k_5} \end{aligned}$$

The reaction $B_3H_9 \xrightarrow{k_5} B_3H_7 + H_2$ is thought to be the rate limiting step¹⁸. It seems reasonable that k_5 should be large because of a high activation energy necessary for the formation of an excited state that would allow the interaction of two hydrogen atoms for the subsequent elimination of H_2 . The reaction $B_3H_9 \xrightarrow{k_4} BH_3 + B_2H_6$ would occur with no internal rearrangement necessary for the elimination of BH_3 and the activation energy would probably be equal to the endothermicity of the reaction. Since the reaction occurs with a net cleavage of one bond, the activation energy would conceivably be comparatively small. In order that the preceding statements may be made somewhat more understandable, the proposed structures for B_3H_9 and B_3H_7 ⁴³ are shown as follows:



The conclusion is that $k_5 \gg k_4$ and

$$\begin{aligned} \frac{da}{dt} &= -2k_3 \sqrt{K} a^{3/2} \\ &= -2k_3 k_1^{1/2} k_2^{-1/2} a^{3/2} \\ &= -2A_3 \left(\frac{A_1}{A_2} \right)^{1/2} \frac{e^{-\frac{E_3}{RT}} e^{-\frac{E_1}{2RT}} a^{3/2}}{e^{-\frac{E_2}{2RT}}} \end{aligned}$$

The equation is seen to agree with the experimental $3/2$ order dependence upon B_2H_6 . The experimental activation energy, $E_{\text{expt.}}$, is then given by

$$E_{\text{expt.}} = E_3 + \frac{E_1}{2} - \frac{E_2}{2}.$$

Since electron impact measurements must include any activation energies that are present⁷⁶, $D(BH_3 - BH_3)$ determined in this thesis is essentially equal to E_1 . The reactivity of the "electron deficient"

molecule BH_3 would appear to justify setting $E_2 = 0$. Whether or not $E_3 = 0$ may well be debated. But based upon the reactivity of BH_3 , as before, as well as the probability that the reaction $\text{BH}_3 + \text{B}_2\text{H}_6 \rightarrow \text{B}_3\text{H}_9$ is exothermic, the assumption that $E_3 = 0$ may not be unfounded. Therefore, assuming E_2 and E_3 are equal to zero, $E_1 = 2E_{\text{expt.}}$ or $E_1 = 51$ to 58 kcal/mole from experimental activation energies¹⁵⁻¹⁸.

APPENDIX F

CALCULATIONS OF KINETIC RATE CONSTANTS

The purpose of this appendix is twofold. First of all, the expression developed in Appendix E describing the initial stages of the B_2H_6 pyrolysis is related to the expression which has been experimentally determined¹⁵⁻¹⁸. Since this work indicates that the rate of disappearance of B_2H_6 may be expressed in the form

$$-\frac{d[B_2H_6]}{dt} = k[B_2H_6]^{3/2}$$

in agreement with experimental findings, the expression for k from Appendix E may be related to $k_{\text{expt.}}$ in order to calculate pre-exponential factors for several of the reaction steps in the pyrolysis mechanism. The reasonableness of the calculated pre-exponential factors may then be taken as a measure of the correctness of the proposed pyrolysis mechanism. Secondly, by utilizing the bond energies determined in this thesis work, activation energies for several of the reaction steps may be calculated which, combined with the previously determined pre-exponential factors, allow expressions for reaction rate constants to be written. More important, however, a comparison of the specific rate constants for the dissociation of B_2H_6 into BH_3 and into BH_2 may be made in order to support the exclusion of BH_2 from the pyrolysis mechanism.

From Appendix E, the following relationship is evident:

$$A_{\text{expt.}} = 2A_3 \left(\frac{A_1}{A_2} \right)^{1/2}$$

where $A_{\text{expt.}}$ is the experimentally determined frequency factor for the pyrolysis of B_2H_6 . At 100°C ,

$$k_{\text{expt.}}^{15} = 0.24 \left(\frac{\text{liter}}{\text{mole}} \right)^{1/2} \text{hr}^{-1}$$

and

$$E_{\text{expt.}}^{15} = 27.4 \text{ kcal/mole.}$$

Therefore,

$$0.24 \left(\frac{\text{liter}}{\text{mole}} \right)^{1/2} \text{hr}^{-1} = A_{\text{expt.}} e^{\frac{-27,400 \text{ cal/mole}}{R \times 373^\circ\text{K}}},$$

or

$$\begin{aligned} A_{\text{expt.}} &= 2.7 \times 10^{15} \left(\frac{\text{liter}}{\text{mole}} \right)^{1/2} \text{hr}^{-1} \\ &= 7.5 \times 10^{11} \left(\frac{\text{liter}}{\text{mole}} \right)^{1/2} \text{sec}^{-1} \\ &= 1.4 \times 10^{11} \text{ atm}^{-1/2} \text{ sec}^{-1} \end{aligned}$$

From the relationship⁸⁰ $\ln(A_1/A_2) = \Delta S/R$ where ΔS refers to the reaction $B_2H_6 \rightarrow 2BH_3$, the ratio

$$\frac{A_1}{A_2} = e^{\frac{34.44 \text{ cal./mole/}^\circ\text{K}}{R}} = 10^{7.53} \quad (A_1 \text{ and } A_2 \text{ in terms of atm})$$

is obtained at 100°C using entropy tables from JANAF DATA.⁵⁵

Therefore,

$$A_3 = \frac{A_{\text{expt.}}}{2} \left(\frac{A_1}{A_2} \right)^{-1/2} = 1.2 \times 10^7 \text{ atm}^{-1} \text{ sec}^{-1}$$

$$= 3.6 \times 10^8 \frac{\text{liter}}{\text{mole sec}} .$$

The value of A_3 is certainly typical of frequency factors for bimolecular reactions^{79,80}.

If A_2 is assumed to be equal to A_3 , then

$$A_1 = 1.2 \times 10^7 \times 10^{7.53} \text{ sec}^{-1} = 4.0 \times 10^{14} \text{ sec}^{-1}.$$

The value of A_1 is also consistent with the values of frequency factors for unimolecular reactions^{79,80}.

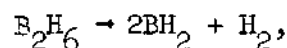
Since E_2 and E_3 were assumed to be zero in Appendix E, the following rate constants are obtained:

$$k_1 = 4.0 \times 10^{14} e^{\frac{-61 \text{ kcal/mole}}{RT}} \text{ sec}^{-1}$$

$$k_2 = k_3 = 3.6 \times 10^8 \frac{\text{liter}}{\text{mole sec}} ,$$

where the activation energy for k_1 is ΔH_{298}° as calculated for the reaction $\text{B}_2\text{H}_6 \rightarrow 2\text{BH}_3$ in Appendix D.

In order to obtain the rate constant for the reaction

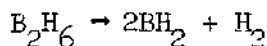


ΔH_{373}° is calculated as 124.8 kcal/mole by assuming $\Delta H_0^{\circ} = D(\text{BH}_3 - \text{BH}_3) + 2D(\text{BH}_2 - \text{H}) - D(\text{H} - \text{H})$, all bond energies being from this research with the exception of $D(\text{H} - \text{H})$, and utilizing $(\text{H}^{\circ} - \text{H}_{298}^{\circ})$ tables from JANAF DATA⁵⁵. This procedure is similar to that used in Appendix D. If the frequency factor for the dissociation into BH_2 is approximately equal to A_1 , and 124.8 kcal/mole is assumed to be the activation energy of k_{BH_2} , then

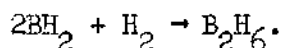
$$\frac{k_1}{k_{\text{BH}_2}} = e^{\frac{(124.8 - 61)\text{kcal/mole}}{RT}} = e^{\frac{63.8 \text{ kcal/mole}}{RT}}$$

where k_{BH_2} is the rate constant for the above reaction. At 373°K, this ratio has a value of 10^{37} and has a value of 10^{23} at 600°K.

In order to calculate k_{BH_2} , the value of $D(\text{BH}_2 - \text{H}) = 3.58$ ev from this research was used to determine the activation energy. Since this value may be too large, as indicated in Chapter III, the activation energy of k_{BH_2} may be recalculated using $D(\text{BH}_2 - \text{H}) = 3.2$ ev, which is then consistent with values determined from isoelectronic curves⁶⁸ and also which represents a reasonable correction to $D(\text{BH}_2 - \text{H})$ from this work. The ratio of k_1/k_{BH_2} is then 10^{27} at 373°K and 10^{17} at 600°K. However, the activation energy of



is actually equal to $\Delta H_r^{\circ} + E'$ where E' refers to the activation energy of the reverse process, i.e.,



Now E' would not be expected to be zero and consequently the activation energy for k_{BH_2} which was calculated using $D(\text{BH}_2 - \text{H}) = 3.2 \text{ ev}$ would represent a minimum value, assuming that 3.2 ev as well as $D(\text{BH}_3 - \text{BH}_3) = 2.56 \text{ ev}$ is actually correct. It then would appear that $k_1/k_{\text{BH}_2} = 10^{37}$ at 373°K is the more reasonable value since this essentially assigns a value of approximately 17 kcal/mole to E' , which is within reason. The accuracy of $D(\text{BH}_3 - \text{BH}_3)$ is of no concern in the ratio of the rate constants since it cancels out leaving essentially

$$\frac{k_1}{k_{\text{BH}_2}} = e^{2D(\text{BH}_2 - \text{H}) - D(\text{H} - \text{H})}.$$

APPENDIX G

RAW DATA FROM H_2BF QUENCHING EXPERIMENTS

This appendix presents typical raw data obtained in a H_2BF synthesis and quenching experiment. The actual ion currents given in Table 5 (all have the same arbitrary units based on an electrometer index setting of 0.4) for various temperatures during the warm-up of the cryogenic inlet system were recorded at 70 volts electron energy. At 115°K and above, the amount of gas being admitted into the ionization region was so great that the trap current had to be reduced to the point that the trap current meter was barely on scale. The inability to control the rate of temperature rise of the system after the refrigerant chambers were emptied of O_2 has been mentioned previously. If this condition did not exist, the temperature could have been held constant at certain points to allow the more volatile species to pump away and, thus, to prevent interference with the detection of species evolved at higher temperatures. When the O_2 coolant had been completely pumped away, the warm-up from 55°K to 150°K took approximately one hour. In Table 5, the letter "a" denotes an ion peak that was off scale, full scale being approximately 140 in the arbitrary units used in the table. A blank indicates either that the ion peak was not present or that the intensity was so small as to be insignificant.

Products, other than HBf_2 , from the rf discharge as tentatively identified either by crude appearance potential measurements, comparison

Table 5. Raw Data for a Typical H_2BF Synthesis Experiment

m/e	Approximate Temperature, °K													
	55	65	70	72	75	85	95	115	130	135	145	155	175	185
	Relative Ion Currents													
10						2	30	a	18	140	12	79	42	47
11			4			23	128	a	70	a	a	a	a	a
12	a	a	a	81	80	100	126			7	7	7		10
13	5	19	7	5		15	135			12	20	21	10	5
14	a	a	a	a	a	a	a			38	30	17	23	17
15	6	77	33	32	25	25	19		11	24	25	10	31	35
16	a	a	a	a	a	a	a		7	60	a	a	135	78
17	104	140	93	140	a	132	131				9	12	25	30
18	a	a	a	a	a	a	a			80	15	25	69	63
19		30			14	28	19	a	130	a	a	a	a	a
20	112	100	60	41	58	38	20						16	8
21							12							
22					3		68				10			
23					6	17	a							
24					7	40	a			53	68	51	30	30
25					5	22	a				17			
26					20	63	a			40	27		16	7
27	30	33	22	32	55	81	a			52	25		36	18
28	a	a	a	a	a	a	a		22	93	60	41	120	140
29	57	140	58	65	125	91	82	54		89	53	37	45	47
30	15	42	65	140	a	a	a	a	40		a	a	140	a
31			16	11	77	127	a	20		28	17	9	a	7
32	a	a	a	a	a	a	a		38	112	a	a		15
33											23			29
34		9									31	37		14
35					10	25					35	12		
36	9	11		10	7		20				30	13		
37											32	13		
38		6		6			12				33	28	20	11
39	15	20	13	8	39	20	29							7
40	a	a	a	a	a	a	a							
41	37	51	52	40	125	73	54		21				12	15
42	9	16	24	17	39	24	15						8	
43	40	68	55	35	108	43	85				12	15	21	
44	10	10	7	11	20	25	29	20			28	20	20	20
45	10	17	9	19	36	25	25				70	14	10	20
46	9	11	5	5	6	8	11				62	68	38	91
47		11	5	3	8		12	37		60	a	94	140	a

(Continued)

with mass spectra data of known substances, or correlation of the temperatures of initial detection of certain ion peaks with vapor pressure data, or by a combination of these identification techniques, were CO, NO, N_2O , SiF_4 , and Si_2F_6 . Impurities that were determined to be present in the feed gases were B_4H_{10} , B_5H_{11} , CO_2 , CF_4 , SiF_4 , and SO_2 .

APPENDIX H

CALCULATION OF PRESSURE IN THE PYROLYSIS REGION
OF THE COAXIAL FURNACE INLET SYSTEM

To calculate the pressure in the pyrolysis region of the coaxial furnace inlet system, it is necessary to know the gas flow rate and the pressure at a particular point. However, only the inlet pressure was obtained in the experimental work since the gas flow rates were too small to be measured by the flow meters available in the laboratory. Therefore, the flow rate of B_2H_6 is calculated by assuming that it is essentially equal to the instantaneous rate of exhaust of a large constant volume, at a pressure equal to the experimental inlet pressure, through the 7-1/2 inch long (1/8 inch diameter) furnace tube. The pressure in the pyrolysis region may then be readily calculated.

A typical inlet pressure in the B_2H_6 pyrolysis experiments was 100 microns. This was indicated by a Consolidated Type 41550 micromanometer with the pressure tap located 6-1/2 inches from the 1 inch heated length of the 1/8 inch diameter stainless steel tube. From Dushman⁸³, we can write the instantaneous rate of exhaust of the volume V of the several inches of 1/4 inch diameter connecting tubing from the pressure tap to the leak valve as

$$-V \frac{dP}{dt} = FP$$

where P designates the pressure in the volume V at any instant. But since V is constant,

$$-\frac{dPV}{dt} = FP$$

or

$$-\frac{d(nRT)}{dt} = FP.$$

The mean free path of a gas may be written as⁸³

$$L = \frac{8.589\eta}{P_{mm}} \left(\frac{T}{M}\right)^{1/2} \text{ cm.}$$

At 100 microns and 25°C, the mean free path of B₂H₆ is

$$L = \frac{8.589 \times 80 \times 10^{-6}}{0.1} \left(\frac{298}{28}\right)^{1/2} \text{ cm} = 2.2 \times 10^{-2} \text{ cm}$$

where η has been experimentally determined⁸⁴ as 80×10^{-6} poise at 25°C.

For the 1/8 inch diameter tube (ID = 0.075 inches),

$$L/a = \frac{2.2 \times 10^{-2} \text{ cm}}{0.0375 \text{ in.} \times \frac{2.54 \text{ cm}}{\text{in.}}} = 0.23.$$

Therefore, transition flow is experienced at these conditions of temperature and pressure since $0.01 < L/a < 1.00$ ⁸³. F may now be written as⁸³

$$F = 30.48 \frac{a^3}{L} \left(\frac{T}{M}\right)^{1/2} \left(0.1472a/L + Z\right) \frac{\text{liters}}{\text{sec}},$$

where

$$Z = \frac{1 + 2.507(a/L)}{1 + 3.095(a/L)}.$$

Substitution into

$$- \frac{d(nRT)}{dt} = - RT \frac{d(n)}{dt} = FP$$

yields

$$- \frac{RTd(n)}{dt} = 6.8 \times 10^{-3} \frac{\text{liters}}{\text{sec}} \times 100 \text{ microns},$$

or

$$- \frac{d(n)}{dt} = 3.6 \times 10^{-8} \frac{\text{g-mole}}{\text{sec}},$$

where $l = 7\text{-}1/2$ inches, i.e., the entire length of the $1/8$ inch diameter tube.

The pressure drop for the $6\text{-}1/2$ inch long distance from the pressure tap to the pyrolysis region is given by⁸³

$$\Delta P = \frac{Q}{F'},$$

where Q is the product of the volumetric flow rate and the pressure at which it is measured and F' is calculated using $l = 6\text{-}1/2$ inches. Therefore, we may write

$$Q = - \frac{d(nRT)}{dt}$$

and consequently

$$\Delta P = - \frac{RTd(n)/dt}{F'},$$

or

$$\Delta P = \frac{F}{F}, P$$

$$= \frac{F}{F}, \times 100 \text{ microns} = 87 \text{ microns.}$$

Therefore, the pressure at the first point of the 1 inch long pyrolysis region is 13 microns or 1.3×10^{-2} mm Hg.

APPENDIX I

IONIZATION EFFICIENCY CURVES FOR EXPERIMENTAL APPEARANCE POTENTIALS

This appendix presents ionization efficiency data in Figures 12-17 for the following: $I(N_2)$; $A(BH^+)$ and $A(BH_2^+)$ from BH_3 ; and $A(B^+)$, $A(BH_2^+)$, and $A(B_2H_5^+)$ from B_2H_6 . The data for $A(BH^+)$ from B_2H_6 are not given. As mentioned in Chapter III, interference, which was due either to the failure of the blanking circuit to completely eliminate the effects of the large B_2H_x peaks or to noise from ion-molecule reactions because of high ion source pressures, permitted only a fraction of the ionization efficiency curve to be utilized for matching with argon. Therefore, the value obtained for $A(BH^+)$ from B_2H_6 was a rough estimate aided by the observation that the difference in $A(BH^+)$ from BH_3 and from B_2H_6 should be about 2.6 ev, as seen from the values of $A(BH_3^+)$ and $A(BH_2^+)$.

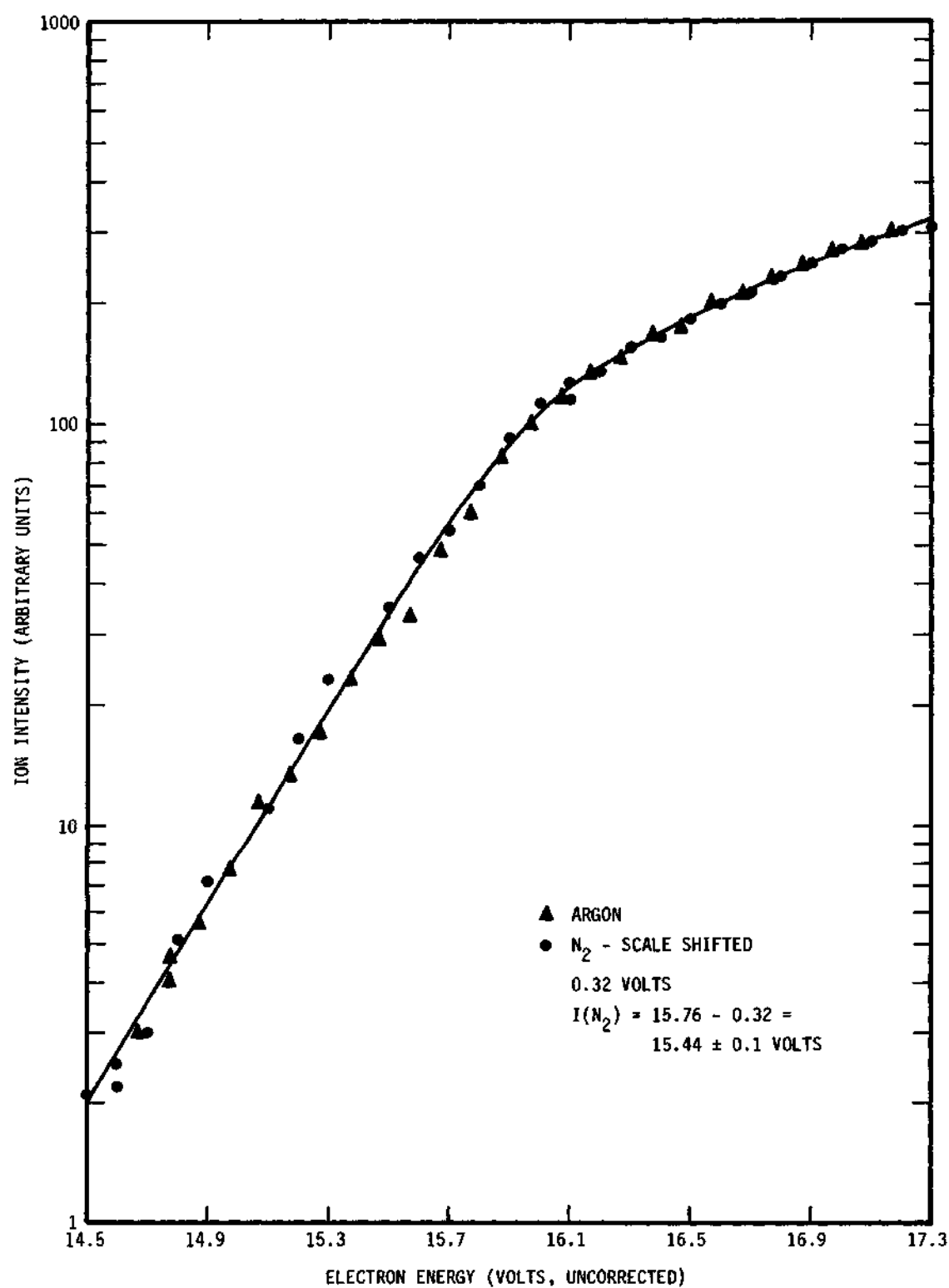


Figure 12. Ionization Efficiency Data for $I(N_2)$ Using the Semi-Log Matching Method.

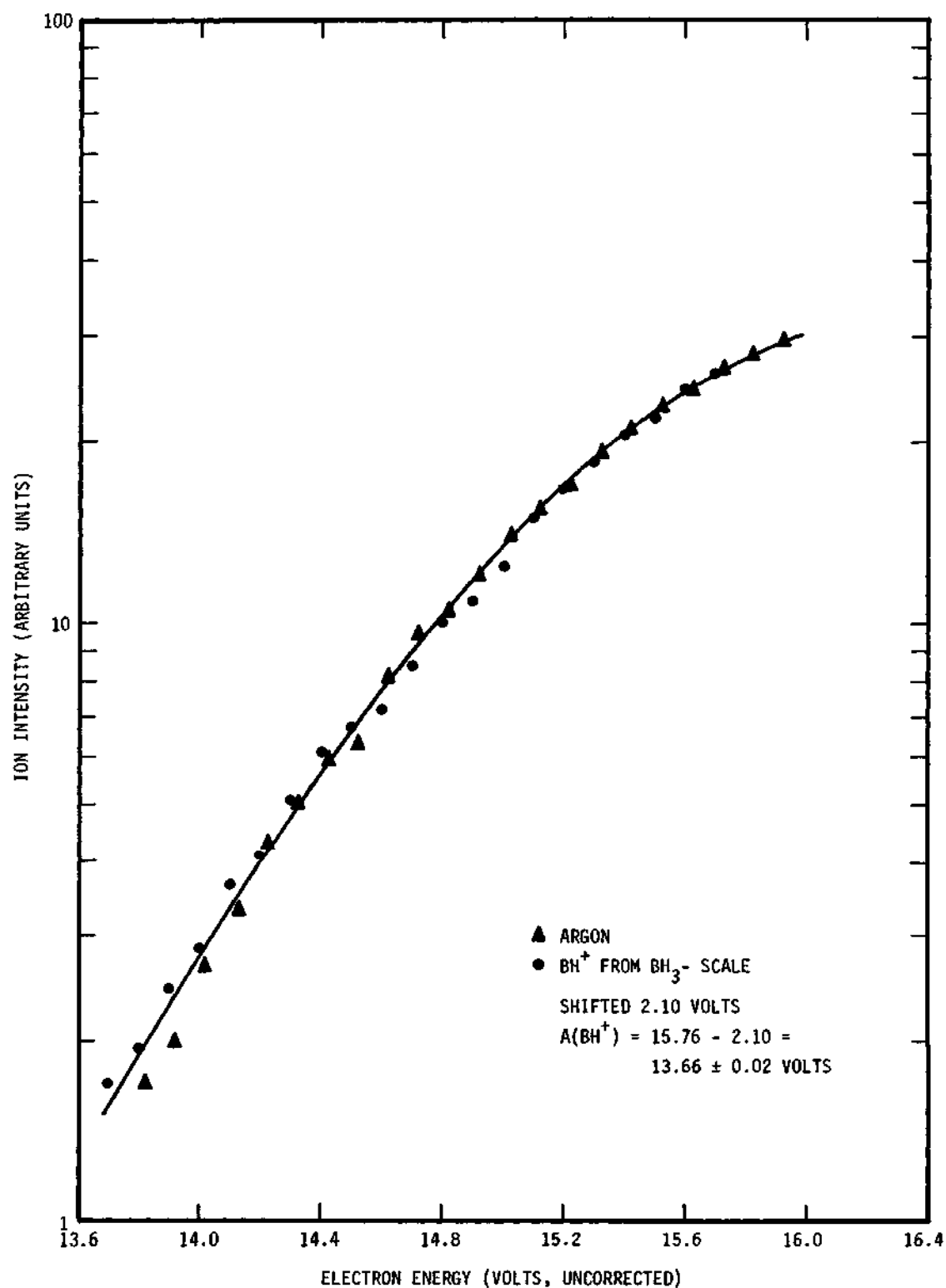


Figure 13. Ionization Efficiency Data for $A(\text{BH}^+)$ from BH_3 Using the Semi-Log Matching Method.

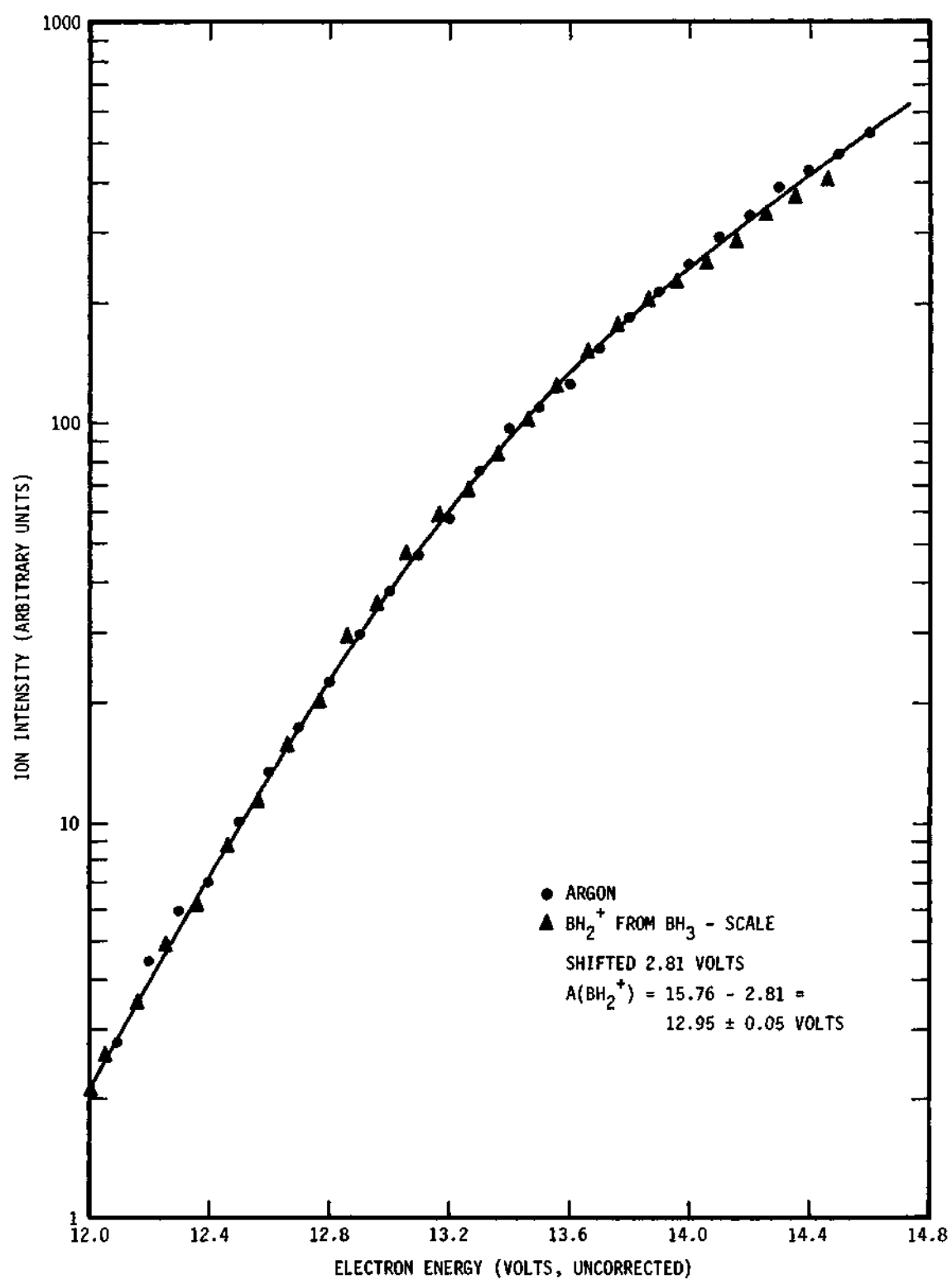


Figure 14. Ionization Efficiency Data for $A(\text{BH}_2^+)$ from BH_3 Using the Semi-Log Matching Method.

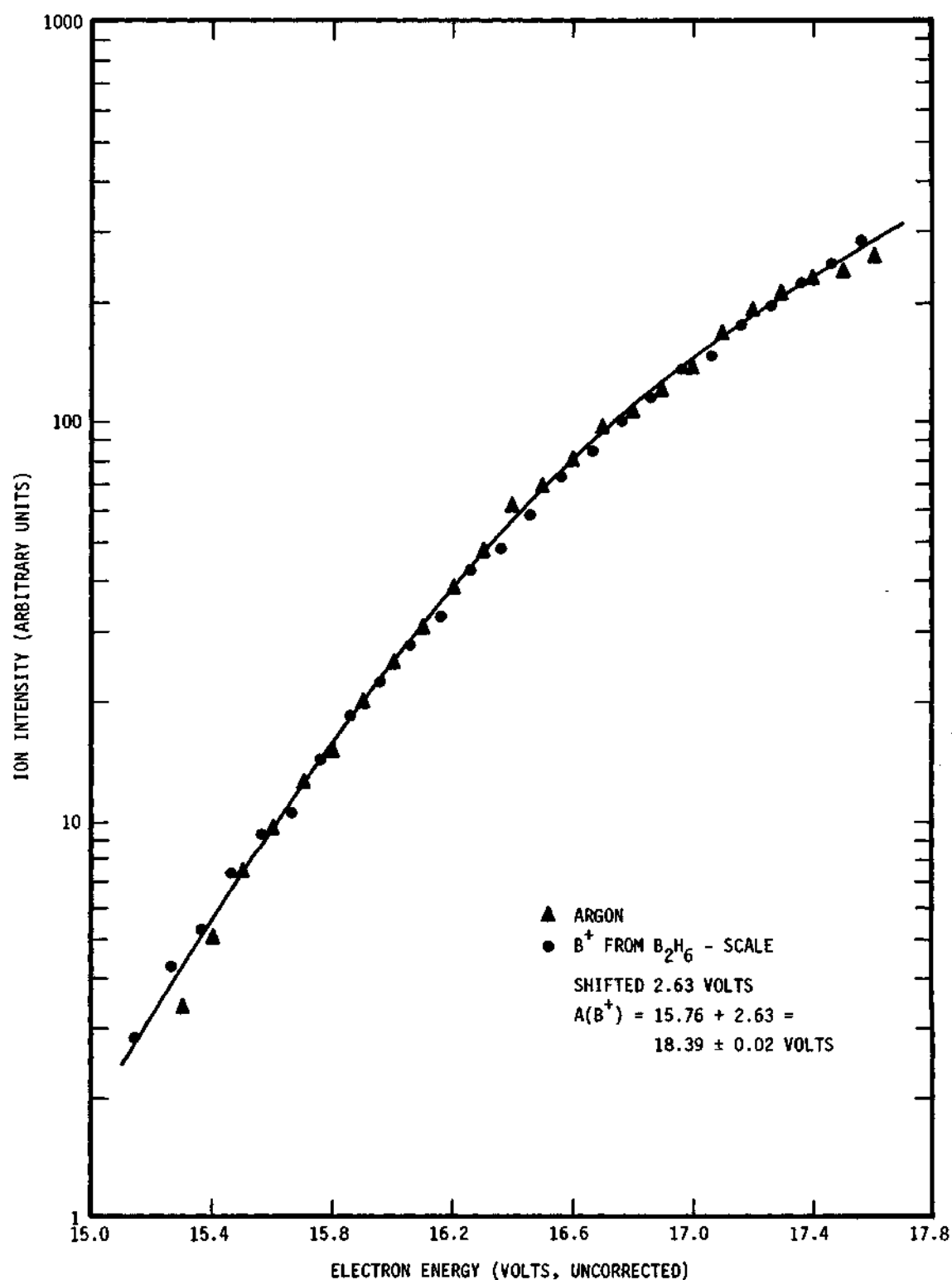


Figure 15. Ionization Efficiency Data for A(B⁺) from B₂H₆ Using the Semi-Log Matching Method.

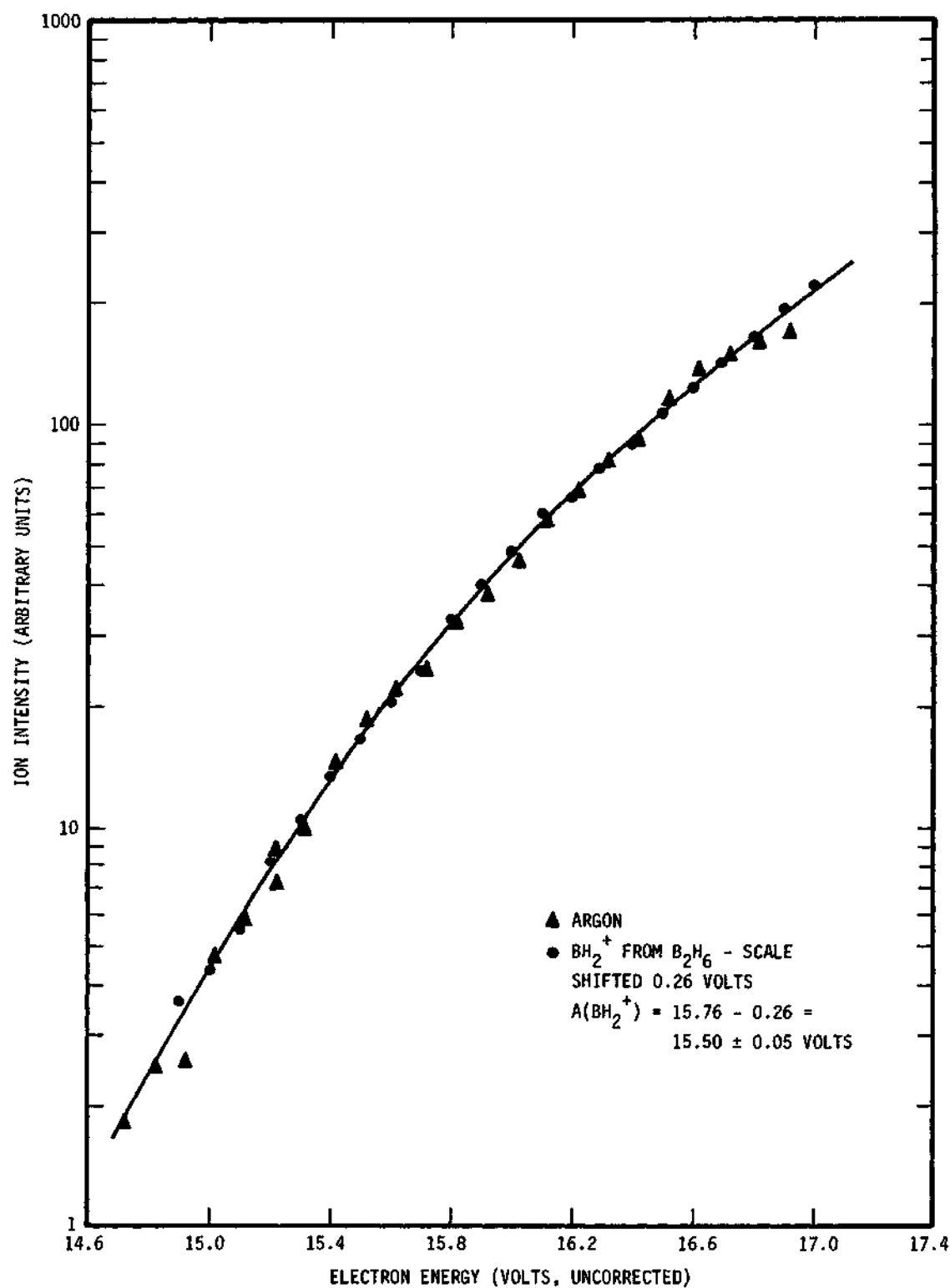


Figure 16. Ionization Efficiency Data for $A(\text{BH}_2^+)$ from B_2H_6 Using the Semi-Log Matching Method.

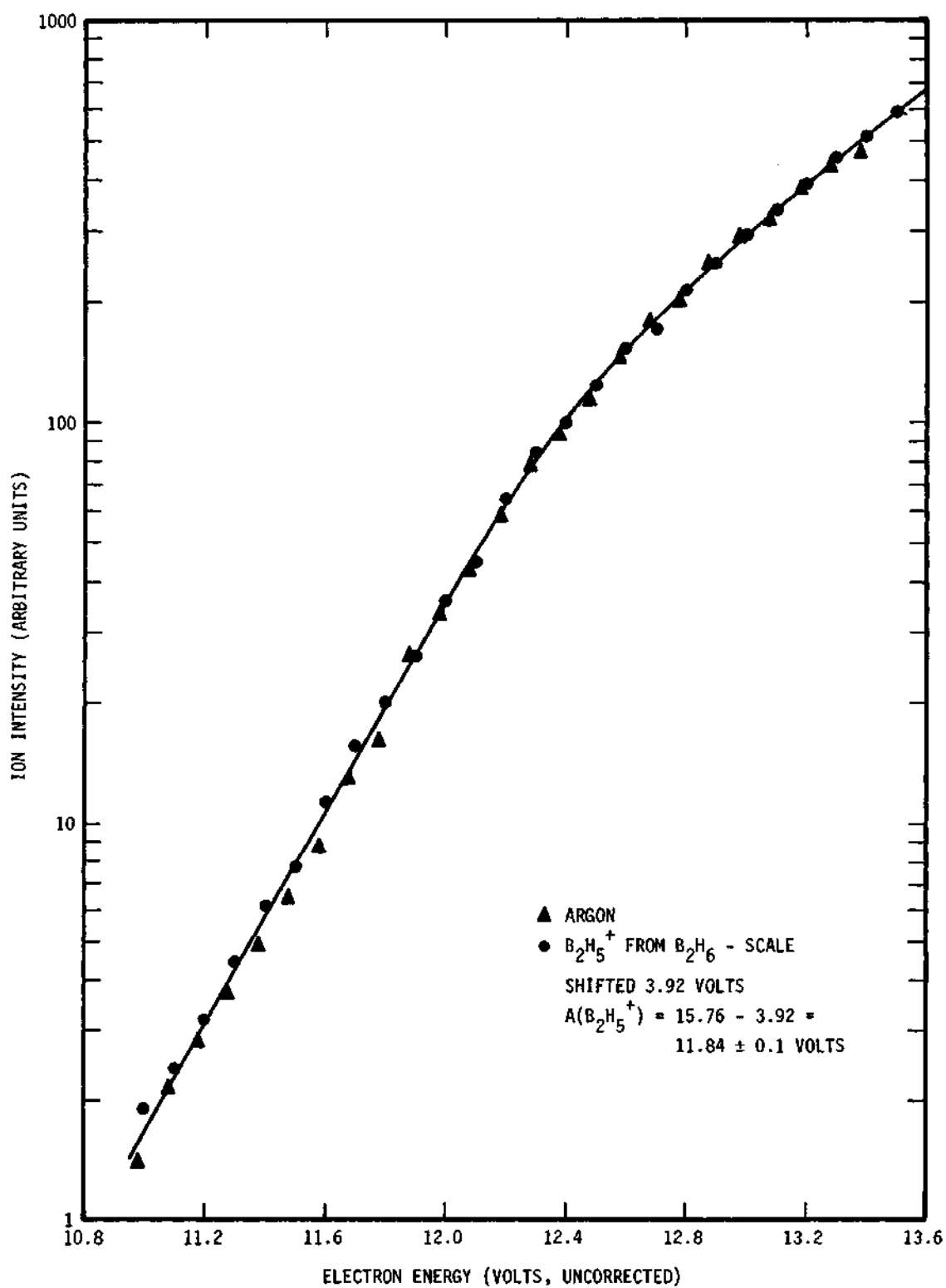


Figure 17. Ionization Efficiency Data for $A(B_2H_5^+)$ from B_2H_6 Using the Semi-Log Matching Method.

BIBLIOGRAPHY*

1. A. Stock, "Hydrides of Boron and Silicon," Cornell University Press, Ithaca, New York, 1933.
2. H. I. Schlesinger and A. B. Burg, Chem. Rev. 31, 1 (1942).
3. W. H. Eberhardt, B. Crawford, and W. N. Lipscomb, J. Chem. Phys. 22, 989 (1954).
4. H. C. Longuet-Higgins, J. Chim. Phys. 46, 268 (1949).
5. C. C. J. Roothaan, Rev. Modern Phys. 23, 69 (1951).
6. W. L. Clinton and B. Rice, J. Chem. Phys. 29, 445 (1958).
7. A. Stock and W. Mathing, Chem. Ber. 69, 1456 (1936).
8. A. B. Burg and H. I. Schlesinger, J. Am. Chem. Soc. 53, 4321 (1931).
9. A. B. Burg and H. I. Schlesinger, J. Am. Chem. Soc. 55, 4009 (1933).
10. A. Stock and W. Siecke, Chem. Ber. 57B, 562 (1924).
11. C. R. Dillard, Doctoral Thesis, University of Chicago (1949).
12. A. Stock and E. Kuss, Chem. Ber. 56B, 789 (1923).
13. G. C. Pimentel and K. S. Pitzer, J. Chem. Phys. 17, 882 (1949).
14. H. I. Schlesinger and A. B. Burg, J. Am. Chem. Soc. 60, 290 (1938).
15. J. K. Bragg, L. V. McCarty, and F. J. Norton, J. Am. Chem. Soc. 73, 2134 (1951).
16. R. P. Clarke and R. N. Pease, J. Am. Chem. Soc. 73, 2132 (1951).
17. K. Borer, A. B. Littlewood, and C. S. G. Phillips, J. Inorg. Nucl. Chem. 15, 316 (1960).
18. R. E. Enrione and R. Schaeffer, J. Inorg. Nucl. Chem. 18, 103 (1961).

* Abbreviations follow the form described in Chemical Abstracts, List of Periodicals, 1961.

19. R. Schaeffer, J. Inorg. Nucl. Chem. 15, 190 (1960).
20. A. B. Burg, J. Am. Chem. Soc. 74, 3482 (1952).
21. Y. C. Fu and G. R. Hill, J. Am. Chem. Soc. 84, 353 (1962).
22. H. G. Weiss and I. Shapiro, J. Am. Chem. Soc. 75, 1221 (1953).
23. A. T. Whatley and R. N. Pease, J. Am. Chem. Soc. 76, 835 (1954).
24. H. Brumberger and R. A. Marcus, J. Chem. Phys. 24, 741 (1956).
25. P. C. Maybury and W. S. Koski, J. Chem. Phys. 21, 742 (1953).
26. R. A. Marcus, J. Chem. Phys. 23, 1107 (1955).
27. I. Shapiro and B. Keilin, J. Am. Chem. Soc. 77, 2663 (1955).
28. W. C. Kreye and R. A. Marcus, J. Chem. Phys. 37, 419 (1962).
29. V. V. Subbanna, L. H. Hall, and W. S. Koski, J. Am. Chem. Soc. 86, 1304 (1964).
30. T. Hirata and H. E. Gunning, J. Chem. Phys. 27, 477 (1957).
31. T. P. Fehlner and W. S. Koski, J. Am. Chem. Soc. 86, 1012 (1964).
32. G. B. Skinner and A. D. Snyder, "Progress in Astronautics and Aeronautics," Vol. 15, (Ed. H. G. Wolfhard, I. Glassman, L. Green, Jr.), Academic Press, New York, 1964.
33. R. E. McCoy and S. H. Bauer, J. Am. Chem. Soc. 78, 2061 (1956).
34. S. H. Bauer, J. Am. Chem. Soc. 78, 5775 (1956).
35. M. E. Garabedian and S. W. Benson, J. Am. Chem. Soc. 86, 176 (1964).
36. L. H. Bolz, F. A. Mauer, and H. S. Peiser, J. Chem. Phys. 31, 1005 (1959).
37. J. R. Morrey, A. B. Johnson, Y. C. Fu, and G. R. Hill, "Borax to Boranes," Advances in Chemistry Series, American Chemical Society, Washington, D. C., 1961.
38. E. J. Sinke, G. A. Pressley, Jr., A. B. Baylis, and F. E. Stafford, J. Chem. Phys. 41, 2207 (1964).
39. T. P. Fehlner and W. S. Koski, J. Am. Chem. Soc. 86, 2733 (1964).
40. A. B. Baylis, G. A. Pressley, Jr., E. J. Sinke, and F. E. Stafford, J. Am. Chem. Soc. 86, 5358 (1964); this paper refers to private

communications with R. W. Diesen in which he reports mass spectrometric identification of BH_3 from a shock tube study, cf., R. W. Diesen, J. Chem. Phys. **39**, 2115 (1964).

41. T. P. Fehlner and W. S. Koski, J. Am. Chem. Soc. **87**, 409 (1965).
42. T. P. Fehlner, J. Am. Chem. Soc. **87**, 4200 (1965).
43. W. N. Lipscomb, "Advances in Inorganic Chemistry and Radiochemistry," Vol. I, (Ed. H. J. Emeleus and A. G. Sharpe), Academic Press, Inc., New York, 1959.
44. J. V. Kerrigan, Inorg. Chem. **3**, 908 (1964).
45. M. Perec and L. N. Becka, J. Chem. Phys. **43**, 721 (1965).
46. L. Lynds and C. D. Bass, J. Chem. Phys. **43**, 4357 (1965).
47. T. D. Coyle, J. J. Ritter, and T. C. Farrar, Proc. Chem. Soc. **1964**, 25.
48. T. C. Farrar and T. D. Coyle, J. Chem. Phys. **41**, 2612 (1964).
49. L. Lynds, J. Chem. Phys. **42**, 1124 (1965).
50. R. F. Porter and S. K. Wason, J. Phys. Chem. **69**, 2208 (1965).
51. R. E. Fox, W. M. Hickam, D. J. Grove, and T. Kjeldaas, Jr., Rev. Sci. Instr. **26**, 1101 (1955).
52. W. J. Martin, Mass Spectrometric Studies and Cryogenic Reactivity of CF_2 and Cl_2 , Ph.D. Thesis, Georgia Institute of Technology (1965).
53. T. J. Malone, Mass Spectrometric Studies of the Synthesis, Reactivity, and Energetics of the Oxygen Fluorides at Cryogenic Temperatures, Ph.D. Thesis, Georgia Institute of Technology (1966).
54. H. A. McGee, Jr., T. J. Malone, and W. J. Martin, Rev. Sci. Instr., in press.
55. Joint Army-Navy-Air Force JANAF "Interim Thermochemical Tables," (D. R. Stull, Project Director), The Dow Chemical Company, Midland, Michigan (1960).
56. G. C. Eltenton, J. Chem. Phys. **15**, 455 (1947).
57. F. P. Lossing, D. G. H. Marsden, and J. B. Farmer, Can. J. Chem. **34**, 701 (1956).
58. J. T. Herron and V. H. Dibeler, J. Res. Natl. Bur. Std. **65A**, 405 (1961).

59. F. P. Lossing, "Mass Spectrometry," (Ed. C. A. McDowell), McGraw-Hill Book Company, Inc., New York, 1963.
60. D. B. Givens, Mass Spectrometric Study of the Products Obtained from Fast Cryogenic Quenching of Several Reactions Involving Atomic Hydrogen or Atomic Oxygen, Ph.D. Thesis, Georgia Institute of Technology (1966).
61. S. N. Foner and R. L. Hudson, J. Chem. Phys. 25, 602 (1956).
62. W. S. Koski, J. J. Kaufman, C. F. Pachucki, and F. J. Shipko, J. Am. Chem. Soc. 80, 3202 (1958).
63. J. L. Margrave, J. Phys. Chem. 61, 38 (1957).
64. C. E. Melton and W. H. Hamill, J. Chem. Phys. 41, 546 (1964).
65. A. C. Hurley, Proc. Roy. Soc. (London) Ser. A 261, 237 (1961).
66. F. O. Ellison, J. Chem. Phys. 43, 3654 (1965).
67. S. H. Bauer, G. Herzberg, J. W. C. Johns, J. Mol. Spectry. 13, 256 (1964).
68. W. C. Price, T. R. Passmore, and D. M. Roessler, Discussions Faraday Soc. 35, 201 (1963).
69. S. R. Gunn and L. G. Green, J. Chem. Phys. 36, 1118 (1962).
70. National Bureau of Standards Report No. 6252, "Thermochemistry and Thermodynamic Functions of Some Boron Compounds," December, 1958.
71. E. J. Prosen, W. H. Johnson, and F. Y. Pergiel, J. Res. Natl. Bur. Std. 61, 247 (1958).
72. S. R. Gunn and L. G. Green, J. Phys. Chem. 65, 779 (1961).
73. S. H. Bauer, A. Shepp, and R. E. McCoy, J. Am. Chem. Soc. 75, 1003 (1953).
74. C. A. Coulson, "Valence," Oxford University Press, London, 1961.
75. L. Burnelle and J. J. Kaufman, J. Chem. Phys. 43, 3540 (1965).
76. F. H. Field and J. L. Franklin, "Electron Impact Phenomena," Academic Press, New York, 1957.
77. M. Szwarc, Chem. Rev. 47, 75 (1950).

78. N. N. Semenov, "Some Problems in Chemical Kinetics and Reactivity," Vol. 1, Princeton University Press, Princeton, New Jersey, (1958).
79. K. J. Laidler, "Chemical Kinetics," McGraw-Hill Book Company, Inc., New York, 1965.
80. S. W. Benson, "The Foundations of Chemical Kinetics," McGraw-Hill Book Company, Inc., 1960.
81. R. W. Law and J. L. Margrave, J. Chem. Phys. 25, 1086 (1956).
82. M. Studier, private communication
83. S. Dushman, "Scientific Foundations of Vacuum Technique," John Wiley and Sons, Inc., New York, 1962.
84. C. A. Thomas and D. K. Eads, Callery Chemical Company Report No. CCC-1024-TR-4, Jan. 29, 1954.
85. W. H. Evans, E. J. Prosen, and D. D. Wagman, "Thermodynamic and Transport Properties of Gases, Liquids, and Solids," American Society of Mechanical Engineers, McGraw-Hill Book Company, Inc., New York, 1959.
86. A. Shepp and S. H. Bauer, J. Am. Chem. Soc. 76, 265 (1954).

VITA

James Howard Wilson was born in Clay, West Virginia, on September 1, 1939. He attended public schools in Clay, West Virginia, and graduated from Clay County High School in May, 1957. He entered Georgia Institute of Technology in September, 1957, and was awarded the degree of Bachelor of Chemical Engineering, Cooperative Plan, with highest honors in June, 1962. His employer under the cooperative plan was the Ashland Oil and Refining Company, Ashland, Kentucky. He received scholarships from the Universal Oil Products Company and the Chemstrand Company during the academic years 1960-61 and 1961-62.

During the summer of 1962, he was employed by the E. I. du Pont de Nemours and Company in Belle, West Virginia.

In September, 1962, he enrolled in the Graduate Division of the Georgia Institute of Technology and completed requirements for the Master of Science in Chemical Engineering in September, 1963. He was employed by the Engineering Experiment Station and received graduate fellowships from the National Science Foundation, the Humble Oil and Refining Company, and the Standard Oil Company of California.

He is a member of Phi Kappa Phi, Tau Beta Pi, the Briaerean Society, and the Society of Sigma Xi.

In 1962 he was married to the former Julia Ann Murray of St. Albans, West Virginia, and they have one daughter, Alice Kristine, and one son, James Michael. He has accepted a position at Orange, Texas, with the Plastics Department of E. I. du Pont de Nemours and Company.